Geoscience Frontiers xxx (2014) 1–33

Contents lists available at ScienceDirect

China University of Geosciences (Beijing)

Geoscience Frontiers

journal homepage: www.elsevier.com/locate/gsf

Focus paper

Four billion years of ophiolites reveal secular trends in oceanic crust formation

Harald Furnes [a,*], Maarten de Wit [b], Yildirim Dilek [c,d]

[a] Department of Earth Science and Centre for Geobiology, University of Bergen, Allegt. 41, 5007 Bergen, Norway
[b] AEON and Earth Stewardship Science Research Institute, Nelson Mandela Metropolitan University 7701, Port Elizabeth 6031, South Africa
[c] Department of Geology and Environmental Earth Science, Miami University, Oxford, OH 45056, USA
[d] State Key Laboratory of Geological Processes and Mineral Resources, and School of Earth Science and Mineral Resources, China University of Geosciences, Beijing 100083, China

ARTICLE INFO

Article history:
Received 29 November 2013
Received in revised form
28 January 2014
Accepted 6 February 2014
Available online xxx

Keywords:
Phanerozoic and Precambrian greenstone belts
Ophiolite classification
Subduction-related ophiolites
Subduction-unrelated ophiolites
Precambrian plate tectonics

ABSTRACT

We combine a geological, geochemical and tectonic dataset from 118 ophiolite complexes of the major global Phanerozoic orogenic belts with similar datasets of ophiolites from 111 Precambrian greenstone belts to construct an overview of oceanic crust generation over 4 billion years. Geochemical discrimination systematics built on immobile trace elements reveal that the basaltic units of the Phanerozoic ophiolites are dominantly subduction-related (75%), linked to backarc processes and characterized by a strong MORB component, similar to ophiolites in Precambrian greenstone sequences (85%). The remaining 25% Phanerozoic subduction-unrelated ophiolites are mainly (74%) of Mid-Ocean-Ridge type (MORB type), in contrast to the equal proportion of Rift/Continental Margin, Plume, and MORB type ophiolites in the Precambrian greenstone belts. Throughout the Phanerozoic there are large geochemical variations in major and trace elements, but for average element values calculated in 5 bins of 100 million year intervals there are no obvious secular trends. By contrast, basaltic units in the ophiolites of the Precambrian greenstones (calculated in 12 bins of 250 million years intervals), starting in late Paleo- to early Mesoproterozoic (ca. 2.0–1.8 Ga), exhibit an apparent decrease in the average values of incompatible elements such as Ti, P, Zr, Y and Nb, and an increase in the compatible elements Ni and Cr with deeper time to the end of the Archean and into the Hadean. These changes can be attributed to decreasing degrees of partial melting of the upper mantle from Hadean/Archean to Present. The onset of geochemical changes coincide with the timing of detectible changes in the structural architecture of the ophiolites such as greater volumes of gabbro and more common sheeted dyke complexes, and lesser occurrences of ocelli (varioles) in the pillow lavas in ophiolites younger than 2 Ga. The global data from the Precambrian ophiolites, representative of nearly 50% of all known worldwide greenstone belts provide significant clues for the operation of plate tectonic processes in the Archean.

1. Introduction

Ophiolites are "suites of temporally and spatially associated ultramafic to felsic rocks related to separate melting episodes and processes of magmatic differentiation in particular oceanic tectonic environments (Dilek and Furnes, 2011). Their geochemical characteristics, internal structure, and thickness are strongly controlled by spreading rate, proximity to plumes or trenches, mantle temperature, mantle fertility, and the availability of fluids". In this new definition, ophiolites are categorized in subduction-unrelated and subduction-related groups. The subduction-unrelated ophiolites include **continental margin-, mid-ocean-ridge-** (*plume-proximal,*

* Corresponding author. Tel.: +47 5558 3530, +47 41326549 (cell); fax: +47 5558 3660.
E-mail address: harald.furnes@geo.uib.no (H. Furnes).

Peer-review under responsibility of China University of Geosciences (Beijing)

Production and hosting by Elsevier

1674-9871/$ – see front matter © 2014, China University of Geosciences (Beijing) and Peking University. Production and hosting by Elsevier B.V. All rights reserved.
http://dx.doi.org/10.1016/j.gsf.2014.02.002

plume-distal, and trench-distal subtypes), and **plume** (*plume-proximal ridge and oceanic plateau* subtypes) **type** ophiolites, whereas the subduction-related ophiolites include **suprasubduction zone** (*backarc to forearc, forearc, oceanic backarc, and continental backarc* subtypes) and **volcanic arc types**. The subduction-unrelated ophiolites represent the constructional stage (rift-drift to seafloor spreading) of oceanic crust formation and contain predominantly mid-ocean-ridge basalts. The subduction-related ophiolite types represent destructive stages of ocean floor recycling (subduction with or without seafloor spreading), and their magmatic products are characterised by showing variable geochemical fingerprints, indicating subduction influence.

In this paper, we summarize the lithological and geochemical characters of 118 representative Phanerozoic ophiolites, as well as four young examples (Tihama Asir, Macquarie, Taitao and Iceland) unrelated to orogenesis (Fig. 1 and Table 1). Using well-established geochemical discrimination diagrams based on stable trace elements, we interpret our global geochemical dataset in light of the new ophiolite classification of Dilek and Furnes (2011). We also use our extensive dataset on the Precambrian greenstone sequences (de Wit and Ashwal, 1997; Furnes et al., 2013), in an attempt to synthesise oceanic crust evolution over 4 billion years of Earth history. Our choice of selected ophiolites and greenstone belts is largely restricted to those from which we have sufficient field observations and geochemical data for a comparative study, though a few well-known ophiolites for which we have not found appropriate geochemical data for this classification are mentioned (shown in italics).

2. Phanerozoic orogenic belts and selected ophiolites

We provide below a short description of the Phanerozoic orogenic belts in which different ophiolite types occur (Fig. 1). For a more complete overview, we refer the reader to Dilek and Robinson (2003), and the literature under the description of each orogenic belt and Table 1. The Paleozoic orogenic belts we describe below are represented by collisional and accretionary types (Isozaki, 1997; Condie, 2007; Windley et al., 2007; Cawood et al., 2009; Wilhem et al., 2011). The examples of the collisional orogenic type include: The Caledonian-Appalachian belt, the Hercynian belt, the Uralian belt, the Maghrebian-Alpine-Himalayan belt, and the Qinling/Qilian/Kunlun belts. The examples of the accretionary type are: the peri-Caribbean type, the Central Asian Orogenic Belt, the Gondwanide-Tasmanide belt, the Andes, and the western Pacific and Cordilleran belts. The Indonesian-Myanmar belt is currently in a transitional position from subduction-accretion in the west to collision with the Australian passive margin in the east (e.g., Timor).

2.1. Caledonian-Appalachian belt

The tectonic history of the Scandinavian Caledonides (e.g., Roberts et al., 1985, 2007; Stephens et al., 1985; Roberts, 2003; Gee, 2005; Gee et al., 2008; Andersen et al., 2012; Hollocher et al., 2012) demonstrates a "Wilson Cycle" evolution (e.g., Dewey, 1969; Dewey and Spall, 1975), lasting over a time period of ca. 200 million years (Gee et al., 2008), starting around 600 Ma with rifting and sedimentation, separating Baltica from Rodinia. For about 80 million years (ca. 500–420 Ma) magmatism associated with oceanic crust and island arc construction took place in the Iapetus Ocean. The first and main oceanic crust-building period was between ca. 500–470 Ma that resulted in the formation of several major ophiolite complexes, and a second but short-lived event during ca. 445–435 Ma that generated two ophiolites (Dunning and Pedersen, 1988; Pedersen et al., 1991; Dilek et al., 1997; Furnes et al., 2012a). The oldest generation is represented by the Lyngen, Leka, Trondheim area, Gulfjell and Karmøy ophiolites, and the youngest generation is represented by the Sulitjelma and Solund-Stavfjord ophiolites (Fig. 1, Table 1).

The northern Appalachians, even though in some respects different from the Scandinavian Caledonides (e.g., Dewey and Kidd, 1974; van Staal et al., 2009; Zagorevski and van Staal, 2011), show much the same timing of oceanic crust and island arc construction processes (e.g., Anniopsquotch, Bay of Islands, Betts Cove, Lac Brompton, Thetford Mines) as those in Ireland (*the Clew Bay ophiolite*, e.g., Chew et al., 2010, and Tyrone Igneous Complex, e.g., Hollis et al., 2013), Scotland (Ballantrae, e.g., Leslie et al., 2008; Sawaki et al., 2010), *the Unst ophiolite* in the Shetlands (Flinn et al., 1979; Prichard, 1985; Cutts et al., 2011) and Scandinavia (Fig. 1, Table 1).

2.2. Hercynian belt

The Hercynian (or Variscan) orogenic belt (e.g., Zwart, 1967) extends from western Europe (Portugal) in the west to the Czech Republic in central Europe and to Turkey in the eastern Mediterranean region (Fig. 1). It represents a complex subduction-accretion-collision belt, developed during the closure of a series of Paleozoic basins during the Ordovician to early Carboniferous, as a result of the convergence of Gondwana and Laurussia (e.g., Matte, 1991; Kroner and Romer, 2013). The Variscan orogeny lasted for about 110 million years (410–300 Ma). Subduction-accretion processes occurred between 410 Ma and 330 Ma, and during this time period ophiolite-, island arc-, continental intra-plate and granitoid magmatism took place; subsequent final magmatic activity was dominated by post-kinematic granitoids (Kroner and Romer, 2013; Uysal et al., 2013). Rifting of the Gondwana margin resulted in bimodal magmatism in the early Paleozoic (e.g., Furnes et al., 1994; Crowley et al., 2000; Floyd et al., 2002), and in the development of small ocean basins (e.g., Finger and Steyrer, 1995). Three of the Hercynian ophiolites, the early Ordovican Internal Ossa-Morena Zone ophiolite sequences (IOMZOS) in SE Spain, and the late Silurian Kaczawa Mts. and the early Devonian Sleza sequences in Poland (Fig. 1, Table 1) are included in our synthesis. Another important magmatic complex is the *Lizard Complex* in SW England, for which we do not have appropriate geochemical data for our magmatic evaluation. Kirby (1979) interpreted this complex of massive and layered gabbro, dikes and peridotites as an ophiolite, whereas Floyd (1984) interpreted it as a fragment of oceanic crust formed in a rifted continental margin. Nutman et al. (2001) suggested that it represents a magmatic complex formed as a result of intra-continental rifting.

2.3. Uralian belt

The Uralides (Fig. 1) define an arc-continent collision orogenic belt (e.g., Zonenshain et al., 1985; Ryazantsev et al., 2008) that is >4000 km long, and extend from the Kara Sea (north) to Kazakhstan (south). The remnants of the early Paleozoic subduction-accretion complexes occur along a suture zone between the East European and the West Siberian cratons (Spadea and D'Antonio, 2006; Pushkov, 2009). We have included three Uralian ophiolites, the Nurali, Magnitogorsk and Kempersay (Fig. 1, Table 1), in this synthesis.

2.4. Maghrebian-Alpine-Himalayan belt

The Magrhebian-Alpine-Himalayan belt, also referred to as the Alpides, extends from Morocco in the west, through the European Alps, the Anatolides, Zagros, Makran, and the Himalayas in the east, defining an orogenic belt with a length of ca. 9000 km. The

Please cite this article in press as: Furnes, H., et al., Four billion years of ophiolites reveal secular trends in oceanic crust formation, Geoscience Frontiers (2014), http://dx.doi.org/10.1016/j.gsf.2014.02.002

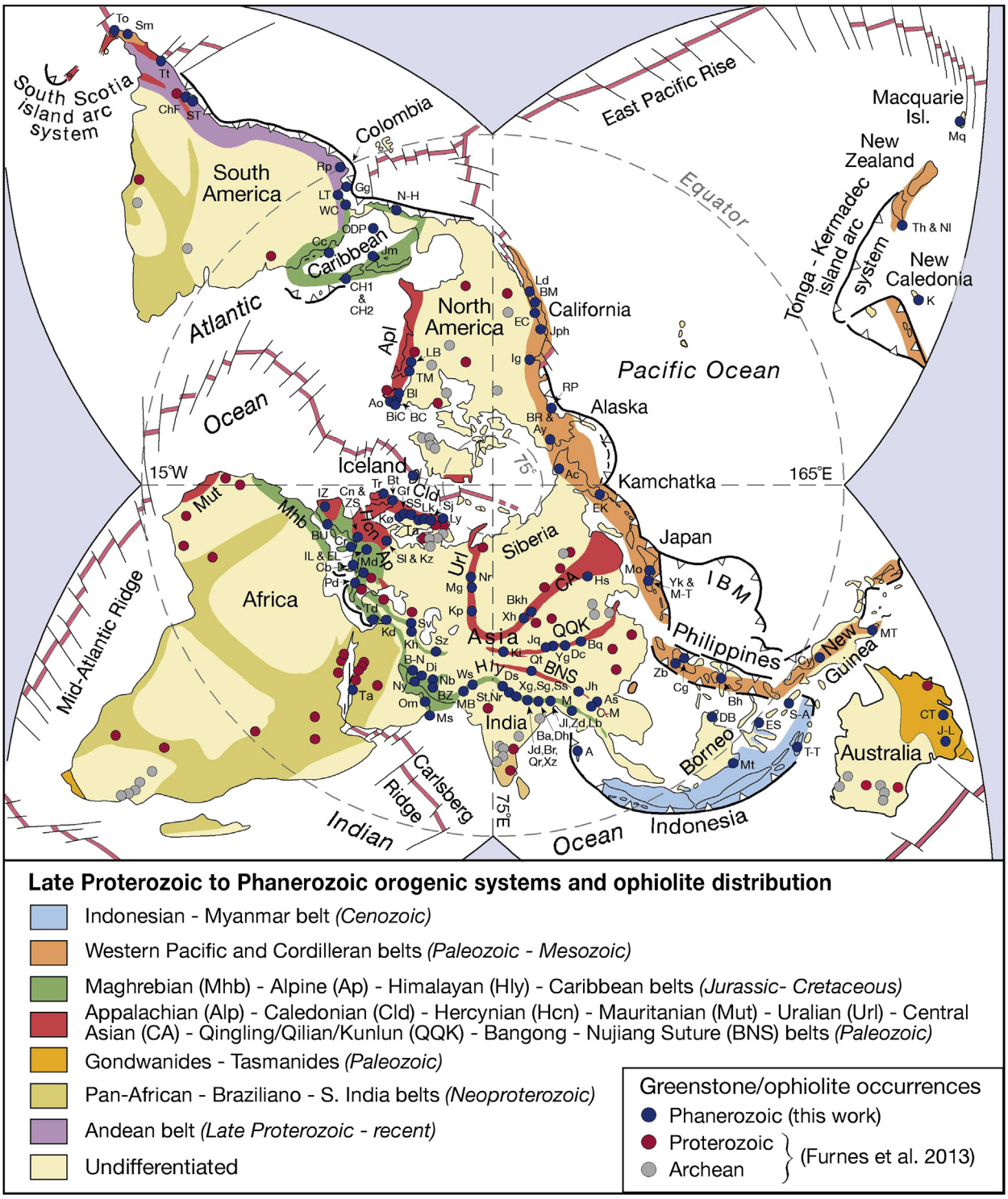

Figure 1. Map showing the global distribution of major Phanerozoic orogenic belts on a north polar projection (modified from Dilek and Furnes, 2011). Blue labelled dots show the location of the Phanerozoic ophiolites listed in Table 1 and red and grey dots show the location of Proterozoic and Archean greenstone sequences, respectively, as investigated in Furnes et al. (2013). Acronym: IBM = Izu-Bonin-Mariana arc-trench rollback system.

production of the ophiolites and island arc sequences and the tectonic processes that shaped this extensive orogenic belt are essentially of Mesozoic–Cenozoic age. The development of this belt occurred during the evolution of the Tethyan Ocean through a prolonged and complicated process whereby the opening and closure of Paleotethys and Neotethys and the production of several backarc basins overlapped in time and space (Dilek et al., 1990; Stampfli and Borel, 2002; Stampfli and Hochard, 2009). Silurian rifting of the northern Gondwana margin adjacent to the Proto-Tethyan Ocean (Rheic and Asiatic oceans) produced the Hun Superterrane. Continued extension led to the opening and development of the Paleo-Tethyan Ocean between the northern

Table 1
Summary of selected ophiolite sequences.

Ophiolitic magmatic complexes	Orogenic belt	Age (Ma)	Lithological components	Suggested tectonic setting	Main references to geology/ geochemistry
	Caledonian				
Lyngen (Ly)	Norway	ca. 480	Basaltic and boninitic pillow lava and mafic volcaniclastic rocks, dykes and gabbro, tonalite intrusions	Incipient oceanic arc	Selbekk et al. (1998); Kvassnes et al. (2004); H. Furnes (unpubl. data)
Leka (Lk)	Norway	497	Basaltic and boninitic pillow lava, sheeted dykes, plagiogranite, gabbro, ultramafic cumulates, mantle peridotites	Intraoceanic subduction	Furnes et al. (1988, 1992)
Sulitjelma (Sj)	Norway	437	Basalt pillow lava, sheeted dykes, varitextured and layered gabbro	Marginal basin	Pedersen et al. (1991)
Trondheim area (Ta) (Løkken, Bymarka, Vassfjell, Resfjell)	Norway	493–481	Basaltic pillow lava, sheeted dykes, plagiogranite, gabbro, ultramafic cumulates	Island arc/backarc	Heim et al. (1987); Grenne (1989); Slagstad (2003)
Solund-Stavfjord (SS)	Norway	442	Basaltic pillowed and massive lava, sheeted dykes, gabbro	Suprasubduction zone	Furnes et al. (2012a)
Gulfjell (Gf)	Norway	498	Basaltic and boninitic pillow lava, sheeted dykes, plagiogranite, gabbro	Forearc	Heskestad et al. (1994)
Karmøy (Kø)	Norway	497–470	Basaltic and bon. pillow lava, sheeted dykes, pl.granite, gabbro, ultram.cum.	Island arc/arc basin	Pedersen and Hertogen (1990)
Ballantrae (Bt)	Scotland	470	Basaltic and boninitic pillow lava, dolerite dykes, gabbro, trondhjemite, wehrlite, harzburgite, dunite	Backarc basin	Smellie et al. (1995); Oliver and McAlpine (1998)
				Forearc accretionay complex	Sawaki et al. (2010)
Tyrone Igneous Complex (Tr)	Ireland	490–475	Tyrone Igneous Complex (oldest): layered and isotropic gabbro, basaltic dykes, pillow lava; Tyrone Volc. Group (youngest): basaltic to rhyolitic volcanic rocks	Suprasubduction zone	Draut et al. (2009); Cooper et al. (2011); Hollis et al. (2012, 2013)
	Appalachian				
Birchy Complex (BiC)	Nfld, Canada	557	Basaltic lava, sediments, serpentinites	Rift-related	van Staal et al. (2013)
Annieopsquotch (Ao)	Nfld, Canada	480	Basaltic and boninitic pillow lava, sheeted dykes, gabbro	Suprasubduction - backarc	Lissenberg et al. (2005)
Bay of Islands (BI)	Nfld, Canada	485	Basaltic and boninitic lava, sheeted dykes, gabbro, mantle peridotites	Marginal basin-arc	Kurth-Velz et al. (2004)
Betts Cove (BC)	Nfld, Canada	488	Basaltic and bon. pillow lava, sheeted dykes, gabbro, px.nite, lay.cum.perid	Suprasubduction zone	Bédard (1999)
Lac Brompton (LB)	Quebec, Canada	480	Boninitic volcanic rocks, gabbro, pyroxenite, harzburgite	Forearc seafloor	De Souza et al. (2008)
Thetford Mines (TM)	Quebec, Canada	479	Basaltic and boninitic pillow lava, volcaniclastic rocks, gabbro, peridotites	Spreading in forearc	Olive et al. (1997); Page et al. (2009)
	Uralian				
Nurali (Nr)	Russia	468–483	Basalt lava (cut by dykes), gabbro, peridotite, set in a melange	Int.oc. arc/cont. marg.	Gaggero et al. (1997)
Magnitogorsk (Mg)	Russia	ca. 400–385	Basaltic and boninitic pillow lava, hyaloclastite, dykes, diorite	Forearc region	Spadea et al. (1998, 2002); Spadea and Scarrow (2000)
Kempersay (Kp)	Kazakhstan	470–485	Basalt lava, sheeted dykes, gabbro, harzburgite, lherzolite	Marginal basin, oceanic crust	Savelieva et al. (1997); Savelieva (2011)
	Central Asian				
Bayankhongor (Bkh)	Mongolia	210–298	Sheeted dykes, leuco- and prophyritic gabbro	Mid-ocean ridge	Buchan et al. (2001, 2002); Jian et al. (2010)
Xiaohuangshan (Xh)	China	340	Basalt, gabbro, serpentinized ultramafic rocks	Arc-basin system	Zheng et al. (2013)
Hegenshan (Hs)	China	400–350	Sparse basaltic lava and dykes; gabbro, serpentinized ultramafic rocks	Island arc-marginal basin	Robinson et al. (1999)
		333–354	Lherzolite dominated group	Mantel upwelling in a subcontinental setting	Jian et al. (2012)
		125–142	Harzburgite-dominated group		Jian et al. (2012)
	Qingling-Qilian-Kunlun				
Dongcaohe (Dc)	China	497	Basalt lava, sheeted dykes, gabbro	Oceanic crust	Tseng et al. (2007)
Yushigou (Yg)	China	550	Basaltic pillow lava, gabbro, keratophyre, dunite, harzburgite	Backarc basin, oc.crust	Hou et al. (2006)
Jiugequan (Jq)	China	490	Basaltic pillow lava, sheeted dykes, gabbro, serpentinites	Backarc basin	Xia and Song (2010)

Table 1 (*continued*)

Ophiolitic magmatic complexes	Orogenic belt	Age (Ma)	Lithological components	Suggested tectonic setting	Main references to geology/ geochemistry
Kudi (Ki)	China	ca. 458	Pillowed and massive lava, diabase dykes, cum. gabbro, px.nite, harzb., dunite	Backarc basin	Wang et al. (2002); Xiao et al. (2002)
Buqingshan (Bq)	China	ca. 470	Pillowed and massive basalt lava, diabase, gabbro, peridotite	Mid-ocean ridge	Bian et al. (2004)
	Bangong-Nujiang Suture				
Ailaoshan (As)	China	ca. 387–374	Ophiolitic melange containing basalt, diabase, gabbro, peridotite	Mid-ocean ridge	Jian et al. (2009)
Jinshajiang (Jh)	China	346–341	Ophiolitic melange containing basalt, diabase, gabbro, peridotite	Mid-ocean ridge	Jian et al. (2009)
Changning-Menglian (C-M)	China	270–264	Ophiolitic melange containing basalt, diabase, gabbro, peridotite	Suprasubduction zone	Jian et al. (2009)
Qiangtang (Qt)	Tibet	ca. 355	Basalt, gabbro, trondhjemite	Mid-ocean ridge	Zhai et al. (2013)
	Hercynian				
Sleza (Sl)	Poland	ca. 400	Basaltic pillow lavas, sheeted dykes, isotropic and layered gabbro	Mid-ocean ridge	Floyd et al. (2002)
Kaczawa Mts. (Kz)	Poland	ca. 420	Pillowed and massive basalt lava and dykes	Rift type	Furnes et al. (1994)
IOMZOS (IZ)	Spain	ca. 480	Basalt dykes, gabbro, dunite, wehrlite, pyroxenite	Mid-ocean ridge	Pedro et al. (2010)
	Alpine-Himalayan				
Betic ophiolitic Unit (BU)	SE Spain	185	Pillow lava and gabbro (eclogites and amphibolites), ultramafic rocks	Mid-ocean ridge, ultraslow	Puga et al. (2011)
Chenaillet (Cn)	France-Italy	165–153	Pillowed and massive flows, hyaloclastites, gabbro, diorite, dolerite dykes, albitites, lherzolite, harzburgite, wehrlite, dunite, pyroxenite	Mid-ocean ridge, ultraslow	Charlot-Prat (2005); Manatschal et al. (2011)
Zermatt-Saas (ZS)	Switerland-Italy	164	Basaltic pillow lava, gabbro, serpentinites	Mid-ocean ridge	Kramer et al. (2003)
External Ligurides (EL)	North Italy	ca. 170–180	Basalt, gabbro, subcontinental mantle	Mid-ocean ridge	Montanini et al. (2008)
Internal Ligurides (IL)	North Italy	ca. 170	Basaltic pillow lava, gabbro, peridotites	Mid-ocean ridge	Ottonello et al. (1984); Rampone et al. (1998)
Calabrian (Cb)	South Italy	150–140	Mafic and ultramafic rocks in melanges	Rift stage	Liberi et al. (2006); Tortorici et al. (2009)
Corsica (Cr)	Corsica	ca. 160	Schistes Lustres Complex: Pillow lava, peridotites Balange Nappe: Pillow lava, gabbro, serpentinite	Rift stage to ocean opening	Saccani et al. (2008)
Mirdita (Md)	Albania	165	Basalt and boninitic pillow lava, sheeted dykes, gabbro, ultramafic cumulates, harzburgite and dunite. Felsic and boninitic lavas on top of sequence	Suprasubduction zone	Dilek and Polat (2008)
Pindos (Pd)	Greece	165	Basalt and boninitic pillow lava, sheeted dykes, gabbro, ultramafic cumulates, harzburgite and dunite. Felsic and boninitic lavas on top of sequence	Suprasubduction zone	Pe-Piper et al. (2004); Dilek and Furnes (2009)
Troodos (Td)	Cyprus	92	Basaltic and boninitic pillow lava, sheeted dykes, gabbro, ultramafic cumulates, harzburgite and dunite	Suprasubduction zone Subduction initiation setting	Rautenschlein et al. (1985) Pearce and Robinson (2010)
Kizildag (Kd)	Turkey	92	Basaltic and boninitic pillow lava, sheeted dykes, gabbro, ultramafic cumulates, harzburgite and dunite	Suprasubduction zone	Dilek and Thy (2009)
Oman (Om)	Oman	96	Basaltic and boninitic pillow lava, sheeted dykes, gabbro, ultramafic cumulates, peridotites (harzburgite and dunite)	Suprasubduction zone	Goodenough et al. (2010)
Masirah (Ms)	Oman	140	Basaltic pillow lava and sheet flows, sheeted dykes, layered and isotropic gabbro, dunite, wehrlite, troctolite, felsic and boninitic lavas on top	Opening of ocean basin	Abbotts (1981); Mahoney et al. (1998); Peters and Mercolli (1998)
Sevan (Sv)	Armenia	165	Pillowed and massive basalt flows, gabbro and peridotites	Slow-spreading oc.crust	Galoyan et al. (2009)
Khoy (Kh)	Iran	ca. 140–130	Pillowed and massive basaltic lava, gabbro (layered and isotropic), mantle lherzolite and harzburgite	Ocean spreading centre	Hassanipak and Ghazi (2000); Khalatbari-Jafari et al. (2006)

(*continued on next page*)

Table 1 (*continued*)

Ophiolitic magmatic complexes	Orogenic belt	Age (Ma)	Lithological components	Suggested tectonic setting	Main references to geology/ geochemistry
Band-e-Zeyarat/Dar Anar (BZ)	Iran	142–141	Basaltic pillow lava, sheeted dykes, gabbro, set in melange	Mid-ocean ridge	Ghazi et al. (2004)
Dehshir (Di)	Iran	ca. 100	Basaltic pillow lava, sheeted dykes, pl.granite, gb., ultram.cum., harzb., dunite	Suprasubduction zone	Shafaii Moghadam et al. (2010)
Baft-Nain (B-N)	Iran	ca. 100	Pillowed and massive basalt lava, sheeted dykes, gabbro, harzburgite	Small backarc basin	Shafaii Moghadam et al. (2008)
Sabzevar (Sz)	Iran	ca. 100–66	Basalts, bas.and., dacite, rhyolite, basanite, gabbro, harzb., dunite, lherzolite	Mid-ocean ridge	Shojaat et al. (2003)
Neyriz (Ny)	Iran	92	Volcanic and volcaniclastic rocks, sheeted dykes, rh.dac., pl.granite, gb, perid.	Suprasubduction zone	Babaie et al. (2006)
Nehbandan (Nb)	Iran	ca. 100–60	Basaltic and boninitic pillowed and massive lava, high-level and cumulate gabbro, mantle tectonite	Mid-ocean ridge to suprasubduction zone	Saccani et al. (2010)
Muslim Bagh (MB)	Pakistan	157–118 87–65	Lower nappe of pillow lava and sediments in melange, upper nappe of gabbro and dolerite dykes	Island arc/ mid-ocean ridge	Khan et al. (2007a)
Waziristan (Ws)	Pakistan	ca. 100	Basaltic pillow lava, sheeted dykes, harzburgite	Island arc/mid-ocean ridge	Khan et al. (2007b)
Yarlung-Zangbo					
Dras (Ds)	India	ca. 135	Basaltic and andesitic lava, mantel tectonites	Intraoceanic arc	Clift et al. (2002)
Spontang (St)	India	130–110	Basaltic pillow lava, dykes, gabbro	Intraoceanic arc	Mahéo et al. (2004)
Nidar (Nr)	India	130–110	Basaltic pillow lava, dykes, gabbro	Intraoceanic arc	Mahéo et al. (2004)
Xiugugabu (Xg)	Tibet	ca. 125	Mafic sills, diabase, harzburgite	Backarc basin	Bezard et al. (2011)
Saga (Sg)	Tibet	155–130	Basalt lava, sills and dykes, gabbro, harzburgite, lherzolite	Backarc-arc	Bédard et al. (2009)
Sangsang (Ss)	Tibet	155–130	Basalt lava, gabbro, harzburgite	Backarc-arc	Bédard et al. (2009)
Jiding (Jd)	Tibet	125	Minor basaltic pillow lava, dykes and sills, gabbro, harzburgite, lherzolite	Backarc basin	Dubois-Côté et al. (2005)
Beimarang (Br)	Tibet	125	Minor basaltic pillow lava, dykes and sills, gabbro, harzburgite, lherzolite	Backarc basin	Dubois-Côté et al. (2005)
Qunrang (Qr)	Tibet	125	Minor basaltic pillow lava, dykes and sills, gabbro, harzburgite, lherzolite	Backarc basin	Dubois-Côté et al. (2005)
Beinang (Ba)	Tibet	125	Minor basaltic pillow lava, dykes and sills, gabbro, harzburgite, lherzolite	Backarc basin	Dubois-Côté et al. (2005)
Dazhugu (Dh)	Tibet	125	Minor basaltic pillow lava, dykes and sills, gabbro, harzburgite, lherzolite	Intraoceanic arc	Dubois-Côté et al. (2005)
Jinlu (Jl)	Tibet	125	Minor basaltic pillow lava, dykes and sills, gabbro, harzburgite, lherzolite	Intraoceanic arc	Dubois-Côté et al. (2005)
Loubusa (Lb)	Tibet	175	Minor basaltic pillow lava, dykes and sills, gabbro, harzburgite, lherzolite	Suprasubduction zone	Malpas et al. (2003), Yang et al. (2007)
Zedong (Zd)	Tibet	170–80	Minor basaltic pillow lava, dykes and sills, gabbro, harzburgite, lherzolite	Intra-oceanic arc	Malpas et al. (2003)
Xigaze (Xz)	Tibet	125–110	Basaltic and boninitic sheeted dykes, gabbro, harzburgite	Suprasubduction zone	Chen and Xia (2008)
Curacao (Cc)	Caribbean	90	Basalts and dolerite sills	Oceanic plateau	Klaver (1987); Kerr et al. (1996a)
Jamaica	Caribbean	90	Pillowed and massive lava, dolerite and gabbro	Oceanic plateau	Hastie et al. (2008)
(Bath-Dunrobin Fm) (Jm)					
Nicoya-Herradura (N-H)	Caribbean	95–86	Pillowed and massive basaltic lava, gabbro and minor plagiogranites	Oceanic plateau	Hauff et al. (2000)
Central Hispaniola (CH1)	Caribbean	115	Basalts, andesite, dacite/rhyolite lavas and equivalent intrusives	Subduction initiation	Escuder-Viruete et al. (2008)
Central Hispaniola (CH2)	Caribbean	79–68	Massive submarine lava flows, dolerite dykes and sills	Plume-related	Escuder-Viruete et al. (2011)
ODP, Leg 165, site 1001	Caribbean	ca. 81	Basalt flows	Plume-related	Kerr et al. (2009)
	Andean				
Western Colombia (WC)	Colombia	100–73	Pillowed and massive mafic lava, dolerite, gabbro, ultramafic rocks	Oc. spreading centre/plume	Kerr et al. (1997)
La Tetilla (LT)	Colombia	ca. 125–120	Basalt lava and breccias, gabbro, wehrlite	Suprasubduction zone	Spadea et al. (1987)
Gorgona Isl. (Gg)	Colombia	ca. 90–76	Basalt and komatiite, gabbro, peridotites	Oceanic plateau	Kerr et al. (1996b); Revillion et al. (2000)
Raspas (Rp)	Ecuador	ca. 140	Metabasalts (eclogites), peridotites	Oc. plateau/mid-oc. Ridge	Bosch et al. (2002); John et al. (2010)

Table 1 (*continued*)

Ophiolitic magmatic complexes	Orogenic belt	Age (Ma)	Lithological components	Suggested tectonic setting	Main references to geology/ geochemistry
Sierra del Tigre (ST)	Argentina	ca. 150	Basalt and gabbro	Rifted margin	Gonzáles-Menéndez et al. (2013)
Chuscho Fm (ChF)	Argentina	ca. 450	Basaltic pillow lavas, dykes and sills	Backarc basin	Ramos et al. (2000); Fauqué and Villar (2003)
Sarmiento (Sm)	Chile	150	Pillowed and massive basalt lava, sheeted dykes, layered gabbro	Marginal basin	Saunders et al. (1979); Stern (1980); Stern and Elthon (1979)
Tortuga (To)	Chile	150	Pillowed and massive basalt lava, sheeted dykes, layered gabbro	Marginal basin	Stern (1979, 1980); Elthon (1979)
	Cordilleran and Western Pacific				
Llanda (Ld)	California, USA	ca. 160	Gabbro and harzburgite	Suprasubduction zone	Giaramita et al. (1998)
Black Mountain (BM)	California, USA	ca. 160	Basalt lava and sheeted dykes, gabbro, harzburgite	Suprasubduction zone	Giaramita et al. (1998)
Ingalls (Ig)	Washington, USA	161	Pillow lava and breccia, sheeted dykes, minor gabbro, mantle tectonite	Suprasubduction zone	MacDonald et al., 2008
Elder Creek (EC)	California, USA	ca. 170	Volcanic rocks, sheeted dykes, gabbro, layered ultramafic rocks, mantel tectonites, abundant felsic plutonic rocks	Suprasubduction zone	Shervais (2008)
Josephine (Jph)	Oregon, USA	164–162	Basaltic and bon. pillow lava, sheeted dykes, gb, ultram.cum., harzb., dunite	Suprasubduction zone	Harper (2003)
Angayucham (Ay)	Alaska, USA	ca. 210–170	Pillow basalt, diabase, gabbro	Oceanic plateau	Pallister et al. (1989)
Brooks Range (BR)	Alaska, USA	ca. 165	Pillow basalt, diabase dykes, ultramafic/ mafic/intermediate intrusions, layered and isotropic gabbro, ultramafic cumulates	Interarc basin	Harris (1995)
Resurrection Peninsula (RP)	Alaska, USA	57	Basalt pillow lava, sheeted dykes, gabbro, trondhjemite, ultramafic rocks	Arc-like mid-ocean ridge	Lytwyn et al. (1997); Kusky and Young (1999)
Aluchin (Ac)	NE Russia	226	Basalt dykes and gabbro	Backarc basin	Ganelin (2011)
East Kamchatka (EK)	NE Russia	ca. 110–60	Basaltic pillow lava, sheeted dykes, gabbro, peridotites	Volcanic arc	Tsukanov et al. (2007)
Mineoka (Mo)	Japan	66	Basaltic lava and serpentinized peridotite (dominant)	Subduction and within-plate	Hirano et al. (2003); Y. Ogawa (pers.com.)
Mino-Tamba (M-T)	Japan	200–185	Massive and pillowed basaltic lava	Intraoceanic plume	Ichiyama et al. (2008)
Yakuno (Yk)	Japan	280	Massive and pillowed basalt lava, dolerite, gabbro, troctolite	Backarc basin	Ichiyama and Ishiwatari (2004)
Zambales (Zb)	Philippines	44–48	Basaltic pillow lava, dyke complex, layered and massive gabbro, serpentinized tectonized ultramafic rocks	Backarc basin	Geary and Kay (1989); Yumul et al. (2000)
Calaguas (Cg)	Philippines	ca. 100	Basaltic pillow lava and dykes, gabbro, harzburgite	Mid-ocean ridge	Geary and Kay (1989); Geary et al. (1989)
Bohol (Bh)	Philippines	ca. 100	Basaltic and boninitic lava, sheeted dykes, gabbro, harzburgite	Marginal basin	Faustino et al. (2006)
Darvel Bay (DB)	Malaysia	ca. 140	Basaltic volcanic rocks, dykes, gabbro, plagiogranites	Suprasubduction zone	Shariff et al. (1996)
Cyclops (Cy)	New Guinea Isl.	43–20	Basaltic and boninitic pillowed and massive lava, sheeted dykes, layered and isotropic gabbro, dunite, harzburgite	Forearc to backarc	Monnier et al. (1999a)
Milne Terrain (MT)	Papua New Guinea	55	Basalts and minor gabbro, ultramafic rocks	Mid-ocean ridge	Smith (2013)
Koh (K)	New Caledonia	220	Basaltic and boninitic pillow lava, gabbro, plagiogranite, serpentinite	Backarc basin	Meffre et al. (1996)
Northland (Nl)	New Zealand	32–26	Basalt and boninite, gabbro, diorite, plagiogranite	Backarc basin	Whattam et al. (2006)
Tangihua (Th)	New Zealand	ca. 100	Basatic pillow lava, massive flows and breccias, sheeted dykes, layered gabbro and ultramafic rocks; wehrlite and serpentinite	Suprasubduction zone	Nicholson et al. (2000)
	Indonesian-Myanmar				
Manipur (M)	NE India	ca. 70	Dykes and gabbro	Mid-ocean ridge	Singh et al. (2012)

(*continued on next page*)

Please cite this article in press as: Furnes, H., et al., Four billion years of ophiolites reveal secular trends in oceanic crust formation, Geoscience Frontiers (2014), http://dx.doi.org/10.1016/j.gsf.2014.02.002

Table 1 (*continued*)

Ophiolitic magmatic complexes	Orogenic belt	Age (Ma)	Lithological components	Suggested tectonic setting	Main references to geology/ geochemistry
Andaman (A)	Andaman isl.	95	Basaltic volcanic rocks, intrusives, cumulate peridotites and gabbro	Mid-ocean ridge	Pedersen et al. (2010)
Meratus (Mt)	SE Borneo	ca. 120	Gabbro, diorite, plagiogranite, ultramafic rocks	Forearc	Monnier et al. (1999b)
Timor-Tanimbar (T-T)	Timor	3–6	Basaltic pillow lava, dykes, gabbro, peridotites	Forearc	Ishikawa et al. (2007)
East Sulawesi (ES)	Sulawesi	80–120 & 10–20	Basaltic pillow lavas and massive flows, sheeted dykes, isotropic and layered gabbro and ultramafic rocks, lherzolite, harzburgite, dunite	Oceanic plateau	Kadarusman et al. (2004)
Seram-Ambon (S-A)	Central Indonesia	ca. 20–10	Basaltic lava, dykes, gabbro, peridotites	Marginal basin	Monnier et al. (2003)
	Tasmanide				
Camilaroi Terrane (CT)	SE Australia	ca. 390–360	Lower felsic volcanic rocks and associated sediments, upper basalt flows, intrusive rocks and sediments	Intraoceanic island arc	Aitchison and Flood (1995)
Jamieson-Licola (J-L)	SE Australia	ca. 500	Basalts, andesite, boninite and rhyolite volcanic rocks, gabbro	Backarc to forearc	Foster et al. (2009)
	Unrelated to orogenic belts				
Tihama Asir (TA)	Red Sea, Saudi Arabia	23–19	Basalt lava and dykes, isotropic and layered gabbro, granophyre	Rift stage, incipient oc.crust	Y. Dilek and H. Furnes (unpublished data)
Macquarie (Mq)	Macquarie Island	10	Basaltic pillow lava, sheeted dykes, gabbro, troctolite, wehrlite, dunite, harzb.	Oc.crust, N- to E-MORB	Kamenetsky et al. (2000); Varne et al. (2000)
Taitao (Tt)	Chile	6	Basaltic pillow lava and breccia, sheeted dykes, gabbro with dykes, ultramafic rocks	Mid-ocean ridge	Le Moigne et al. (1996); Guivel et al. (1999); Velozo et al. (2005)
Iceland	Mid-Atlantic Ridge	<1	Mainly basaltic lava	Plume/mid-ocean ridge	Hemond et al. (1993)

Abbreviations: bon = boninite/boninitic; pl.granite = plagiogranite; ultram.cum. = ultramafic cumulate; px.nite = pyroxenite; lay.cum.perid. = layered cumulate peridotite; cont.marg. = continental margin; Int.oc. = intra-oceanic; oc.crust = oceanic crust; harzb. = harrxburgite; gb = gabbro; bas.and. = basaltic andesite; rh.dac. = rhyodacite.

Gondwana margin and the Hun Superterrane, at the same time as the Rheic Ocean closed during Devonian time. The renewed Permian rifting of the northern margin of Gondwana, with detachment of the Cimmerian continent, led to the development of the Neo-Tethyan Ocean and the contemporary closure of Paleo-Tethys in the Triassic (for details, see Stampfli and Borel, 2002).

The Himalayan-Tibetan orogen developed as a result of the collision of India with Eurasia (e.g., Allegre et al., 1984; Dewey et al., 1989; Yin and Harrison, 2000; Searle et al., 2006; Guilmette et al., 2009). This collision started about 65 million years ago (Klootwijk et al., 1992), and the amalgamation of the involved continental blocks (e.g., Klootwijk et al., 1992; Matte et al., 1997; Yin and Harrison, 2000) occurred along the Yarlung-Zangbo Suture Zone in the late Cretaceous to early Tertiary (e.g., Windley, 1988; Hébert et al., 2012). Some of the ophiolites along this suture zone (e.g. the Loubusa ophiolite) contain in-situ diamonds and ultra high-pressure minerals in their upper mantle peridotites and chromitites (Yang et al., 2007).

The ophiolite occurrences in the Alpine belt (as included in this study) represent different types (continental margin, mid-ocean ridge to SSZ types) and are related to the opening, rift-drift development and closure of Neotethys (Whitechurch et al., 1984; Dilek and Delaloye, 1992; Dilek and Eddy, 1992; Lagabrielle and Lemoine, 1997; Dilek et al., 1999; Robertson, 2000; Malpas et al., 2003; Garfunkel, 2004; Manatschal and Müntener, 2009; Sarifakioglu et al., 2013). They are principally of two age groups (Table 1), an older group around 170–140 Ma (Betic, Chenaillet, Zermatt-Saas, External and Internal Ligurides, Calabrian, Corsica, Mirdita, Pindos, Eldivan, Refahiye, Sevan, Khoy, Band-e-Zeyarat/Dar Anar, Muslim Bagh, Saga, Sangsang) and a younger group around 125–90 Ma (Troodos, Kizildag, Oman, Neyriz, Nehbandan, Muslim Bagh, Waziristan, plus most of the examples of the Yarlung-Zangbo Suture Zone).

2.5. Caribbean region

The Caribbean region is characterized by a Cretaceous large igneous province (LIP) (e.g., Hauff et al., 2000; Kerr et al., 2009; Escuder-Viruete et al., 2011). This LIP was built during three main phases of magmatism, i.e. 124–112 Ma, 94–83 Ma, and 80–72 Ma (Escuder-Viruete et al., 2011, and references therein). The on-land remnants of LIP-related ophiolites that we have examined in this study include (Fig. 1, Table 1), from the oldest to the youngest include: central Hispaniola (115 Ma), Nicoya-Herradura, Curacao, Jamaica (95–86 Ma), central Hispaniola (youngest sequence, 79–68 Ma). In addition, we have included some geochemical data from the core samples recoved from the ODP Leg 165, Site 1001 in our database (Table 1).

2.6. Central Asian-Qingling/Qilian/Kunlun belts

The central Asian orogenic belt (Fig. 1) is situated between the Siberian and North China cratons (Tarim and Sino-Korean cratons). Its development involved the accretion of a series of island arcs, ophiolites and continental blocks to the bounding cratons during the evolution of the paleo-Asian Ocean from the late Mesoproterozoic to the Mesozoic (Kröner et al., 2008; Jian et al., 2010; Wakita et al., 2013; Zheng et al., 2013). We have included in our synthesis three ophiolite complexes, i.e., the younger part (210–298 Ma) of the Bayankhongur (the older part is ca. 645 Ma), the

Xiaohuangshan (340 Ma) and the Hegenshan (Table 1). The Hegenshan ophiolite consists of four different mafic-ultramafic massifs (Jian et al., 2012), which consist of two lithological groups with different crystallization ages, one lherzolite-dominated early Carbonifereous group (354–333 Ma) and the other harzburgite-dominated early Cretaceous group (142–125 Ma). However, there are contrasting viewpoints on the origin of the Hegenshan magmatic complex: Robinson et al. (1999) interpreted it as an ophiolite, whereas Jian et al. (2012) interpreted it as in-situ intrusive complex that was emplaced during episodic mantle upwelling and melting in a subcontinental setting.

The Qingling/Qilian/Kunlun fold belt (Fig. 1), also known as the central China orogenic belt, extends ca. 5000 km in a W–E direction and is located between the North China and Tarim cratons to the North and the Yangtze Craton to the southeast. This orogenic belt developed during the closure of the Qilian Ocean, which evolved following the late Proterozoic break-up of Rodinia. The Cambrian to Ordovician backarc ophiolites and island arcs formed during the latest stages of the evolution of this ocean (Song et al., 2013). We have chosen the following five ophiolite sequences from this belt in our synthesis: Dongcaoche, Yushigou, Jiugequan, Kudi and Buqingshan (Fig. 1, Table 1).

The ~1200-km-long Bangong-Nujiang Suture Zone (Fig. 1) in central Tibet is situated between the southern Lhasa and the northern Qingtang blocks. It is an E–W-trending, discontinuous belt of Paleozoic melanges and ophiolites. We have examined the Paleotethyan Ailaoshan, Jinshajiang, Changning-Menglian, Qiangtang ophiolites, ranging in age from ca. 380–270 Ma (Table 1) in this study (Jian et al., 2009).

2.7. Gondwanide-Tasmanide belt

The Tasmanides (Fig. 1) occupy approximately one third of the eastern Australian continent and include a collage of orogenic belts that formed during a time span of nearly 500 million years. The break-up of the Rodinia supercontinent during 750–525 Ma was followed by ca. 300 million years of mainly convergent margin tectonics and magmatism (e.g., Glen, 2005). We have investigated two main ophiolites from the Tasmanides, the early Ordovician Jamieson-Licola sequence of the Lachlan orogeny, and the Devonian Camilaroi Terrane of the New England orogen (Fig. 1, Table 1).

2.8. Andean belt

The Andean belt (Fig. 1), stretching over more than 8000 km between the Caribbean to the north and the Scotia Seas to the south, represents the largest active orogenic system developed by oceanic subduction along a continental margin for nearly 600 myrs, beginning soon after the break-up of Rodinia in the late Proterozoic (Oncken et al., 2006; Ramos, 2009). In the Paleozoic a number of exotic terranes accreted to this continental margin, whose geologic history includes an intricate record of accretion, collision, and subduction of different types of oceanic lithosphere (Ramos, 2009). The Andean system is divided up into the northern, central, and southern Andes. The northern and southern segments are characterized by Jurassic and Cretaceous metamorphic rocks as well as diverse occurrences of oceanic crust emplaced into the continental margin. The central Andes constitute the type locality of an Andean-type orogen and lack Mesozoic and Cenozoic metamorphic and ophiolitic rocks. They formed by subduction of oceanic crust and associated overlying mantle-wedge processes.

The northern Andes record a series of collisions of island arcs and oceanic plateaus from the early Cretaceous to the middle Miocene, and include the Cretaceous komatiite-bearing sequences of Gorgona Island (e.g., de Wit and Ashwal, 1997; Revillion et al., 2000). The geological record of the central and southern Andes includes mountain building and orogenic episodes alternating with periods of quiescence and absence of deformation. An orogenic cycle related to shallowing and steepening of the subduction zones dipping beneath western South America through time best accounts for the episodes of quiescence, minor arc magmatism, expansion and migration of the volcanic fronts, deformation, subsequent lithospheric and crustal delamination, and final foreland fold-and-thrust development (Ramos, 2009, and references therein).

The selected ophiolitic sequences for this study are: Colombian examples represented by those from western Colombia, La Tetilla and Gorgona Island, the Raspas ophiolite in Equador, the Sierra del Tigre and Chuscho Formation sequences in Argentina, and the Sarmiento and Tortuga ophiolites in southern Chile (Fig. 1, Table 1).

2.9. Western Pacific and Cordilleran belts

The Circum-Pacific orogenic system, referred to here as the western Pacific and the Cordilleran belts of western North America, extends along a great circle for more than 25,000 km in the Pacific Rim (Fig. 1). At an early stage in the Cordilleran evolution was the Neoproterozoic rifting of Rodinia. The characteristic features of the Circum-Pacific orogenic system stem largely from a long-term subduction of the Pacific oceanic lithosphere, from Triassic time onwards, along the active continental margins and island arc systems (e.g., Dickinson, 2004). Most of the early models invoke a Jurassic–Cretaceous eastward-dipping subduction zone, with oceanic crust being subducted underneath the continental margin (Burchfiel and Davis, 1975; Saleeby, 1983; Harper and Wright, 1984). More recent models envision, however, a series of fringing Triassic–Jurassic arc systems and backarc basins with opposite subduction polarities off the coast of North America that collapsed into the continental margin through arc-trench collisions in the latest Jurassic (e.g., Coleman, 2000; Dilek, 1989; Dilek et al., 1991; Dickinson et al., 1996; Godfrey and Dilek, 2000; Ingersoll, 2000). Collisional models in which the leading edge of the North American continent was subducted to the west beneath ensimatic arc systems have been also proposed (Moores and Day, 1984; Hildebrand, 2009, 2013). In Japan the subduction history has been shown to go back to ca. 500 Ma (Isozaki et al., 2010).

We show some of the most salient ophiolites along the Pacific Rim in Fig. 1. These are (Table 1): Llanda, Black Mountain, Ingalls, Eder Creek, Josephine, Angayucham, Brooks Range and Resurrection Island (USA); Aluchin, East Kamchatka (Russia); Mineoka, Mino-Tamba, Yakuno (Japan); Zambales, Calaguas, Bohol (Philippines); Darvel Bay (Malaysia); Cyclops, Milne Terrain (New Guinea), Koh (New Caledonia); Northland, Tangihua (New Zealand).

2.10. Indonesian-Myanmar belt

The Mesozoic–Cenozoic Indonesian-Myanmar orogenic belt (Hall, 2012) reveals a complex magmatic and tectonic history that evolved during the closure of the Meso-Tethyan Ocean. Continental blocks, rifted from East Asia (Luconia-Dangerous Grounds) and western Australia (Banda – SW Borneo and Argo – East Java and West Sulawesi) in the late Jurassic–early Cretaceous became part of the Sundaland region at a later stage. During much of the Cenozoic subduction has occurred under most of the Indonesian region. Rollback of subduction zones at different times has opened up backarc basins such as the Celebes and Philippine Seas (starting at ~45 Ma) and the Banda Sea (starting at ca. 15 Ma). For a complete picture of the reconstruction of the tectonic evolution of the Indonesian region, the reader is referred to the comprehensive work of Hall (2012). The ophiolites included in this synthesis

Please cite this article in press as: Furnes, H., et al., Four billion years of ophiolites reveal secular trends in oceanic crust formation, Geoscience Frontiers (2014), http://dx.doi.org/10.1016/j.gsf.2014.02.002

include (Table 1): Manipur (India); Andaman; Meratus (SE Borneo); Timor-Tanimbar (Timor); East Sulawesi; Seram-Ambon (Central Indonesia).

3. Phanerozoic and Precambrian ophiolites

3.1. Age distribution

The age distribution of the investigated greenstone sequences (Fig. 2) displays pronounced maxima during the time intervals 50–200 Ma (particularly the 100–150 Ma), 450–1000 Ma, and 2500–2750 Ma. The second most abundant greenstone complexes occur in the time intervals 0–50 Ma, 2000–2250 Ma, and 2750–3500 Ma. A third group is represented by the ophiolite complexes of 350–400 Ma, 1000–1500 Ma, and 1750–2000 Ma. The remaining complexes, defined in the time intervals, 200–300 Ma, 1500–1750 Ma, 2250–2500 Ma, and >3500 Ma, are rare. This variation in the temporal distribution is to some degree artificial, since only the greenstone sequences with reliable and easily accessible geochemical data have been chosen in this study; but it may also reflect the time periods when less greenstone material was preserved (Furnes et al., 2013).

3.2. Components of the investigated greenstone sequences

Composite stratigraphic columnar sections of the most representative Archean (10), Proterozoic (7) greenstone sequences, Phanerozoic (6) ophiolites, and two *in-situ* oceanic crustal sequences (represented by the Izu-Bonin-Mariana system and the Macquarie Island) are shown in Fig. 3. The Precambrian greenstone belts are dominated by pillowed to massive basaltic lava flows, with komatiitic rocks commonly represented, albeit in minor amounts in the 2.7 Ga and older sequences. Boninite-like rocks are minor constituents in the Precambrian greenstone sequences, but they have been reported from the amphibolites of the 3.8 Ga Isua supracrustal belt, SW Greenland (Polat et al., 2002; Furnes et al., 2009; Hoffmann et al., 2010) and the 3.12 Ga Whudo greenstone sequence of western Australia (Smithies et al., 2005) (Fig. 3). However, the origin of komatiite formation is controversial. In one model, Arndt et al. (2008) envisioned komatiites to have formed by high degrees of melting of dry peridotites through mantle plume activity, whereas Parman and Grove (2004) regarded komatiites as the Archean equivalent of modern boninites formed during partial melting of hydrated mantle. Thus, if some of the komatiitic rocks represent the boninite affinity, the magmatic evolution of some of the Archean greenstone sequences may be the equivalents of subduction-related Proterozoic ophiolites.

Intermediate to felsic volcanic and intrusive rocks are widespread in some Phanerozoic ophiolites and also in the Archean greenstone sequences, as documented for example from the IOG, Whundo, Kustomuksha and Wawa greenstone sequences (Fig. 3). Chert and BIFs are interlayered with the lava piles of the 3.0 Ga and older sequences. Sheeted dyke complexes are more common in the 2.7 Ga and younger sequences (Fig. 3), but they have been also reported from the Archean greenstone belts, i.e., the 3.8 Ga Isua and 2.7 Yellowknife complexes (Fig. 3), as well from the ca. 2.6 Ga Point Lake Greenstone Belt (e.g., Kusky, 1990).

The available lithological data from some Phanerozoic and Precambrian greenstone sequences are summarized in Fig. 4. In the Phanerozoic examples (Fig. 4A) mafic volcanic rocks have been reported from nearly all sequences (average 92%), with sparse occurrence of felsic rocks. Boninitic rocks are represented in variable amounts, from scarce (particularly in the 150–100 Ma interval) to abundant (in the 500–450 Ma interval), and on the average make up ca. 21%. The occurrences of sheeted dyke complexes are highly variable, ranging from zero to ca. 50% (average 34%), whereas individual dykes or dyke swarms are more common. Gabbro is a common lithology in most of the Phanerozoic greenstone complexes, as well as peridotites, on average 83% and 68% (respectively). Fig. 4B shows the lithology of the investigated greenstone sequences (this work and Furnes et al., 2013) through all times (Archean–Proterozoic–Phanerozoic). Mafic volcanic rocks are by far the most common lithology represented in most time windows, and felsic rocks are common in the Archean and lower Proterozoic greenstone sequences. Similarly, komatiites are commonly described from the Archean and lower Proterozoic greenstone complexes, but they are hardly reported in rocks younger than 2 billion years. In contrast, boninitic magmatic rocks have been reported throughout the 4 billion years investigated here. Sheeted dyke

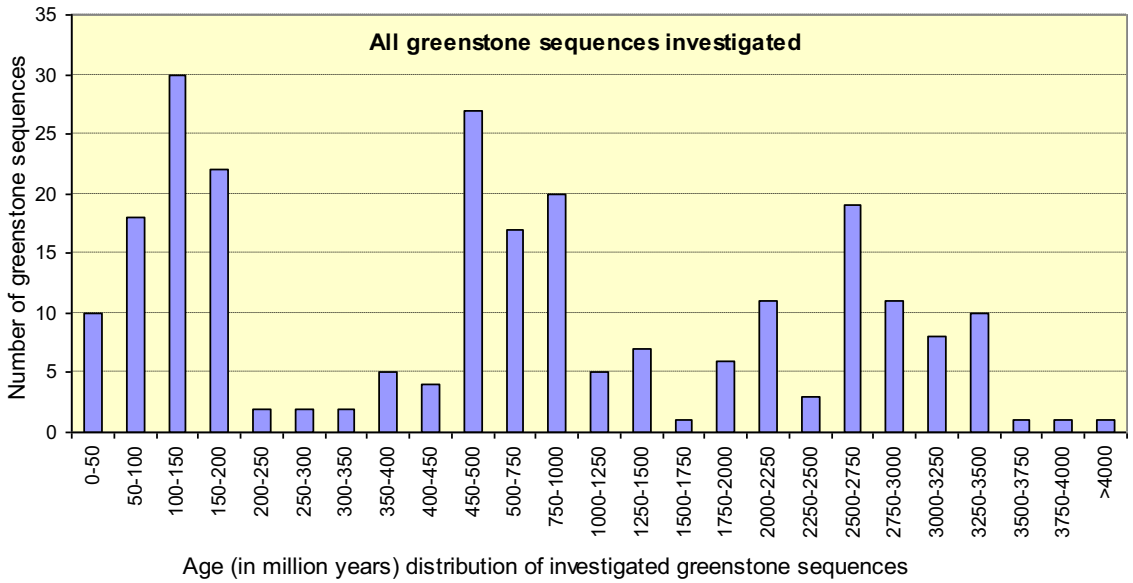

Figure 2. Age distribution of investigated greenstone sequences through geological time. Data for the Phanerozoic ophiolites are listed in Table 1, and the Precambrian greenstone sequences are shown in Table 1 of Furnes et al. (2013).

Please cite this article in press as: Furnes, H., et al., Four billion years of ophiolites reveal secular trends in oceanic crust formation, Geoscience Frontiers (2014), http://dx.doi.org/10.1016/j.gsf.2014.02.002

complexes are scarce, and gabbro and peridotites are minor lithological constituents in the Archean greenstone complexes; but these rock units become more abundant in ophiolite complexes younger than 2 billion years.

In the basaltic pillow lavas, ocelli (or alternatively referred to as "varioles") are common and striking features in the Archean and early Proterozoic ophiolites (e.g., Gelinas et al., 1976; de Wit and Ashwal, 1997; Sandstå et al., 2011). These mm- to cm-sized leucocratic globular objects are uncommon in younger ophiolites and in modern oceanic crust (Upadhyay, 1982; Kerr et al., 1996a). The origin of these features is controversial and has been explained as representing immiscible liquids, mingling of felsic and mafic liquids, or the result of secondary alteration (see summary and appropriate references in Sandstå et al., 2011). However, the shape, distribution, texture and composition of well-preserved ocelli in the interior part of pillow lavas of the Barberton greenstone belt in South Africa (e.g., de Wit et al., 2011; Furnes et al., 2011) indicate an origin by spherulitic crystallization of plagioclase from highly undercooled basalt melt and glass during rapid cooling (Sandstå et al., 2011). This interpretation suggests that the absence of gabbros and dolerites may be related to higher rates of cooling of mafic magmas in the Archean.

4. Geochemistry

We consider only the mafic rocks; all intermediate to felsic rocks as well as rocks regarded as cumulate units have been omitted from the geochemical plots presented here. Also, among Archean rocks, silicification of mafic and ultramafic volcanic rocks is a common phenomenon, and the analytical data representing such units have been excluded in our plots. We define intermediate to felsic rocks primarily as high SiO_2 (>55%), low MgO (<3%) magmatic units. For mafic-ultramafic volcanic rocks that underwent silicification, both SiO_2 and MgO, Ni and Cr concentrations are high. For the komatiites that we regard as cumulates (mainly olivine), we have set an upper MgO limit of 35%, and for the gabbroic rocks (mainly plagioclase) an upper Al_2O_3 limit of 20% has been chosen.

Numerous studies have been completed to evaluate the element behaviour during low-temperature alteration and greenschist to amphibolite grade metamorphism of basaltic rocks. A general conclusion is that Ti, Al, P, Cr, Ni, Sc, Co, V, Y, Zr, Nb, REE (particularly HREE) and Th are relatively stable (e.g., Scott and Hajash, 1976; Staudigel and Hart, 1983; Seyfried et al., 1988; Komiya et al., 2004; Hofmann and Wilson, 2007; Dilek et al., 2008; Furnes et al., 2012b). For this study we have used the major oxides TiO_2, Al_2O_3, FeO^t, Na_2O and P_2O_5, the incompatible trace elements Sr, Y, Zr, Nb, and the compatible trace elements Cr, Ni, Sc, Co to characterize the concentration levels as a function of age. For the discrimination diagrams, we have used the elements Ti, Y, Zr, Nb, V, Yb, Th, in the combinations of Zr/Ti–Nb/Y, Th/Yb–Nb/Yb, V–Ti/1000, and TiO_2/Yb–Nb/Yb. Na and Sr are generally reported as highly mobile; however, it is interesting to note (see description below) that in our study they show the same patterns as defined by the stable incompatible elements.

4.1. Age-related geochemical patterns

Fig. 5A shows the concentration of the major oxides TiO_2, Al_2O_3, FeO^t, Na_2O and P_2O_5 plotted against time. There is a large spread in their concentration at any given age. For TiO_2, Na_2O and P_2O_5 the spread increases with decreasing age; for Al_2O_3 the spread appears highest in the Archean rocks, whereas for FeO^t there is no particular trend. For the Phanerozoic (0–517 Ma) and Precambrian analyses, averages of 100 and 250 million years, respectively, have been calculated. Apart from the two oldest greenstone sequences, i.e. Isua (SW Greenland) and Nuvvuagittuq (NE Canada), the average concentrations of the major oxides show rather small variations. There is a decrease in TiO_2, Na_2O and P_2O_5 with increasing age, a feature also demonstrated for the incompatible trace elements Sr, Zr, Y and Nb (Fig. 5B). This relationship is best demonstrated by Sr and Nb. During the Phanerozoic and Proterozoic eons there are only minor changes in the average concentrations of incompatible trace elements. There is, however, some variability in the concentration of the stable elements Ti, Zr and Nb during the first 400 million years of the Phanerozoic that relate to the predominant basalt type represented within the following time intervals: the high Ti, Zr and Nb contents in the time interval 100–200 Ma (Fig. 5A and B) reflect the high proportion of subduction-unrelated basalts in the time interval 150–200 Ma (Fig. 8A); the low average Nb contents in the time interval of 200–400 Ma (Fig. 5A and B) can be explained, on the other hand, by the predominance of subduction-related magmatism during that period (Fig. 8); the low average contents of Al_2O_3 in the 2750–3000 Ma, 3250–3500 Ma and 4000 Ma (Fig. 5A) may be attributed to relatively high content of ultramafic magmatism during these time intervals. However, when taking the average concentrations of the above-mentioned incompatible elements for the Archean Eon, there is a decrease of 30–50% compared with the average Phanerozoic values. For the compatible elements Cr and Ni, there is a marked increase in their concentrations in the older sequences, particularly in Archean examples in which the average values are about three times higher than for those of the Phanerozoic greenstones. The elements Sc and Co, on the other hand, do not show any particular trend with increasing age.

These average secular geochemical changes may reflect variations in the degree of partial melting. Since the heat production in the upper mantle was higher in the Archean than today, it is generally assumed that melting of the Archean mantle was more extensive than today, yielding hotter and greater volumes of oceanic lithosphere (e.g., Foley et al., 2003; Komiya, 2004; Korenaga, 2006; Herzberg et al., 2010). Exactly how much higher the temperatures may have been in the Archean than that of the modern mantle, is conjectural. Komiya (2004) suggested 150–200 °C, whereas Grove and Parman (2004) proposed even lower (ca. 100 °C) temperatures. Tholeiitic melts are produced by 5–25% partial melting of mantle peridotites (e.g., McDonough et al., 1985); by contrast komatiitic magmas are modelled to be generated at ca. 30–50% partial melting of the mantle peridotites (e.g., Arndt, 2003; Maier et al., 2003).

In order to evaluate the cause of the observed decrease in the incompatible elements and the increase in the compatible elements, we have performed partial batch melting modelling (Brownlow, 1996) of spinel and garnet lherzolite with respect to Ni, Cr, Co, Sc, Y, Zr and Nb, and with bulk distribution coefficients of 8, 4, 2, 0.5, 0.05, 0.02, 0.01, respectively (Pearce and Parkinson, 1993). For Co, Sc, Y, Zr and Nb the differences in the average concentrations of the Phanerozoic and Archean greenstones could be modelled by 20% and 40% partial melting, respectively. The concentrations of Ni and Cr, on the other hand, are too high in the Archean rocks to be compatible with this modelling, and a possible explanation is that many of the komatiites, particularly those with more than 35% MgO, represent cumulates and that their high Ni and Cr do not represent the values of true magmatic liquids.

Exactly when and why the decrease in the incompatible elements took place is difficult to pinpoint. But judging on the basis of Ti and Nb (in particular), this appears to commence at around 2 Ga or somewhat later. At about this time, there were also major changes in the lithological composition of the greenstones complexes, i.e. in complexes older than 2 Ga, komatiites are more common, sheeted dyke complexes are rare, and gabbro is

Please cite this article in press as: Furnes, H., et al., Four billion years of ophiolites reveal secular trends in oceanic crust formation, Geoscience Frontiers (2014), http://dx.doi.org/10.1016/j.gsf.2014.02.002

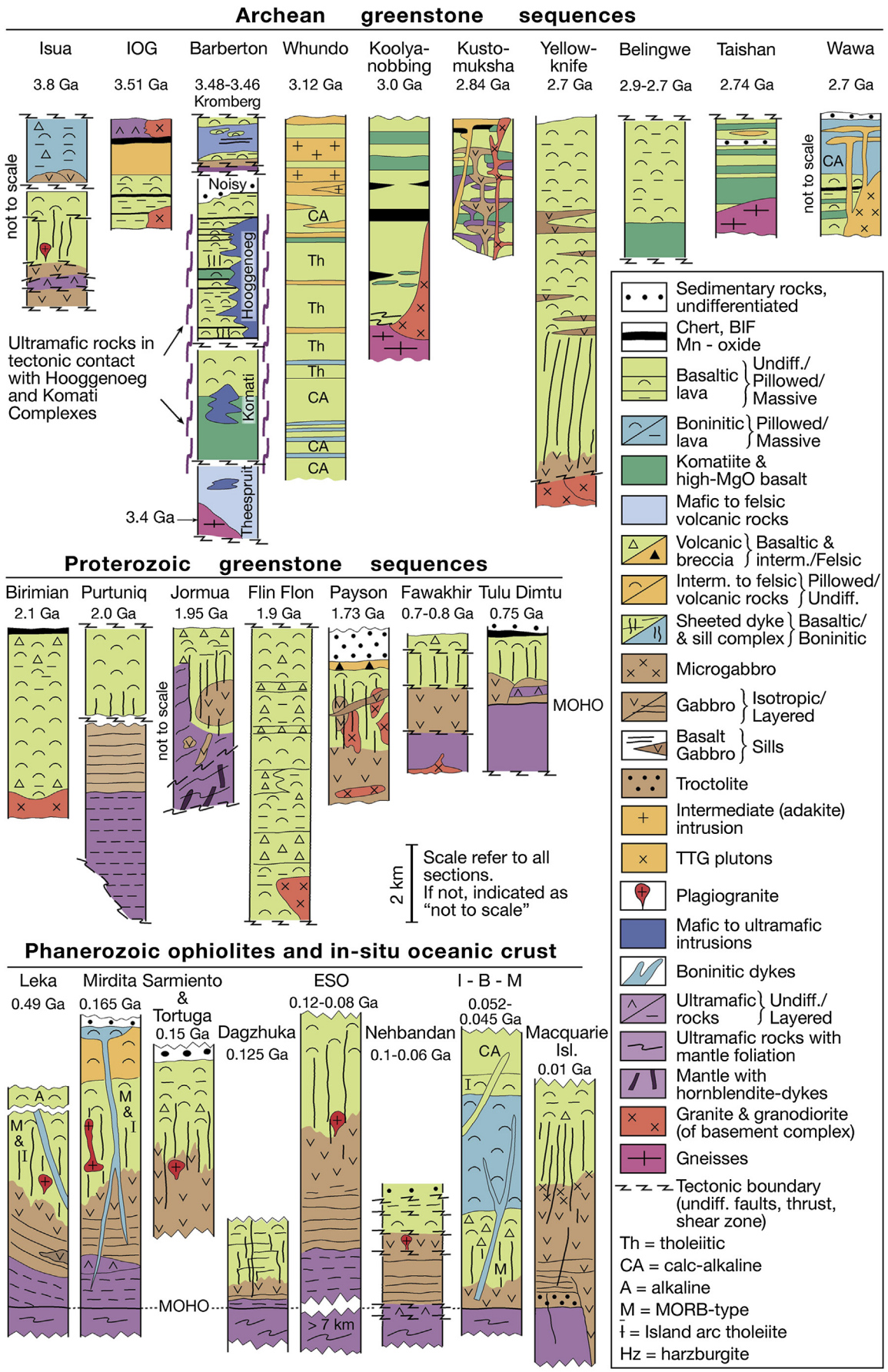

Please cite this article in press as: Furnes, H., et al., Four billion years of ophiolites reveal secular trends in oceanic crust formation, Geoscience Frontiers (2014), http://dx.doi.org/10.1016/j.gsf.2014.02.002

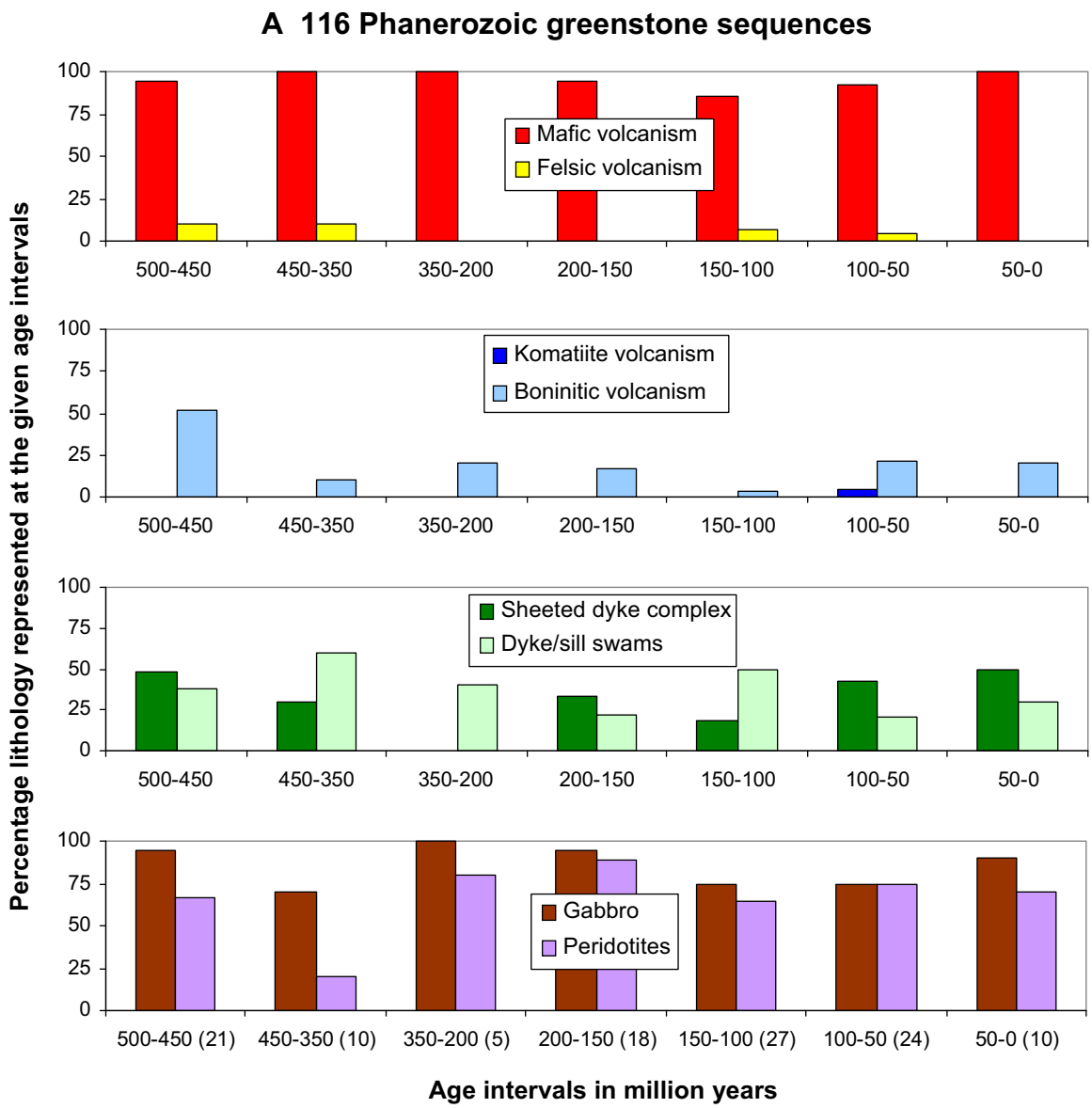

Figure 4. Percentage lithology represented at given age intervals (e.g. at the 450–350 age interval 10 sequences are presented, as shown in brackets at the bottom. In these 10 sequences all (i.e. 100%) contain mafic volcanic rocks, 3 contain sheeted dyke complexes (30%), etc.). A: The data information for all the Phanerozoic greenstone sequences is shown in Table 1. B: The data information for the Precambrian greenstone sequences is from Table 1 of Furnes et al. (2013).

subordinate and ocelli are abundant compared to the younger complexes (Fig. 4B).

4.2. Discrimination diagrams

In addition to the filtration of the geochemical data as outlined above, we have applied the Zr/Ti–Nb/Y diagram of Floyd and Winchester (1975) in order to better group the data that truly represent basaltic compositions (Fig. 6A). The use of the Th/Yb–Nb/Yb discrimination of Pearce (2008) further separates subduction-related basalts from the subduction-unrelated basalts (Fig. 6A). Samples that plot above the MORB-OIB array are analysed using the V–Ti plot of Shervais (1982). The V/Ti ratio can be used as a proxy for supra-subduction zone (SSZ) melting, and the V–Ti diagram, as modified by Pearce (in press), can be subdivided into fields defined by boninites, island arc tholeiites (IAT), and MORB, the latter being the most distal to the subduction zone (Fig. 6A). Samples that plot within the MORB-OIB array are further analysed in a TiO_2/Yb–Nb/Yb diagram in which the TiO_2/Yb ratio is a proxy for the depth of melting. Since Yb is an element that is highly partitioned into garnet, the Ti/Yb ratio in a melt is sensitive to whether or not garnet is present in the residue after melting; it is high if garnet is present.

Figure 3. Selected stratigraphic columnar sections from ten Archean and seven Proterozoic greenstone belts, seven Phanerozoic ophiolite complexes, and the oceanic *in-situ* Izu-Bonin-Mariana sequence. Data from: Isua, Greenland (Furnes et al., 2009); IOG, India (Mukhopadhyay et al., 2012); Barberton, South Africa (de Wit et al., 2011; Furnes et al., 2012b); Whundo, Australia (Smithies et al., 2005); Koolyanobbing, Australia (Angerer et al., 2013); Kustomuksha, Karelia, Russia (Puchtel et al., 1998); Belingwe, South Africa (Hofmann and Kusky, 2004); Taishan, China (Polat et al., 2006); Wawa, Canada (Polat et al., 1998); Yellowknife, Canada (Corcoran et al., 2004); Birimian, West African Craton (Sylvester and Attoh, 1992); Purtuniq, Canada (Scott et al., 1992); Flin Flon, Canada (Lucas et al., 1996); Jormua, Finland (Peltonen et al., 1996); Payson, North America (Dann, 1997); Fawakhir, Egypt (Abd El-Rahman et al., 2009); Tulu Dimtu, Etiopia (Tadesse and Allen, 2005); Leka, Norway (Furnes et al., 1988); Mirdita, Albania (Dilek and Furnes, 2009); Sarmiento and Tortuga, Chile (de Wit and Stern, 1978); Dagzhuka, Tibet (Xia et al., 2003); ESO (East Sulawesi Ophiolite), Indonesia (Kadarusman et al., 2004); Nehbandan, Iran (Saccani et al., 2010); I-B-M (Izu-Bonin-Mariana), southwestern Pacific Ocean (Ishizuka et al., in press); Macquarie Island, southern Pacific Ocean (Goscombe and Everard, 1999).

Please cite this article in press as: Furnes, H., et al., Four billion years of ophiolites reveal secular trends in oceanic crust formation, Geoscience Frontiers (2014), http://dx.doi.org/10.1016/j.gsf.2014.02.002

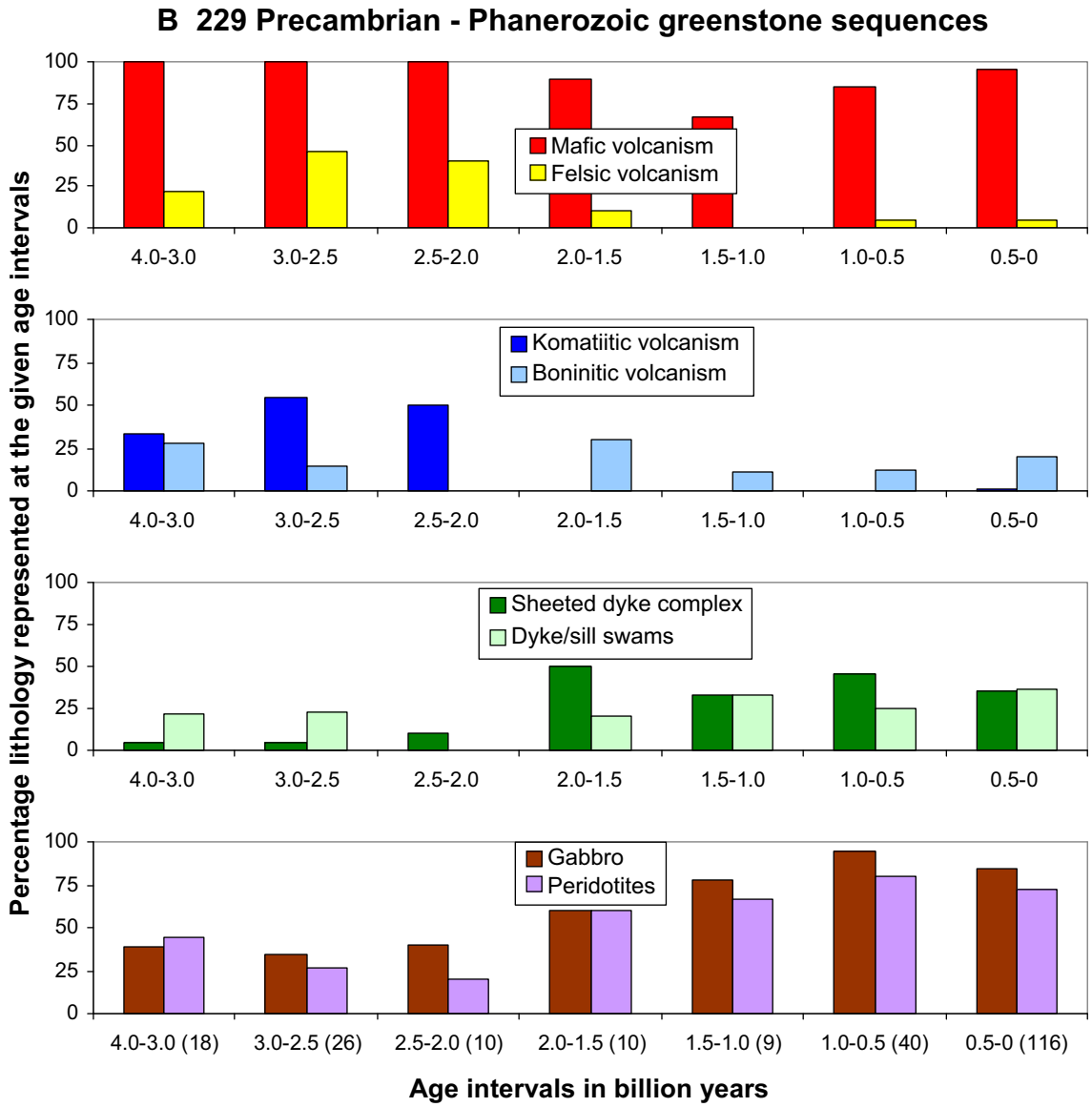

Figure 4. (*continued*).

Hence, the Ti/Yb ratio may function as a proxy for the depth of melting (Fig. 6A).

In Fig. 6B–D, the Phanerozoic, Proterozoic and Archean geochemical data are plotted in the various discrimination diagrams as outlined above. On all diagrams the vast majority of the investigated ophiolites plot in the subalkaline basalt field. The Th/Yb–Nb/Yb diagram reveals that the majority of the data are subduction-related, with the highest proportion in the Archean. In the V–Ti/1000 diagram, the subduction-related data show a large spread through the boninite, island arc tholeiite (IAT) and mid-ocean-ridge basalt (MORB) fields indicating different tectonic settings of subduction-related melt generation above the Benioff Zone. All the geochemical data are approximately equally distributed between the OIB and MORB arrays (i.e., deep and shallow melting regimes, respectively) in the TiO_2/Yb–Nb/Yb diagram.

5. Classification of ophiolites through time

We are aware of the short-comings in providing a waterproof classification of the ophiolites, particularly the oldest, and we are also aware of the many conflicting views regarding many of the Precambrian greenstone sequences, and also some of the Phanerozoic examples. For most of the sequences it is probably difficult, if not impossible, to meet all the criteria 100%. We have used the available geochemical data for greenstone sequences that have been (at least by some authors) considered to represent some sort of oceanic crust, and then applied the geochemical approach to classify them according to the recently introduced ophiolite classification of Dilek and Furnes (2011).

Using the compilation of the geochemical data presented in Fig. 6 and field, regional tectonics, and lithological characters of the ophiolites summarized in Table 1, we provide combined analyses of the Phanerozoic and Precambrian ophiolite complexes in which we first divide the data into subduction-related and subduction-unrelated sequences (Table 2 and Fig. 7). This analysis shows that 75% and 85% of the Phanerozoic and Precambrian greenstone sequences, respectively, are subduction-related. The subduction-related ophiolites are further divided into SSZ-backarc, SSZ-backarc to forearc, SSZ-forearc, and SSZ to Volcanic Arc, and the estimated percentage of each type is shown in Fig. 7. The SSZ-backarc type, represented by a predominance of MORB-type greenstones, is by far the dominant Phanerozoic ophiolites (56%), as are also for the

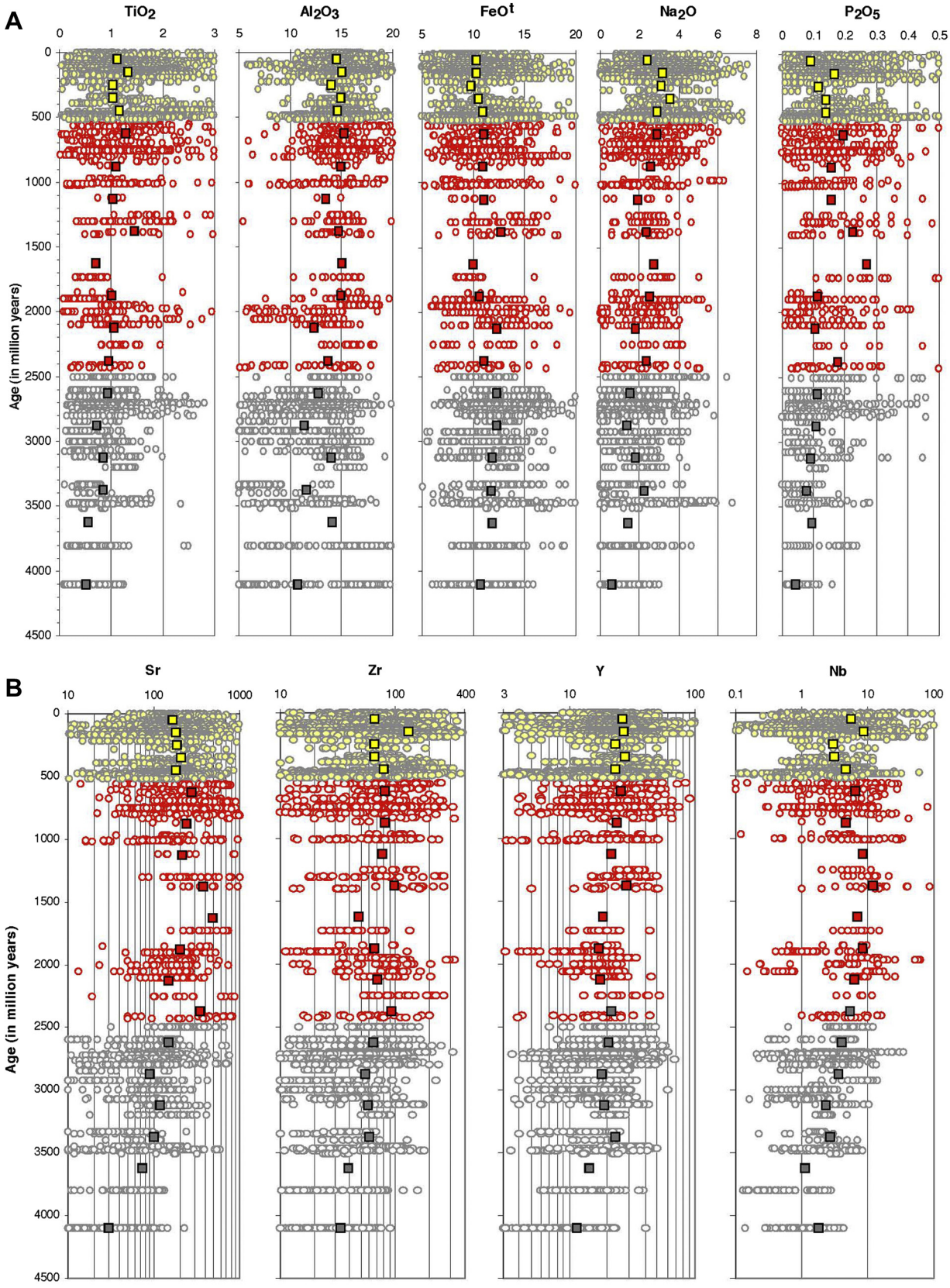

Figure 5. All geochemical data plotted against age. Yellow, red, and grey circles represent Phanerozoic, Proterozoic and Archean greenstones, respectively. References to the Phanerozoic greenstones are listed in Table 1 of this paper, whereas those for Precambrian age are shown in Table 1 of Furnes et al. (2013). (A) Major elements, (B) incompatible trace elements, and (C) compatible trace elements.

Please cite this article in press as: Furnes, H., et al., Four billion years of ophiolites reveal secular trends in oceanic crust formation, Geoscience Frontiers (2014), http://dx.doi.org/10.1016/j.gsf.2014.02.002

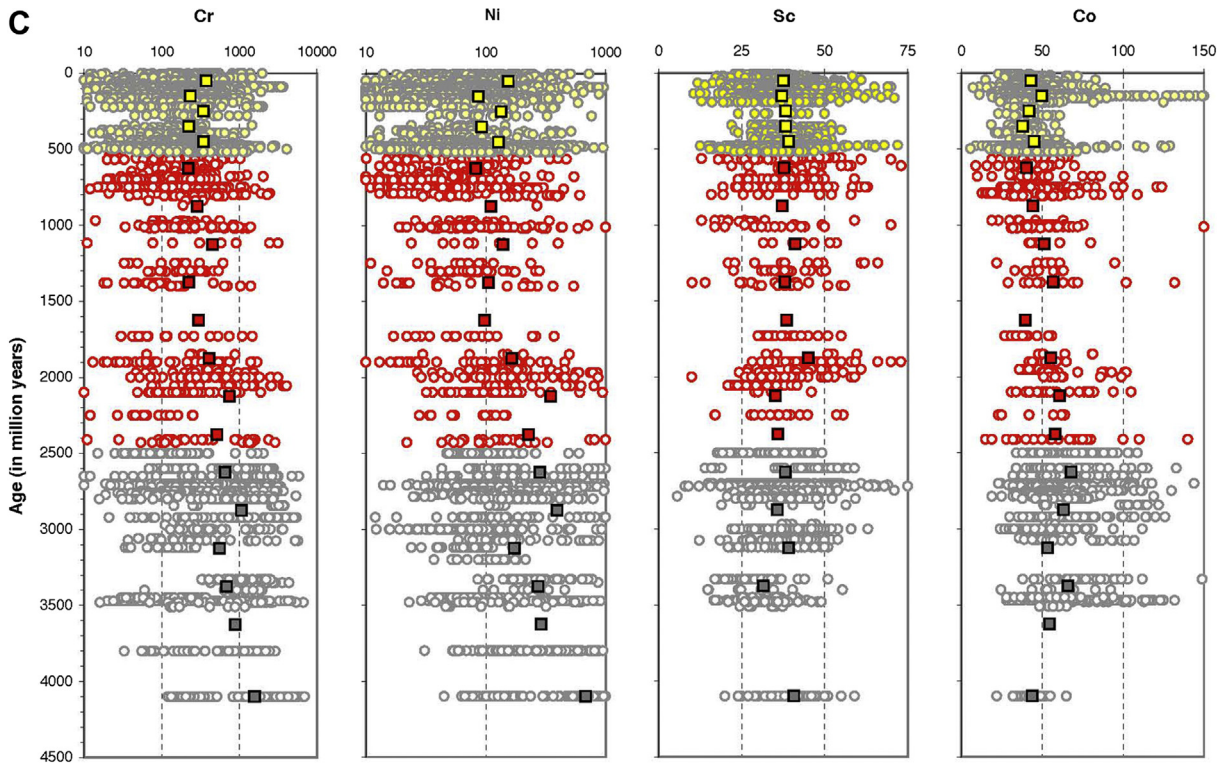

Figure 5. (*continued*).

Precambrian greenstones (45%). The SSZ-backarc to forearc, represented by the sequences that show approximately equal proportions of MORB, IAT and Boninites (Table 2), are the second most abundant group of the Phanerozoic ophiolites (27%), and are also well represented (22%) with the Precambrian greenstone sequences. The SSZ-forarc ophiolite type, characterized by the sequences consisting of boninites, is of minor abundance among the Phanereozoic and Precambrian greenstones. The ophiolites classified as SSZ to Volcanic Arc type have a dominant continental arc signature in the Th/Yb–Nb/Yb diagram (see Fig. 6), but variable character in the V–Ti discrimination diagram (Table 2). This type is rarely represented among the Phanerozoic ophiolites, but defines a significant proportion (26%) among the Precambrian examples (Fig. 7).

The subduction-unrelated ophiolites, classified as Rift/Continental Margin-, MORB- and Plume-types, are much less abundant than the subduction-related types both in the Phanerozoic and in the Precambrian. We consider that the stages from rift-drift to seafloor spreading (Dilek and Rowland, 1993; Dilek et al., 2005) represent a continuous development from the incipient dyke and gabbro intrusions in continental crust through super-extension into fully developed oceanic crust that in turn also may show differences depending on the spreading rates. Here, we have combined the two types into one single class. Amongst the Phanerozoic ophiolites the MORB type is the dominant (74%), whereas for the Precambrian greenstones there is an equal distribution of the three types (Fig. 7).

6. Time-related distribution of ophiolite types

Fig. 8 shows the relationship between the types of the investigated ophiolitic greenstone sequences and time. The undifferentiated subduction-related and subduction-unrelated ophiolites are shown in Fig. 8A. This compilation indicates that the highest proportion of subduction-unrelated greenstone sequences are represented during the time intervals 0–50, 50–100, 150–200, and 2000–2250 million years. For the remaining time intervals, subduction-unrelated sequences are sparsely represented, or absent. Among the subduction-related ophiolites (Fig. 8B), the backarc type, i.e. those with a high proportion of MORB component, are the dominant for most of the time intervals, backarc to forearc types pre-dominate among those older than 2750 Ma. This observation suggests a stronger subduction influence in the magmatic evolution of the Archean greenstone sequences. In Fig. 8C we show the subdivided subduction-unrelated ophiolites. This compilation suggests that the MORB type is the pre-dominant among the Phanerozoic to late Proterozoic sequences, whereas Rift/Continental Margin- and Plume-types are the dominant ones in the Archean.

7. Degree of subduction-influence upon the ophiolites

7.1. Variations within the Phanerozoic orogens

The extent of subduction-influence detected in the greenstones of the investigated ophiolites varies significantly along and across the orogenic belts. This is demonstrated in Fig. 9, where each point represents the average subduction-influence of individual ophiolite occurrences, taken from Table 2. In this compilation, for example, the majority of all of the greenstone samples of the Appalachian ophiolites are subduction-influenced, whereas those of the Caledonian orogen show a much larger range, though none appears to be subduction-unrelated. The ophiolites of the Alpine-Himalayan orogen, the Cordilleran and the western Pacific orogens, the Uralian/Asian and the Indonesian-Myanmar orogens demonstrate a complete variation from zero to 100% subduction-influence. Those of the Hercynian and Andean orogenic belts show less variation from subduction-unrelated to those which are only sparsely subduction-related. Surprisingly, the four Andean ophiolite examples on which we could estimate the subduction-influence (Table 2) gave the average lowest value (Fig. 9).

Please cite this article in press as: Furnes, H., et al., Four billion years of ophiolites reveal secular trends in oceanic crust formation, Geoscience Frontiers (2014), http://dx.doi.org/10.1016/j.gsf.2014.02.002

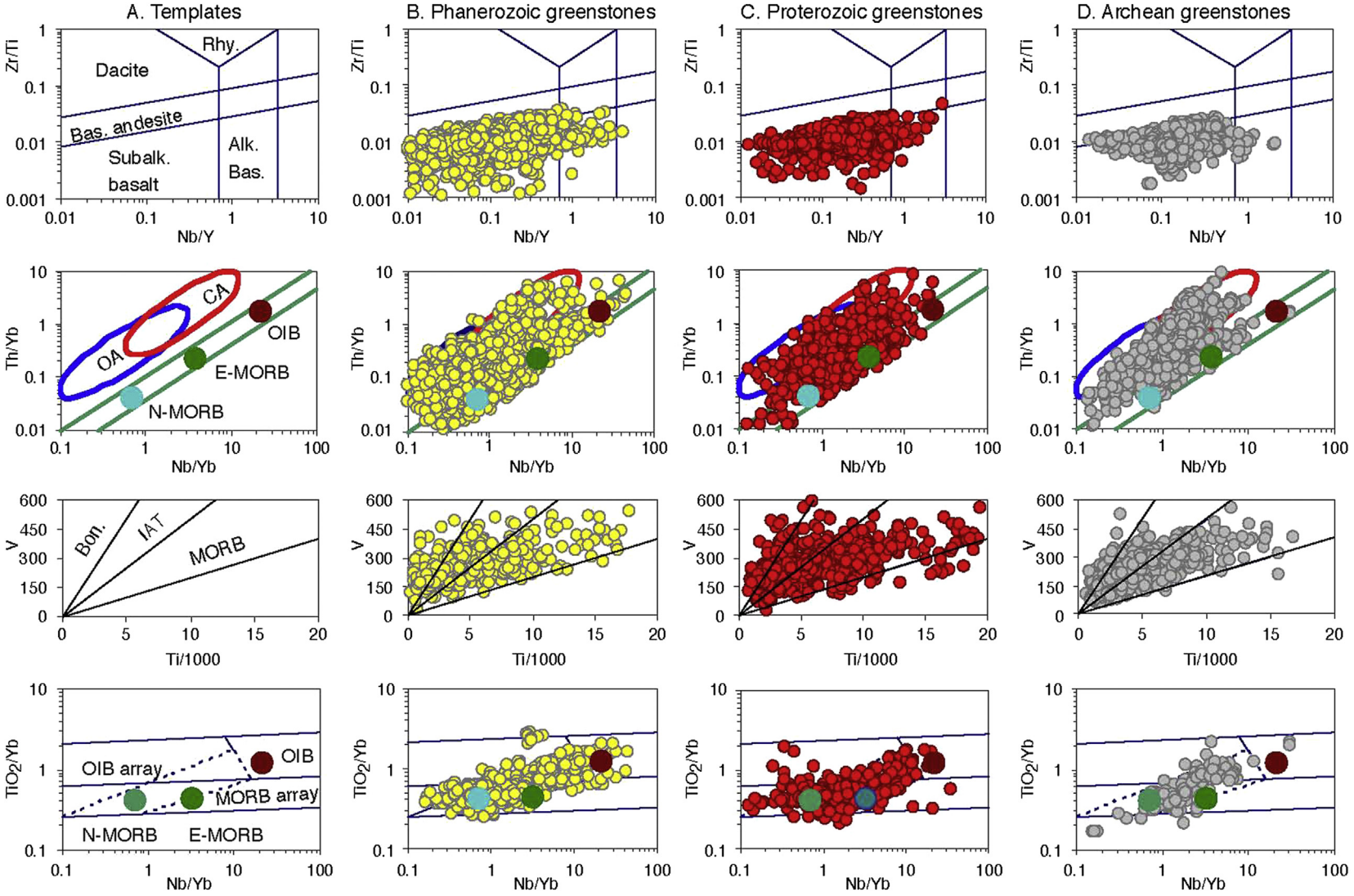

Figure 6. Zr/Ti – Nb/Y, Th/Yb – Nb/Yb, V – Ti/1000, and TiO_2/Yb – Nb/Yb diagrams for rock classification and tectonic setting (after Shervais, 1982; Pearce, 2008, in press). (A) Templates for the above-mentioned diagrams; (B) plots of all Phanerozoic greenstone analyses used in this paper; (C) and (D) plots of Proterozoic and Archean greenstone analyses (from Furnes et al., 2013).

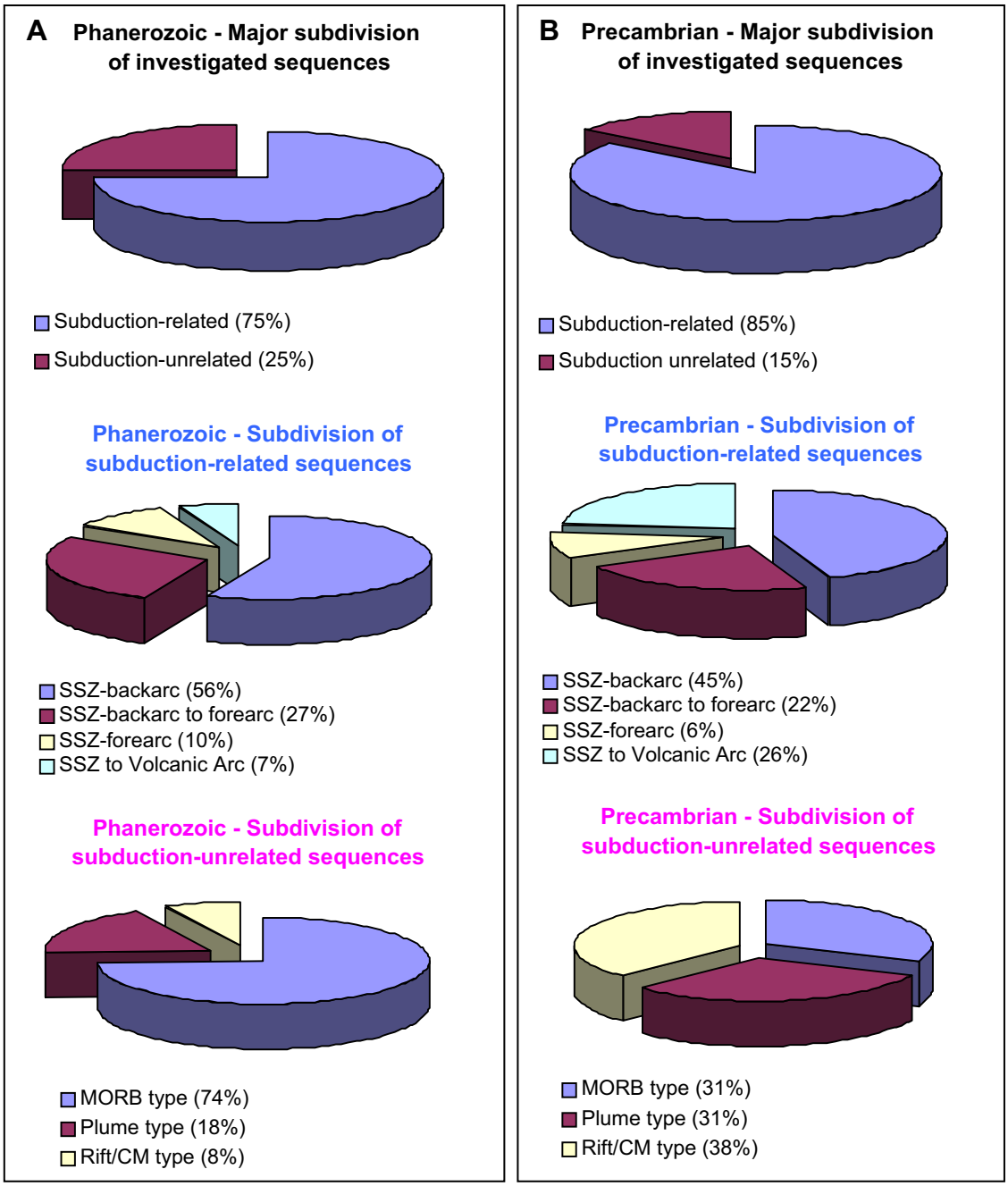

Figure 7. Pie-diagram showing the proportion of subduction-related and subduction-unrelated greenstone sequences, subdivisions of the subduction-related, and the subduction-unrelated investigated greenstone sequences. (A) Compilation of Phanerozoic greenstone sequences based on the information provided by the lithological (Table 1) and the geochemical data summarized in Table 2. (B) Precambrian greenstone sequences (modified from Furnes et al., 2013).

7.2. Subduction-signals through time

Fig. 10 shows the average subduction-influence against time for the greenstones from each of the investigated ophiolite complexes. For Phanerozoic ophiolites (Table 2, Fig. 10A) the highest proportion of subduction-unrelated ophiolites are among those younger than 200 Ma. When all the greenstone complexes, i.e. the Phanerozoic data from this work (Table 2), and the Proterozoic and Archean data from Furnes et al. (2013) are plotted against time, a pattern of increasing subduction-influence with increasing age appears (Fig. 10B). The reason for this variation is not immediately obvious, but one suggestion may be that this is either because less total continental margins may have been present in the early Archean, although this may be counter-intuitive if we think that the average size of tectonic plates was smaller then (e.g., Abbott and Hoffman, 1984; Pollack, 1997; de Wit, 1998), or that continental margin ophiolites are more prone to recycling/subduction than other plate boundary ophiolites.

Archean igneous rocks commonly show arc signature by the enrichment of LILE (large ion lithophile elements) over HFSE (high field strength elements), and have been interpreted as subduction-related (e.g., van Hunen and Moyan, 2012). The invariably common arc signature in basaltic rocks can be explained by (1) melt production from depleted mantle in a subduction setting; or (2) contamination of mantle-derived magmas (without having been subduction-influenced) by continental crust. It is conceivable that

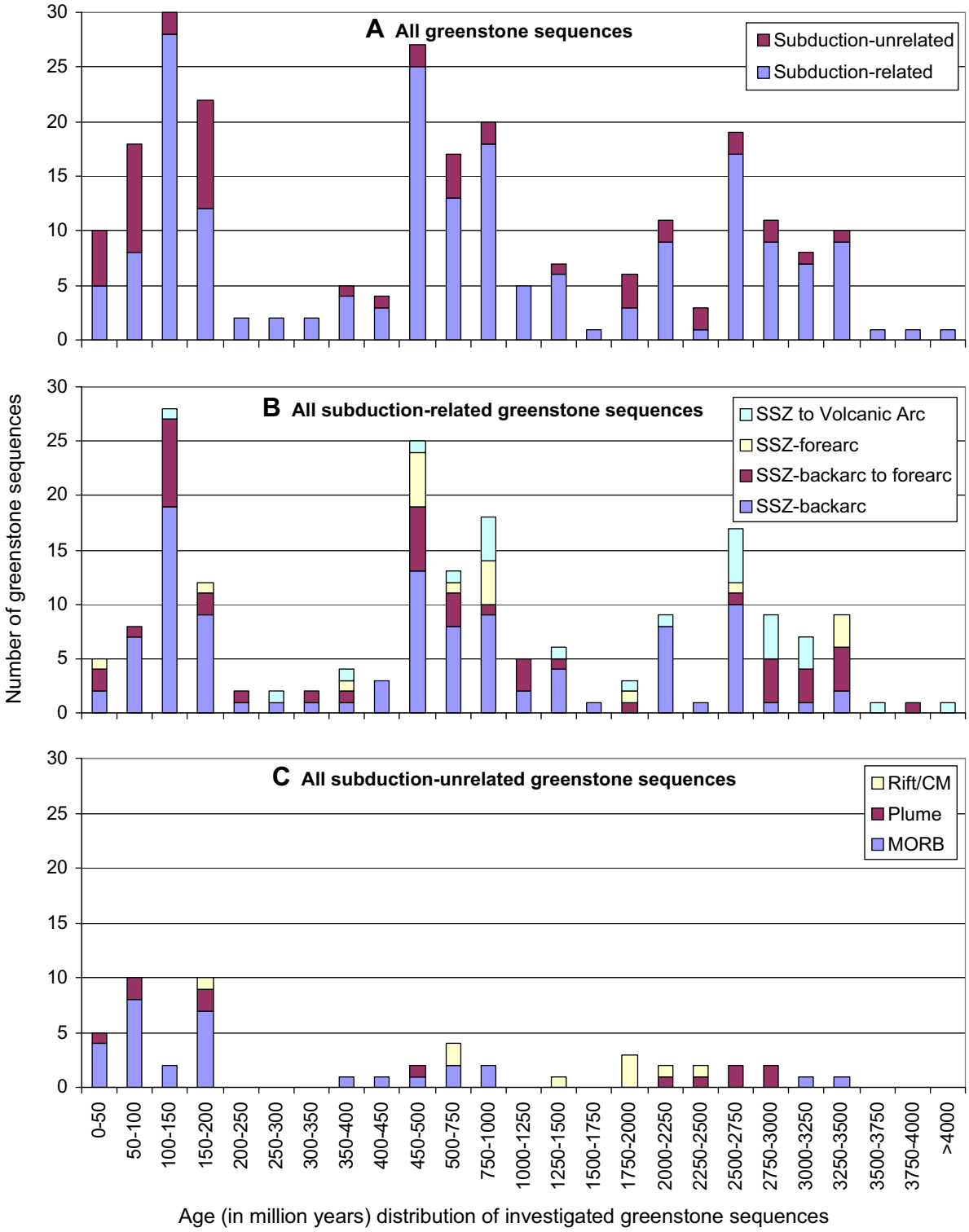

Figure 8. Histograms showing the age-related distinction of greenstone sequences divided into (A) subduction-related and subduction-unrelated types; (B) the division of subduction-related into four different subtypes; and (C) the division of subduction-unrelated into three different subtypes. The data on the Phanerozoic greenstones are all from Table 2 of this account, whereas all the Precambrian data are from Table 2 in Furnes et al. (2013).

high-MgO magma with high liquidus temperature on its passage through continental crust can partially melt the host, and may thus acquire an arc-like signature through contamination.

This is a possible scenario that has been discussed widely in the literature (e.g., Redman and Keays, 1985; Arndt and Jenner, 1986; Barley, 1986; Puchtel et al., 1997; Polat et al., 2006). In the Archean komatiites of the Taishan greenstone belt of the north China craton, for example, Polat et al. (2006) found strong linear relationships between negative Nb anomalies (represented as Nb/Nb* ratios, calculated from N-MORB normalised values, and $Nb^* = (La + Th)/2$) and the major oxides TiO_2, MgO and Al_2O_3, a feature regarded as diagnostic for crustal contamination. We have

Table 2
Th/Yb, V-Ti, and Ti/Yb geochemical proxies and proposed classification of the selected ophiolite sequences, according to the ophiolite classification of Dilek and Furnes (2011).

Ophiolitic magmatic complex – no. of samples	Orogenic belt	Age (Ma)	% Subd. infl.	Th/Yb-proxy for subduction (%)					V vs. Ti-proxy for SSZ melting (%)			Ti/Yb-proxy for plume melting (%)					Suggested ophiolite type and tectonic environment on the basis of the various proxies shown.
				None mantle array	Various subduction signal							MORB shallow melting			OIB deep melting		
					Weak	Oceanic arc (oa)	Cont. arc (ca)	Joint Oa-ca	Bon	IAT	MORB	N	T	E	Thol.	Alk.	*In italics: Suggested from literature*
	Caledonian																
Lyngen (Ly) – 29	Norway	c. 480	55	45	17		31	7	19	25	56			92	8		SSZ-backarc to forearc to VA + major MORB
Leka (Lk) – 16	Norway	497	81	19	12	69			8	23	69	67			33		SSZ-backarc to forearc + minor MORB & OIB
Sulitjelma (Sj) – 7	Norway	437	14	86	14						100						SSZ-backarc + major MORB
Trondheim area (Ta) – 26	Norway	493–481	42	58	12	23		7		11	89	80	20				SSZ-backarc + major MORB
Solund-Stavfjord (SS) – 27	Norway	442	30	70	30			6			100	78	11		11		SSZ-backarc + major MORB
Gulfjellet (Gf) – 15	Norway	498	73	27	20	47						100					SSZ-backarc + moderate MORB
Karmøy (Kø) – 10	Norway	497–470	70	30		20	10	40	40	20	40						SSZ-backarc to forearc
Ballantrae (Bt) – 10	Scotland	470	90	10		90			75	25							SSZ-forearc
Tyrone Ign. Compl. (Tr) – 76	Ireland	490–475	67	33	20	26	16	5	6	65	29				100		SSZ-backarc to forearc + moderate OIB
	Appalachian																
Birchy Complex (BiC)	Nfld, Canada	557															*Rift-related*
Annieopsquotch (Ao) – 46	Nfld, Canada	480	80	20	72	10				15	858	100					SSZ-backarc + moderate MORB
Bay of Islands (BI) – 7	Nfld, Canada	485	86	14	29	29		28	25		75		100				SSZ-backarc to forearc + minor MORB
Betts Cove (BC) – 23	Nfld, Canada	488	91	9	13	56		22	78	12		100					SSZ-forearc + minor MORB
Lac Brompton (LB) – 7	Quebec, Canada	480	100		29	29	13	29	100								SSZ-forearc
Thetford Mines (TM) – 19	Quebec, Canada	479	100		11	32		57	75	17	8						SSZ-backarc to forearc
	Uralian																
Nurali (Nr)	Russia	468–483															*Intraoceanic arc/continental margin*
Magnitogorsk (Mg) – 13	Russia	c. 400–385	100		23	46		31	7	73	20						SSZ-backarc to forearc
Kempersay (Kp)	Kazakhstan	470–485															*Marginal basin, normal oceanic crust*
	Central Asian																
Bayankhongor (Bkh) – 5	Mongolia	210–298	0	100										100			MORB-type
Xiaohuangshan (Xh) – 9	China	340	100		33		11	56		100							SSZ-backarc to forearc
Hegenshan (Hs)	China	400–350															*Island arc-marginal basin*
	Qingling-Qilian-Kunlun																
Dongcaohe (Dc) – 3	China	497	33	67	33							100					SSZ-backarc + major MORB
Yushigou (Yg)	China	550															*Mature backarc basin*
Jiugequan (Jq)	China	490															*Backarc basin*
Kudi (Ki) – 15	China	c. 458	100		7	20		73									SSZ-backarc
Buqingshan (Bq) – 14	China	c. 470	43	57	43							100					SSZ-backarc + major MORB

	Bangong-Nujiang Suture																
Ailaoshan (As) – 4	China	c. 387–374	0	100								100					MORB-type
Jinshajiang (Jh) – 5	China	346–341	40	60	40						100			100			SSZ-backarc/MORB-type
Changning-Menglian (C-M) – 10	China	270–264	80	20	50	20		10		25	75	50		50			SSZ-backarc + moderate MORB
Qiangtang (Qt) – 19	Tibet	c. 355	63	37	63						100	86	14				SSZ-backarc/MORB-type
	Hercynian																
Sleza (Sl) – 8	Poland	c. 400	0	100								100					MORB-type
Kaczawa Mts. (Kz) – 7	Poland	c. 420	43	57		14		29				50		50			SSZ-backarc + major MORB
IOMZOS (IZ) – 36	Spain	c. 480	8	92	8							13	33	15	39		MORB-type + Plume (?)
	Alpine-Himalayan																
Betic ophiolitic Unit (BU) – 8	SE Spain	185	0	100													MORB-type
Chenaillet (Cn) – 59	France-Italy	165–153	0	100								100					MORB-type
Zermatt-Saas (ZS)	Switerland-Italy	164															*Mid-ocean ridge*
External Ligurides (EL) – 10	North Italy	c. 170–180	10	90				10			100		100				MORB-type
Internal Ligurides (IL) – 22	North Italy	c. 170	0	100								100					MORB-type
Calabrian (Cb) – 2	South Italy	150–140	0	100													MORB-type/*rift*
Corsica (Cr) – 25	Corsica	c. 160	0	100								36	32		32		MORB-type + Plume (?)
Mirdita (Md) – 30	Albania	165	87	13	30	57			12	60	28	100					SSZ-backarc to forearc + minor MORB
Pindos (Pd) – 5	Greece	165	80	20	20	20	40		66	17	17	100					SSZ-backarc to forearc to VA + mod. MORB
Troodos (Td) – 8	Cyprus	92	100		25	75											SSZ-backarc
Kizildag (Kd) – 34	Turkey	92	85	15	64	18		3	3	90	7	100					SSZ-backarc to forearc + minor MORB
Oman (Om) – 56	Oman	96	50	50	30	20			57	14	29	79		17		4	SSZ-backarc to forearc + major MORB
Masirah (Ms) – 7	Oman	140	0	100													MORB-type
Sevan (Sv) – 8	Armenia	165	100		25	63		12		25	75						SSZ-backarc to forearc
Khoy (Kh) – 57	Iran	c. 140–130	36	64	21			15		15	85		98		2		SSZ-backarc + major MORB
Band-e-Zeyarat/ Dar Anar (BZ) – 17	Iran	142–141	47	53	29	6		12			100			100			SSZ-backarc + major MORB
Dehshir (Di) – 8	Iran	c. 100	88	12	13	50		25	28	58	14	100					SSZ-backarc to forearc + minor MORB
Baft-Nain (B-N) – 21	Iran	c. 100	86	14	19	62	5		5	81	14	100					SSZ-backarc to forearc + minor MORB
Sabzevar (Sz) – 13	Iran	c. 100–66	77	23	54	23					100						SSZ-backarc
Neyriz (Ny) – 8	Iran	92	25	75	25					33	67	80		20			SSZ-backarc + major MORB
Nehbandan (Nb) – 11	Iran	c. 100–60	18	82	18						100	44		56			SSZ-backarc + moderate MORB
Muslim Bagh (MB) – 13	Pakistan	157–118	77	23	39	31		7	10	50	40	100					SSZ-backarc + moderate MORB
Waziristan (Ws)	Pakistan	87–65 c. 100															*Island arc/mid-ocean ridge*
Yarlung-Zangbo																	
Dras (Ds) – 12	India	c. 135	92	8	16	8	43	25									SSZ/VA
Spontang (St) & Nidar (Nr) – 14	India	130–110	28	72	21			7		100		100					SSZ-backarc + major MORB
Xiugugabu (Xg) – 14	Tibet	c. 125	100		28	72											SSZ-backarc

(*continued on next page*)

Table 2 (*continued*)

Ophiolitic magmatic complex – no. of samples	Orogenic belt	Age (Ma)	% Subd. infl.	Th/Yb-proxy for subduction (%)					V vs. Ti-proxy for SSZ melting (%)			Ti/Yb-proxy for plume melting (%)					Suggested ophiolite type and tectonic environment on the basis of the various proxies shown.
				None mantle array	Various subduction signal							MORB shallow melting			OIB deep melting		
					Weak	Oceanic arc (oa)	Cont. arc (ca)	Joint Oa-ca	Bon	IAT	MORB	N	T	E	Thol.	Alk.	*In italics: Suggested from literature*
Saga (Sg) – 13	Tibet	155–130	23	77	15			8			100	64		18		18	SSZ-backarc + major MORB & mod. OIB
Sangsang (Ss) – 10	Tibet	155–130	30	70	20	10					100	29			71		SSZ-backarc + mod. MORB & major OIB
Jiding (Jd) & Beimarang (Br) & Qunrang (Qr) – 8	Tibet	125	62	38	50	12				14	86	100					SSZ-backarc + major MORB
Beinang (Ba) & Dazhugu (Dh) – 8	Tibet	125	75	25	50	25				17	83	100					SSZ-backarc + moderate MORB
Jinlu (Jl) & Loubusa (Lb) & Zedong (Zd) – 7	Tibet	125	43	57	14			29		100		100					SSZ-backarc to forearc + major MORB
Xigaze (Xz) – 16	Tibet	125–110	69	31	69						100	100					SSZ-backarc + moderate MORB
Curacao (Cc) – 21	Caribbean	90	0	100							100			100			MORB-type
Jamaica – 17	Caribbean	90	6	94	6						100	100					MORB-type
Nicoya-Herradura (N-H) – 26	Caribbean	95–86	0	100									96		4		MORB-type
Central Hispaniola (CH1) – 32	Caribbean	115	41	59	22	6		13	38	31	31	26	47		11	16	SSZ-backarc + major MORB & mod. OIB
Central Hispaniola (CH2) – 8	Caribbean	79–68	0	100											100		Plume-type
ODP, Leg 165, site 1001 – 14	Caribbean	c. 81	0	100								100					MORB-type
	Andean																
Western Colombia (WC) – 13	Colombia	100–73	8	92	8					100			84		8	8	MORB-type
La Tetilla (LT)	Colombia	c. 125–120															*Suprasubduction zone*
Gorgona Isl. (Gg)	Colombia	c. 90–76															*Oceanic plateau*
Raspas (Rp) – 13	Ecuador	c. 140	15	85	15						100	100					SSZ-backarc + major MORB
Sierra del Tigre (ST) – 13	Argentina	c. 150	0	100											100		Plume/*rifted margin*
Chuscho Fm (ChF) – 9	Argentina	c. 450	0	100											100		Plume-type
Sarmiento (Sm)	Chile	150															*Marginal basin*
Tortuga (To)	Chile	150															*Marginal basin*
	Cordilleran and Western Pacific																
Llanada (Ld) – 7	California, USA	c. 160	57	43	57					75	25	67	33				SSZ-backarc + major MORB
Black Mountain (BM) – 13	California, USA	c. 160	31	69	31						100	100					SSZ-backarc + major MORB
Ingalls (Ig) – 8	Washington, USA	161	25	75		25					100	100					SSZ-backarc + major MORB
Elder Creek (EC)	California, USA	c. 170															*Suprasubduction zone*
Josephine (Jph) – 10	Oregon, USA	164–162	40	60	40						100		67		33		SSZ-backarc + major MORB & OIB
Angayucham (Ay) – 34	Alaska, USA	c. 210–170	6	94	6								59	10	31		Plume-type
Brooks Range (BR)	Alaska, USA	c. 165															*Interarc basin*
Resurrection Peninsula (RP) –	Alaska, USA	57															*MORB-type*
Aluchin (Ac) – 10	NE Russia	226	60	40	10	40		10		60	40	100					SSZ-backarc to forearc + major MORB

East Kamchatka (EK) – 21	NE Russia	c. 110–60	33	67	14	19			14	58	28	86		14			SSZ-backarc to forearc + major MORB
Mineoka (Mo) – 57	Japan	66	6	94	4	2						83			17		SSZ-backarc + major MORB & minor OIB
Mino-Tamba (M-T) – 20	Japan	200–185	10	90	10						100				69	33	Plume-type
Yakuno (Yk) – 5	Japan	280	100				40	60		40	60						VA-type
Zambales (Zb) – 11	Philippines	44–48	55	45	36	19						100					SSZ-backarc + major MORB
Calaguas (Cg) – 7	Philippines	c. 100	0	100								100					MORB-type
Bohol (Bh) – 12	Philippines	c. 100	58	42	8	33		17		43	57	60			40		SSZ-backarc + major MORB & OIB
Darvel Bay (DB)	Malaysia	c. 140															*Suprasubduction zone*
Cyclops (Cy) – 8	New Guinea Isl.	43–20	25	75	13			12	50	50		100					SSZ-backarc to forearc + major MORB
Milne Terrain (MT) – 18	Papua New Guinea	55	6	94		6				100		6	94				MORB-type
Koh (K)	New Caledonia	220															*Backarc basin*
Northland (Nl) – 9	New Zealand	32–26	78	22	78						100	100					SSZ-backarc + moderate MORB
Tangihua (Th) – 10	New Zealand	ca.100	40	60		20		20		50	50	100					SSZ-backarc to forearc + major MORB
	Indonesian-Myanmar																
Manipur (M) – 9	NE India	c. 70	0	100									33		67		MORB-type
Andaman (A)	Andaman isl.	95															*Mid-ocean ridge*
Meratus (Mt) – 10	SE Borneo	c. 120	60	40	10	10	10	30		50	50	50		50			SSZ-backarc to forearc + major MORB
Timor-Tanimbar (T-T)	Timor	3–6															*Forearc*
East Sulawesi (ES) – 10	Sulawesi	80–120 & 10–20	80	20		60		20				100					SSZ-backarc to forearc + moderate MORB
Seram-Ambon (S-A) – 13	Central Indonesia	c. 20–10	100			92	8			71	29						SSZ-backarc to forearc
	Tasmanide																
Camilaroi Terrane (CT)	SE Australia	c. 390–360															*Intraoceanic island arc*
Jamieson-Licola (J-L) – 7	SE Australia	c. 500	29	71			14	15	100				100				SSZ-forearc + major MORB
	Unrelated to orogenic belts																
Tihama Asir (TA) – 19	Red Sea, Saudi Arabia	23–19	0	100								6		26	68		MORB-type/Plume
Macquarie (Mq) – 12	Macquarie Island	10	0	100										100			MORB-type
Taitao (Tt) – 5	Chile	6	0	100										100			MORB-type
Iceland – 32	Mid-Atlantic Ridge	<1	0	100									68		32		MORB-type/Plume

Abbreviations: Subd. infl. = subduction influence; oc = oceanic arc; ca = continental arc; Bon = boninite; IAT = island arc tholeiite; MORB = mid-ocean-ridge basalt; OIB = ocean island basalt; N = normal; T = transitional; E = enriched; Thol = tholeiitic; Alk = alkaline.

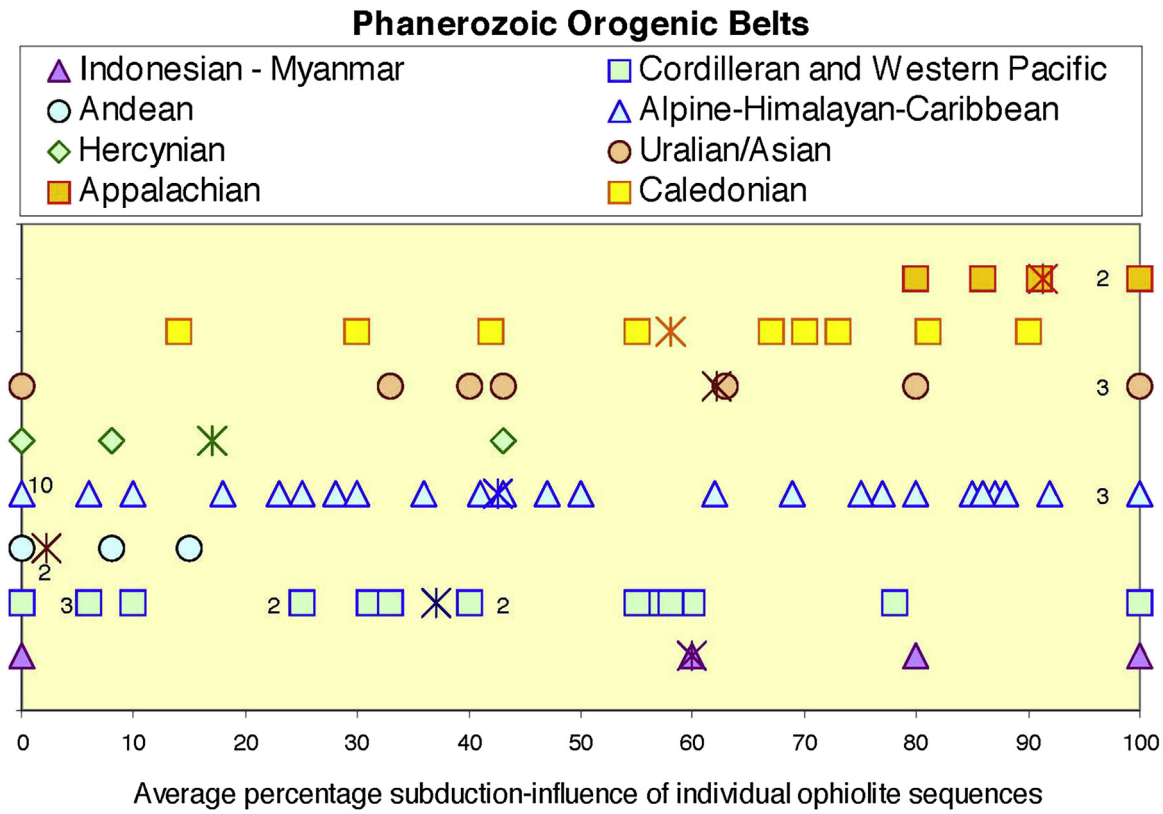

Figure 9. Average percentage subduction-influence upon the greenstones (taken from Table 2) of individual ophiolite sequences from the different orogenic belts shown in Fig. 1. The crosses show the average value for each of the orogenic belts. A digit adjacent to a symbol shows the number of ophiolites with the same average percentage subduction influence.

tested these relationships for each of the Phanerozoic, Proterozoic and Archean sequences presented in this work, and have calculated the least squares regression (R^2) values, in which $R^2 = 1$ represent perfect correlation and $R^2 = 0$ shows no correlation. The relationship between Nb/Nb* versus TiO_2, Al_2O_3 and MgO show poor correlation, i.e. ca. 90% of the sequences define $R^2 << 0.5$. This observation suggests that the vast majority of the examined sequences were unaffected by crustal contamination, and that the basalts with "subduction-signal" indeed represent melts from recycled lithosphere and metasomatically-influenced mantle segments above subduction zones.

8. Early onset of subduction processes

Processes that sustain plate tectonics include seafloor spreading to generate new oceanic crust and OPS (ocean plate stratigraphy), and subduction as its dominant driver that also recycles lithosphere back to the mantle. But, the search for compelling geological evidence documenting the initiation of modern plate tectonics is a challenging task, and the timing for the onset of plate tectonics ranges over more than 3 billion years, from as far back as ca. 3 to 3.2 Ga (Van Kranendonk, 2007, 2011; Wyman et al., 2008; Shirey and Richardson, 2011), to 3.6 Ga (Nutman et al., 2007), 3.8 Ga (Furnes et al., 2007; Dilek and Polat, 2008; Maruyama and Komiya, 2011), 4.0 Ga (de Wit, 1998; Friend and Nutman, 2010), 4.2 Ga (Cavosie et al., 2007), and even 4.4 Ga (Harrison et al., 2008; Maruyama et al., 2013), to as late as 1.0–0.5 Ga (e.g., Bickle et al., 1994; Hamilton, 1998, 2007, 2011; Stern, 2005, 2008; Maurice et al., 2009).

The presence or absence of ophiolites, arc-backarc sequences, accretionary prisms and ocean plate stratigraphy (OPS), blueschists and ultra high-pressure metamorphic rocks in the rock record of deep time in earth history have been thoroughly discussed in the recent literature (e.g., Condie and Kröner, 2008). Here, we focus specifically on the lithological character of some of the early Archean greenstone complexes, and the geochemical fingerprints of their greenstones. Important in this context is the "lithological character" of the oldest greenstone belt, containing all the components of a subduction-related ophiolite, including the presence of a sheeted dyke complex (e.g. the 3.8 billion-years old Isua sequence in SW Greenland; Furnes et al., 2007, 2009; Fig. 3). The preservation of an accretionary prism complex in the Isua greenstone belt (Komiya et al., 1999) provides an independent line of evidence for subduction and obduction tectonics in the evolution of this early Archean greenstone belt (e.g., de Wit and Furnes, 2013).

In a previous compilation of Cenozoic to early Archean relics of oceanic crust and OPS, Kusky et al. (2013) have found consistent similarities in all complexes with respect to structural style, major rock components, sequence of accretion and trace element geochemistry, and have concluded that there is a 3.8 billion years history of sea-floor spreading, subduction and accretion. Thus, they were able to trace plate tectonic processes back to the early Archean. This extrapoation is consistent with the geochemical compilation shown in Figs. 6D, 8B and 10B. Particularly, the greenstones of the three oldest complexes (see Table 1 in Furnes et al., 2013), i.e. the 3.51 Ga Southern Iron Ore Group (Singhbhum Craton, NE India), the 3.8 Ga Isua supracrustal complex (SW Greenland), and the 3.8–4.3 (?) Ga Nuvvuagittuq greenstone complex (NE Canada), are all strongly subduction-influenced (Figs. 8B and 10B), indicating that subduction-like processes were operative in the Archean. Thus, if the Nuvvuagittuq greenstone complex truly is of Hadean age (>4 Ga), as proposed by O'Neil et al.

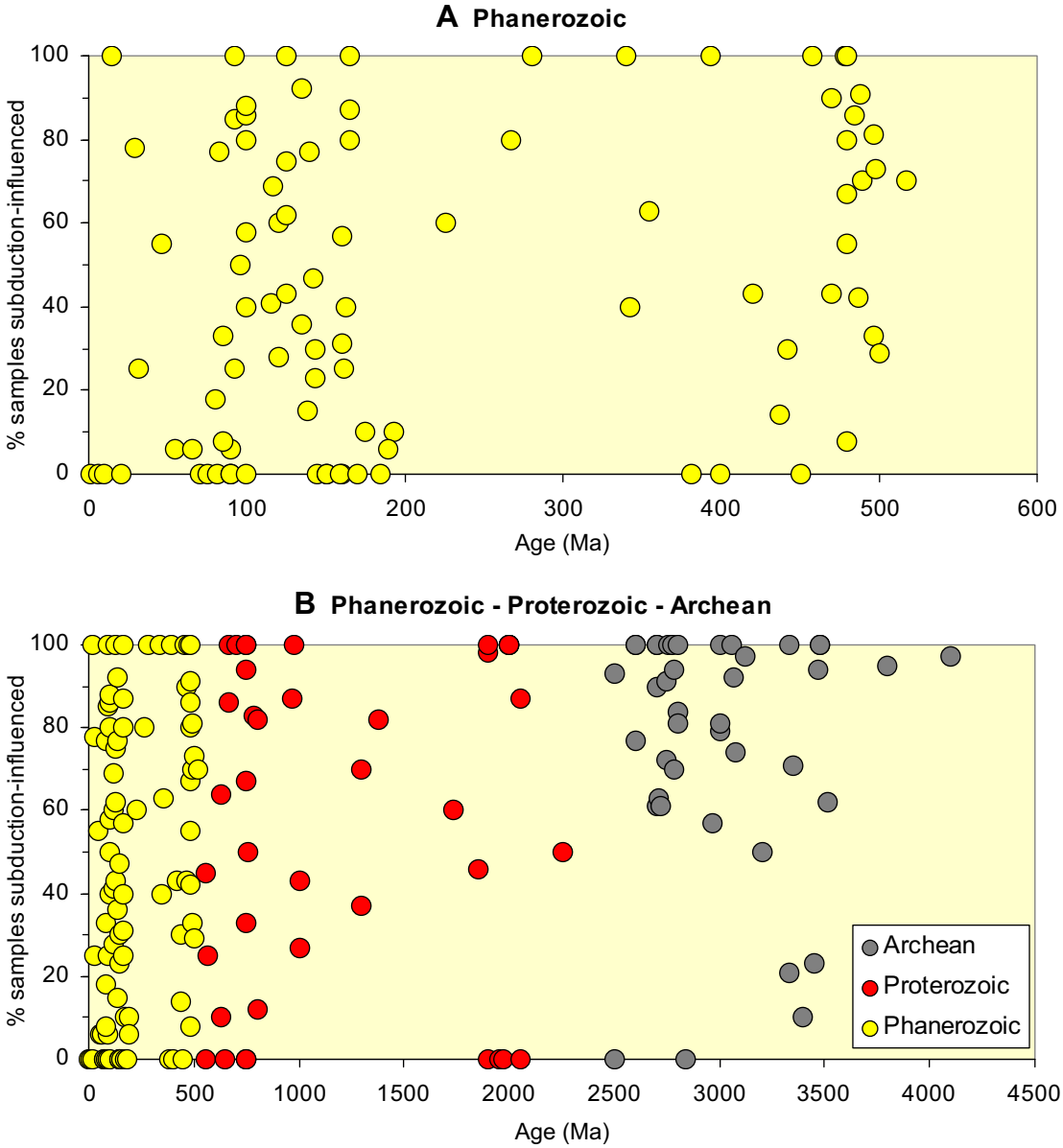

Figure 10. Percentage samples within each greenstone complex that is subduction-influenced. (A) Phanerozoic ophiolites (data from Table 2), (B) Phanerozoic and Precambrian (Proterozoic–Archean) ophiolites. The Precambrian data are taken from Table 2 of Furnes et al. (2013).

(2008, 2011) and Adam et al. (2012), but questioned by Cates et al. (2013), it is plausible that subduction-like processes were operative already by the end of the Hadean Aeon.

9. Greenstone data synthesis

One of the most striking features of the Archean ophiolites is the near-absence of sheeted dyke complexes, as well as the scarcity of gabbro in ophiolites older that ca. 1.8–2.0 Ga. Absence of a sheeted dyke complex is frequently used to dismiss a greenstone sequence as an ophiolite (e.g., Stern, 2005). However, a sheeted dyke complex is not a necessary component of a greenstone sequence for being classified as an ophiolite (Robinson et al., 2008). Among the Phanerozoic SSZ-type ophiolites (Table 1), the occurrence of a sheeted dyke complex has only been reported for 47% of them.

The Archean greenstone sequences (Fig. 3) generally define a layered structure of thick basaltic (and occasionally komatiitic) lava accumulation (commonly with sills, as for example in the Barberton greenstones). Sheeted dyke complexes are more abundant in 2.0 Ga and younger ophiolites, although they do occur in the 3.8 Ga Isua and 2.7 Ga Yellowknife (Fig. 3). Thus, the physical conditions during the Archean apparently were less favourable to meet those that produced sheeted dykes complexes, as compared to Proterozoic and Phanerozoic times. Further, from the evaluation of the ophiolite types (Fig. 8) and the time-related subduction influence (Fig. 10) it appears that subduction-related ophiolites are the most common type throughout the Archean, in accordance with the suggestion of Santosh (2010), that the first 2 billion years of Earth history was dominated by subduction-related processes in the oceanic environment.

The lesser amount of gabbro preserved in the Archean greenstone sequences, compared to those of Proterozoic and Phanerozoic ages (Figs. 3 and 4B), is the other marked secular feature, which, together with the scarcity of the sheeted dykes complexes,

probably relates to the thermal conditions during the Archean. Even without absolute constraints on the temperature conditions of the Archean mantle (on which there is no general consensus, as discussed above), it is reasonable to conclude that higher heat fluxes would result in greater magma production and greater mantle flux to the surface. We suggest that this physical scenario prevented stagnation and solidification of magma chambers, and hence reduced potential for gabbro formation and sheeted dyke complexes. Instead, the magmas erupted predominantly as lavas and formed accumulations with ocelli (e.g., Sandstå et al., 2011) as ubiquitous in the extrusive sequences of the Archean greenstones.

Our analyses shows that 85% of the Precambrian greenstone sequences are subduction-related, including those from the oldest belts, and that of the total related backarc ophiolites nearly 50% are MORB-type. Thus, there is no evidence that (deep) plume activity was the dominant driving force of surface tectonic processes over the last 4 billion years. Even in today's plate-tectonic environment some of the largest volcanos in our solar system formed as oceanic plateau built on oceanic crust (e.g., Sager et al., 2013). The lack of abrupt changes in our geochemical data also precludes that episodic mantle overturn 'reset' the chemistry of the global oceanic lithosphere (e.g., Davis, 2007; Kump et al., 2001). Thus, the most conservative interpretation is that subduction processes, as inferred from the geochemical proxies in our datasets covering the ca. 4 billion years, were counterbalanced by upper mantle influenced spreading processes. By inference then, modern style plate tectonic processes likely dominated over this period. However, subtle but detectible changes that occurred around 2 billion years ago, as reported here in both the lithological make up of ophiolites and the incompatible elements such as Ti, P, Zr, Y and Nb, and compatible elements Ni and Cr, may well reflect linked changes in oxidation states of both the mantle and atmosphere at that time (c.f., Kump et al., 2001). Further examination of the chemistry of the relevant basalts is needed to test this inference.

10. Summary and conclusions

We present a geological and geochemical compilation of 118 Phanerozoic ophiolite complexes and 111 ophiolite-like sequences from 106 Precambrian greenstone belts worldwide. The following are the main observations and conclusions of this global study:

- The most important ophiolite sequences are preserved in the time intervals of 50–200 Ma, 450–1000 Ma, and 2500–2750 Ma. The next abundant group is represented in the time intervals 0–50 Ma, 2000–2250 Ma, and 2750–3500 Ma.
- In terms of their lithological make-up the Phanerozoic and Precambrian ophiolites are relatively similar until ca. 2 Ga. Prior to 2 Ga, ophiolites contain notably less gabbro, dykes (sheeted dyke complexes and dyke swarms). Further, ocelli-bearing komatiites and basalts are common in the Archean and lower Proterozoic lavas, and rare in the younger occurrences. This observation is consistent with magma formation and crust development without long residence time in magma chambers.
- Over 4.0 Ga, ophiolite complexes show variations in their geochemical character. The average values of incompatible and compatible elements at 100 million-year time intervals (for the Phanerozoic ophiolites) and 250 million-year time intervals for the Precambrian ophiolites, change around 2–1.8 Ga. Before then, from 2.0 to 4.0 Ga there is a notable decrease in the incompatible elements and increase in the compatible elements. This geochemical change can be linked to an increasing degree of partial melting of the mantle in the Archean and into the early Proterozoic; it also coincides with a broad change in the lithological construction of ophiolites.
- The Phanerozoic ophiolites are predominantly (75%) of the subduction-related type and the majority (56%) of these ophiolites can be attributed to the generation of ancient oceanic lithosphere in a backarc tectonic environment, similar to the major Precambrian ophiolite division.
- The subduction-signal of the greenstones generally shows a large variation among the Phanerozoic orogenic belts from 0 to 100%.
- In general, there appears to be a tendency of increasing subduction-signal as the ophiolite complexes get older. For the oldest (the 3.8 Ga Isua in SW Greenland and the 3.8–4.3 (?) Ga Nuvvuagittuq in NE Canada) greenstones, nearly all the geochemical indicators show subduction-influence, suggesting that these oldest ophiolites were generated as a result of processes at convergent plate margins. Throughout the Archean these were counterbalanced by at least 50% MORB-like sequences, suggesting modern-like plate tectonic processes as the most conservative interpretation for surface tectonics for near 4 billion years of earth history.

Acknowledgements

We express our sincere thanks to the Co-Editor-in-Chief, Professor M. Santosh, for the invitation to write this contribution as a Focus Review paper for Geoscience Frontiers. Financial support over many years of fieldwork in Phanerozoic ophiolites and Precambrian greenstone belts, and numerous geochemical analyses have been supported by the Norwegian Research Council and the Meltzer Foundation at the University of Bergen (HF), the National Research Foundation of South Africa (MdeW), and the National Science Foundation (NSF) and Miami University, USA (YD). Jane Ellingsen helped with some of the illustrations. We acknowledge the insightful and constructive reviews for the journal by Brian Windley and Tim Kusky that helped us improve the paper. This is AEON publication No. 121.

References

Abbott, D.H., Hoffman, S.E., 1984. Archaean plate tectonics revisited 1. Heat flow, spreading rate, and the age of subducting oceanic lithosphere and their effects on the origin and evolution of continents. Tectonics 3 (4), 429–448.

Abbotts, I.L., 1981. Masirah (Oman) Ophiolite sheeted dykes and pillow lavas: geochemical evidence of the former ocean ridge environment. Lithos 14, 283–294.

Abd El-Rahman, Y., Polat, A., Dilek, Y., Fryer, B.J., El-Sharkawy, M., Sakran, S., 2009. Geochemistry and tectonic evolution of the Neoproterozoic incipiant arc-forearc crust in the Fawakhir area, Central Eastern Desert of Egypt. Precambrian Research 175, 116–134.

Adam, J., Rushmer, T., O'Neil, J., Francis, D., 2012. Hadean greenstones from the Nuvvuagittuq fold belt and the origin of the Earth's early continental crust. Geology 40 (4), 363–366.

Aitchison, J.C., Flood, P.G., 1995. Camilaroi Terrane: a Devonian rifted intra-oceanic island-arc assemblage, NSW, Australia. In: Smellie, J.L. (Ed.), Volcanism Associated with Extension at Consuming Plate Margins, Geological Society Special Publications 81, pp. 155–168.

Allegre, C.J., Courtillot, V., Tapponnier, P., 32 others, 1984. Structure and evolution of the Himalaya – Tibet orogenic belt. Nature 307, 17–22.

Andersen, T.B., Corfu, F., Labrousse, L., Osmundsen, P.-T., 2012. Evidence for hyper-extension along the pre-Caledonian margin of Baltica. Journal of the Geological Society, London 169, 601–612.

Angerer, T., Kerrich, R., Hagemann, S.G., 2013. Geochemistry of a komatiitic, bonitic, and tholeiitic basalt association in the Mesoarchean Koolyanobbing greenstone belt, Southern Cross Domain, Yilgarn craton: Implications for mantle sources and geodynamic setting of banded iron formation. Precambrian Research 224, 110–128.

Arndt, N., 2003. Komatiites, kimberlites, and boninites. Journal of Geophysical Research 108 (B6), 2293. http://dx.doi.org/10.1029/2002JB002157.

Arndt, N.T., Jenner, G.A., 1986. Crustally contaminated komatiites and basalts from Kambalda, Western Australia. Chemical Geology 56, 229–255.

Arndt, N.T., Lesher, C.M., Barnes, S., 2008. Komatiite. Cambridge University Press, Cambridge, 488 pp.

Babaie, H.A., Babaei, A., Ghazi, A.M., Arvin, M., 2006. Geochemical, $^{40}Ar/^{39}Ar$ age, and isotopic data for crustal rocks of the Neyriz ophiolite, Iran. Canadian Journal of Earth Sciences 43, 57–70.

Barley, M.E., 1986. Incompatible-element enrichment in Archean basalts: a consequence of contamination by older sialic crust rather than mantle heterogeneity. Geology 14, 947–950.

Bédard, J.H., 1999. Petrogenesis of boninites from the Betts Cove ophiolite, Newfoundland, Canada: identification of subducted source components. Journal of Petrology 40 (12), 1853–1889.

Bédard, É., Hébert, R., Guilmette, C., Lesage, G., Wang, C.S., Dostal, J., 2009. Petrology and geochemistry of the Saga and Sangsang ophiolitic massifs, Yarlung Zangbo Suture Zone, Southern Tibet: evidence for an arc-back-arc origin. Lithos 113, 48–67.

Bezard, R., Hébert, R., Wang, C., Dostal, J., Dai, J., Zhong, H., 2011. Petrology and geochemistry of the Xiugugabu ophiolitic massif, western Yarlung Zangbo suture zone, Tibet. Lithos 125, 347–367.

Bian, Q.-T., Li, D.-H., Pospelov, L., Yin, L.-M., Li, H.-S., Zhao, D.-S., Chang, C.-F., Lou, X.-Q., Gao, S.-L., Astrakhantsev, O., Chamov, N., 2004. Age, geochemistry and tectonic setting of Buqingshan ophiolites, North Qinghai-Tibet Plateau, China. Journal of Asian Earth Sciences 23, 577–596.

Bickle, M.J., Nesbit, E.G., Martin, A., 1994. Archean greenstone belts are not oceanic crust. The Journal of Geology 102, 121–128.

Bosch, D., Gabriele, P., Lapierre, H., Malfere, J.-L., Jaillard, E., 2002. Geodynamic significance of the Raspas Metamorphic Complex (SW Ecuador): geochemical and isotopic constraints. Tectonophysics 345, 83–102.

Brownlow, A.H., 1996. Geochemistry, second ed. Prentice Hall, Upper Saddle River, New Jersey, 580 pp.

Buchan, C., Cunningham, D., Windley, B.F., Tomurhuu, D., 2001. Structural and lithological characteristics of the Bayankhongur Ophiolite Zone, Central Mongolia. Journal of the Geological Society, London 158, 445–460.

Buchan, C., Pfänder, J., Kröner, A., Brewer, T.S., Tomurtogoo, O., Tomurhuu, D., Cunningham, D., Windley, B.F., 2002. Timing of accretion and collisional deformation in the Central Asian Orogenic Belt: implications of granite geochronology in the Bayankhongor Ophiolite Zone. Chemical Geology 192, 23–45.

Burchfiel, B.C., Davis, G.A., 1975. Nature and controls of Cordilleran orogenesis, western United States: extensions of an earlier synthesis. American Journal of Science 275-A, 363–396.

Cates, N.L., Ziegler, K., Schmitt, A.K., Mojzsis, S.J., 2013. Reduced, reused and recycled: detrital zircons define a maximum age for the Eoarchean (ca. 3750–3780 Ma) Nuvvuagittuq Supracrustal Belt, Québec (Canada). Earth and Planetary Science Letters 362, 283–293.

Cavosie, A.J., Valley, J.W., Wilde, S.A., 2007. The oldest terrestrial mineral record: a review of 4400–4000 Ma detrital zircons from Jack Hills, Western Australia. In: Van Kranendonk, M.J., Smithies, R.H., Bennet, V.C. (Eds.), Earth's Oldest Rocks, Development in Precambrian Geology 15. Elsevier, Amsterdam, pp. 91–111.

Cawood, P.A., Kröner, A., Collins, W.J., Kusky, T.M., Mooney, W.D., Windley, B.F., 2009. Accretionary Orogens through Earth History. In: Geological Society, London, Special Publications 318, pp. 1–36.

Charlot-Prat, F., 2005. An undeformed ophiolite in the Alps: field and geochemical evidence for a link between volcanism and shallow plate tectonic processes. In: Foulger, G.R., Natland, J.H., Presnall, D.C., Anderson, D.L. (Eds.), Plates, Plumes and Paradigms, Geological Society of America Special Papers 388, pp. 751–780.

Chen, G., Xia, B., 2008. Platinum-group elemental geochemistry of mafic and ultramafic rocks from the Xigaze ophiolite, southern Tibet. Journal of Asian Earth Sciences 32, 406–422.

Chew, D.M., Daly, J.S., Magna, T., Page, L.M., Kirkland, C.L., Whitehouse, M.J., Lam, R., 2010. Timing of ophiolite obduction in the Grampian orogen. Geological Society of America Bulletin 122 (11/12), 1787–1799.

Clift, P.D., Hannigan, R., Blusztajn, J., Draut, A.E., 2002. Geochemical evolution of the Dras-Kohistan Arc during collision with Eurasia: evidence from the Ladakh Himalaya, India. Island Arc 11, 255–273.

Coleman, R.J., 2000. Prospecting for ophiolites along the California continental margin. In: Dilek, Y., Moores, E.M., Elthon, D., Nicolas, A. (Eds.), Ophiolites and Oceanic Crust: New Insights from Field Studies and the Oceanic Drilling Program. Boulder, Colorado, Geological Society of America Special Paper 349, pp. 351–364.

Cooper, M.R., Crowley, Q.G., Hollis, S.P., Noble, S.R., Roberts, S., Chew, D., Earls, G., Herrington, R., Merriman, R.J., 2011. Age constraints and geochemistry of the Ordovician Tyrone Igneous Complex, Northern Ireland: implications for the Grampian orogeny. Journal of the Geological Society, London 168, 837–850.

Condie, K.C., 2007. Accretionary orogens in space and time. In: Hatcher Jr., R.D., Carlson, M.P., McBride, J.H., Marinez Catalán, J.R. (Eds.), 4-D Framework of Continental Crust, Geological Society of America Memoir 200, pp. 145–158.

Condie, K.C., Kröner, A., 2008. When did plate tectonics begin? In: Condie, K.C., Pease, V. (Eds.), When Did Plate Tectonics Begin on Planet Earth?, The Geological Society of America Special Paper 440, pp. 281–294.

Corcoran, P.L., Mueller, W.U., Kusky, T.M., 2004. Inferred ophiolites in the Archean Slave Craton. In: Kusky, T.M. (Ed.), Precambrian Ophiolites and Related Rocks, Development in Precambrian Geology 13. Elsevier, Amsterdam, pp. 363–404.

Crowley, Q.G., Floyd, P.A., Winchester, J.A., Franke, W., Holland, J.G., 2000. Early Palaeozoic rift-related magmatism in Variscan Europe: fragmentation of the Armorican Terrane Assemblage. Terra Nova 12 (4), 171–180.

Cutts, K.A., Hand, M., Kelsey, D.E., Strachan, R.A., 2011. P-T constraints and timing of Barrovian metamorphism in the Shetland Islands, Scottish Caledonides: implications for the structural setting of the Unst ophiolite. Journal of the Geological Society, London 168, 1265–1284.

Dann, J.C., 1997. Pseudostratigraphy and origin of the Early Proterozoic Payson ophiolite, central Arizona. Geological Society of America Bulletin 109 (3), 347–365.

Davis, G.F., 2007. Controls on density stratification in the early mantle. Geochemistry, Geophysics, Geosystems 8 (4), Q04006. http://dx.doi.org/10.1029/2006GC001414.

De Souza, S., Tremblay, A., Daoust, C., Gauthier, M., 2008. Stratigraphy and geochemistry of the Lac-Brompton ophiolite, Canada: evidence for extensive forearc magmatism and mantle exhumation in the Southern Quebec Ophiolite Belt. Canadian Journal of Earth Sciences 45, 999–1014.

Dewey, J.F., 1969. Continental margins: a model for conversion of Atantic type to Andean type. Earth and Planetary Science Letters 6, 189–197.

Dewey, F.J., Kidd, W.S.F., 1974. Continental collisions in the Appalachian-Caledonian orogenic belt: Variations related to complete and incomplete suturing. Geology 2, 543–546.

Dewey, F.J., Spall, H., 1975. Pre-Mesozoic plate tectonics. Geology 3, 422–424.

Dewey, F.J., Cande, S., Pitman, W.C., 1989. Tectonic evolution of the India-Eurasia collision zone. Eclogae Geology Helvetica 82, 717–734.

de Wit, M.J., Stern, C., 1978. Pillow talk. J. Volcanol. Geotherm. Res. 4, 55–80.

de Wit, M.J., 1998. On Archean granites, greenstones, cratons and tectonics: does the evidence demand a verdict? Precambrian Research 91, 181–226.

de Wit, M.J., Ashwal, L.D. (Eds.), 1997. Greenstone Belts. Clarendon Press, Oxford, p. 809.

de Wit, M.J., Furnes, H., Robins, B., 2011. Geology and tectonostratigraphy of the Onverwacht Suite, Barberton Greenstone Belt, South Africa. Precambrian Research 186, 1–27.

de Wit, M.J., Furnes, H., 2013. Earth's oldest unconformity – prospect of a beginning in the tectono-sedimentary continental cycle? Gondwana Research 23, 429–435.

Dickinson, W.R., 2004. Evolution of the North American Cordillera. Annual Reviews of Earth and Planetary Sciences 32, 13–45.

Dickinson, W.R., Hopson, C.A., Saleeby, J.A., 1996. Alternate origins of the Coast Range Ophiolite (California): introduction and implications. GSA Today 6, 1–10.

Dilek, Y., 1989. Tectonic significance of post-accretion rifting of a Mesozoic island-arc terrane in northern Sierra Nevada, California. The Journal of Geology 97, 503–518.

Dilek, Y., Eddy, C.A., 1992. The Troodos (Cyprus) and Kizildag (S. Turkey) ophiolites as structural models for slow-spreading ridge segments. The Journal of Geology 100, 305–322.

Dilek, Y., Delaloye, M., 1992. Structure of the Kizildag ophiolite, a slow-spread Cretaceous ridge segment north of the Arabian Promontory. Geology 20, 19–22.

Dilek, Y., Rowland, J.C., 1993. Evolution of a conjugate passive margin pair in Mesozoic southern Turkey. Tectonics 12, 954–970.

Dilek, Y., Robinson, P.T., 2003. Ophiolites in Earth History: Introduction. In: The Geological Society, London, Special Publication 218, pp. 1–8 doi: 10.1144/gsl.sp.2003.218.01.01.

Dilek, Y., Polat, A., 2008. Suprasubduction zone ophiolites and Archean tectonics. Geology 36 (5), 431–432.

Dilek, Y., Furnes, H., 2009. Structure and geochemistry of Tethyan ophiolites and their petrogenesis in subduction rollback systems. Lithos 113, 1–20.

Dilek, Y., Thy, P., 2009. Island arc tholeiite to boninitic melt evolution of the Cretaceous Kizildag (Turkey) ophiolite: model for multi-stage early arc-forearc magmatism in Tethyan subduction factories. Lithos 113, 68–87.

Dilek, Y., Furnes, H., 2011. Ophiolite genesis and global tectonics: geochemical and tectonic fingerprinting of ancient oceanic lithosphere. Geological Society of America Bulletin 123 (3/4), 387–411.

Dilek, Y., Thy, P., Moores, E.M., Ramsden, T.W., 1990. Tectonic evolution of the Troodos Ophiolite within the Tethyan Framework. Tectonics 9, 811–823.

Dilek, Y., Thy, P., Moores, E.M., 1991. Episodic dike intrusion in the northwestern Sierra Nevada, California: implications for multistage evolution of a Jurassic arc terrane. Geology 19, 180–184.

Dilek, Y., Furnes, H., Skjerlie, K.P., 1997. Propagating rift tectonics of a Caledonian marginal basin: multi-stage seafloor spreading history of the Solund-Stavfjord ophiolite in western Norway. Tectonophysics 280, 213–238.

Dilek, Y., Thy, P., Hacker, B., Grundvig, S., 1999. Structure and petrology of Tauride ophiolites and mafic dike intrusions (Turkey): implications for the Neotethyan ocean. Geological Society of America Bulletin 111, 1192–1216.

Dilek, Y., Shallo, M., Furnes, H., 2005. Rift-drift, seafloor spreading, and subduction tectonics of Albanian ophiolites. International Geology Review 47, 147–176.

Dilek, Y., Furnes, H., Shallo, M., 2008. Geochemistry of the Jurassic Mirdita ophiolite (Albania) and the MORB to SSZ evolution of a marginal basin oceanic crust. Lithos 100, 174–209.

Draut, A.E., Clift, P.D., Amato, J.M., Blusztajn, J., Schouten, H., 2009. Arc-continent collision and the formation of continental crust: a new geochemical and isotopic record from the Ordovician Tyrone Igneous Complex, Ireland. Journal of the Geological Society, London 166, 485–500.

Dubois-Côté, V., Hébert, R., Dupuis, C., Wang, C.,S., Li, Y.L., Dostal, J., 2005. Petrology and geochemical evidence for the origin of the Yarlung Zangbo ophiolites, southern Tibet. Chemical Geology 214, 265–286.

Dunning, G.R., Pedersen, R.B., 1988. U/Pb ages of ophiolites and arc-related plutons of the Norwegian Caledonides: implications for the development of Iapetus. Contributions to Mineralogy and Petrology 98, 13–23.

Please cite this article in press as: Furnes, H., et al., Four billion years of ophiolites reveal secular trends in oceanic crust formation, Geoscience Frontiers (2014), http://dx.doi.org/10.1016/j.gsf.2014.02.002

Elthon, D., 1979. High magnesia liquids as the parental magma for ocean floor basalts. Nature 278, 514–518.
Escuder-Viruete, J., Díaz de Neira, A., Hernáiz Huerta, P.P., Monthel, J., García Senz, J., Joubert, M., Lopera, E., Ullrich, T., Friedman, R., Mortensen, J., Pérez-Estaún, A., 2008. Magmatic relationships and ages of Caribbean Island arc tholeiites, boninites and related felsic rocks, Dominican Republic. Lithos 90, 161–186.
Escuder-Viruete, J., Pérez-Estaún, A., Joubert, M., Weis, D., 2011. The Pelona-Pico Duarte basalts Formation, Central Hispaniola: an on-land section of Late Cretaceous volcanism related to the Caribbean large igneous province. Geologica Acta 9 (3–4), 307–328.
Fauqué, L.E., Villar, L.M., 2003. Stratigraphic reinterpretation and petrology of the Cerro Chuscho Formation. Precordillera of La Rioja. Rev. Asoc. Geol. Argent. 58 (2), 218–232.
Faustino, D.V., Yumul Jr., G.P., Dimalanta, C.B., de Jesus, J.V., Zhou, M.-F., Aitchison, J.C., Tamayo Jr., R.A., 2006. Volcanic-hypabyssal rock geochemistry of a subduction-related marginal basin ophiolite: Southeast Bohol Ophiolite-Cansiwang Mélange Complex, Central Philippines. Geosciences Journal 10 (3), 291–303.
Finger, F., Steyrer, H.P., 1995. A tectonic model for the Eastern Variscides: indicators from the chemical study of amphibolites in the southeastern Bohemian Massif. Geologica Carpathica 46, 137–150.
Flinn, D., Frank, P.L., Brook, M., Pringle, I.R., 1979. Basement cover relastions in Shetland. In: Harris, A.L., Holland, C.H., Leake, B.E. (Eds.), The Caledonides of the British Isles Reiewed, Geological Society, London, Special Publication 8, pp. 109–115.
Floyd, P.A., Winchester, J.A., 1975. Magma type and tectonic setting discrimination using immobile elements. Earth and Planetary Science Letters 27, 211–218.
Floyd, P.A., 1984. Geochemical characteristics and comparison of the basic rocks of the Lizard Complex and the basaltic lavas within the Hercynian troughs of SW England. Journal of the Geological Society, London 141, 61–70.
Floyd, P.A., Kryza, R., Crowley, Q.G., Winchester, J.A., Abdel Wahed, M., 2002. Ślęża Ophiolite: geochemical features and relationship to Lower Palaeozoic rift magmatism in the Bohemian Massif. In: Winchester, J.A., Pharaoh, T.C., Verniers, J. (Eds.), Palaeozoic Amalgamation of Central Europe, The Geological Society, London, Special Publications 201, pp. 197–215.
Foley, S.F., Buhre, S., Jacob, D.E., 2003. Evolution of the Archaean crust by lamination and shallow subduction. Nature 421, 249–252.
Foster, D.A., Gray, D.R., Spaggiari, C., Kamenov, G., Bierlein, F.P., 2009. Palaeozoic Lachlan orogen, Australia; accretion and construction of continental crust in a marginal ocean setting: isotopic evidence from Cambrian metavolcanic rocks. In: Cawood, P.A., Kröner, A. (Eds.), Earth Accretionary Systems in Space and Time, The Geological Society, London, Special Publications 318, pp. 329–349.
Friend, C.R.L., Nutman, A.P., 2010. Eoarchean ophiolites? New evidence for the debate on the Isua supracrustal belt, Southern West Greenland. American Journal of Science 310, 826–861.
Furnes, H., Pedersen, R.B., Stillman, C.J., 1988. The Leka Ophiolite Complex, central Norwegian Caledonides: field characteristics and geotectonic significance. Journal of the Geological Society, London 145, 401–412.
Furnes, H., Pedersen, R.B., Hertogen, J., Albrektsen, B.A., 1992. Magma development of the Leka Ophiolite Complex, central Norwegian Caledonides. Lithos 27, 259–277.
Furnes, H., Kryza, R., Muszynski, A., Pin, C., Garmann, L.B., 1994. Geological evidence for progressive, rift-related early Palaeozoic volcanism in the western Sudetes. Journal of the Geological Society, London 151, 91–109.
Furnes, H., de Wit, M., Staudigel, H., Rosing, M., Muehlenbachs, K., 2007. A vestige of Earth's oldest ophiolite. Science 315, 1704–1707.
Furnes, H., Rosing, M., Dilek, Y., de Wit, M., 2009. Isua supracrustal belt (Greenland) – a vestige of a 3.8 Ga suprasubduction zone ophiolite, and implications for Archean geology. Lithos 113, 115–132.
Furnes, H., de Wit, M.J., Robins, B., Sandstå, N.R., 2011. Volcanic evolution of the upper Onverwacht Suite, Barberton Greenstone Belt, South Africa. Precambrian Research 186, 28–50.
Furnes, H., Dilek, Y., Pedersen, R.B., 2012a. Structure, geochemistry, and tectonic evolution of trench-distal backarc oceanic crust in the western Norwegian Caledonides, Solund-Stavfjord ophiolite (Norway). Geological Society of America Bulletin 124, 1027–1047.
Furnes, H., Robins, B., de Wit, M.J., 2012b. Geochemistry and petrology of lavas in the upper Onverwacht Suite, Barberton Mountain Land, South Africa. South African Journal of Geology 115 (2), 171–210.
Furnes, H., Dilek, Y., de Wit, M., 2013. Precambrian greenstone sequences represent different ophiolite types. Gondwana Research. http://dx.doi.org/10.1016/j.gr.2013.06.004.
Gaggero, L., Spadea, P., Cortesogno, L., Savelieva, G.N., Pertsev, A.N., 1997. Geochemical investigation of the igneous rocks from the Nurali ophiolitic mélange zone, Southern Urals. Tectonophysics 276, 139–161.
Galoyan, G., Rolland, Y., Sosson, M., Corsini, M., Billo, S., Verati, C., Melkonyan, R., 2009. Geology, geochemistry and $^{40}Ar/^{39}Ar$ dating of Sevan ophiolites (Lesser Caucasus, Armenia): evidence for Jurassic back-arc opening and hot spot event between the South Armenian Block and Eurasia. Journal of Asian Earth Sciences 34, 135–153.
Ganelin, A.V., 2011. Geochemistry and geodynamic significance of the dike series of the Aluchin Ophiolite Complex, Verkhoyansk-Chukotka fold zone, Northeast Russia. Geochemistry International 49 (7), 654–675.
Garfunkel, Z., 2004. Origin of the Eastern Mediterranean basin: a reevaluation. Tectonophysics 391, 11–34.
Geary, E.E., Kay, R.W., 1989. Identification of an Early Cretaceous ophiolite in the Camarines Norte-Calaguas Islands basement complex, eastern Luzon, Philippines. Tectonophysics 168, 109–126.
Geary, E.E., Kay, R.W., Reynolds, J.C., Kay, S.M., 1989. Geochemistry of mafic rocks from the Coto Block, Zambales ophiolite, Philippines: trace element evidence for two stages of crustal growth. Tectonophysics 168, 43–63.
Gee, D.G., 2005. Scandinavian Caledonides (with Greenland). In: Selley, R.C., Cocks, L.R.M., Plimer, I.R. (Eds.), Encyclopedia of Geology. Elsevier, Oxford, pp. 64–74.
Gee, D.G., Fossen, H., Henriksen, N., Higgins, A.K., 2008. From the Early Paleozoic Platforms of Baltica and Laurentia to the Caledonide Orogen of Scandinavia and Greenland. Episodes 31 (1), 44–51.
Gelinas, L., Brooks, C., Trzcienski, W.E., 1976. Archean variolites – quenched immiscible liquids. Canadian Journal of Earth Sciences 13, 210–230.
Ghazi, A.M., Hassanipak, A.A., Mahoney, J.J., Duncan, R.A., 2004. Geochemical characteristics, $^{40}Ar–^{39}Ar$ ages and original tectonic setting of the Band-e-Zeyarat/Dar Anar ophiolite, Makran accretionary prism, S.E. Iran. Tectonophysics 393, 175–196.
Giaramita, M., MacPherson, G.J., Phipps, S.P., 1998. Petrologically diverse basalts from a fossil oceanic forearc in California: the Llanada and Black Mountain remnants of the Coast Range ophiolite. Geological Society of America Bulletin 110 (5), 553–571.
Glen, R.A., 2005. The Tasmanides of eastern Australia. In: Vaughan, A.P.M., Leat, P.T., Pankhurst, R.J. (Eds.), Terrane Processes at the Margins of Gondwana, The Geological Society, London, Special Publications 246, pp. 23–96.
Godfrey, N.J., Dilek, Y., 2000. Mesozoic assimilation of oceanic crust and island arc into the North American continental margin in California and Nevada: insights from geophysical data. In: Dilek, Y., Moores, E.M., Elthon, D., Nicolas, A. (Eds.), Ophiolites and Oceanic Crust: New Insights from Field Studies and the Oceanic Drilling Program. Boulder, Colorado, Geological Society of America Special Paper 349, pp. 365–382.
Goodenough, M.K., Styles, M.T., Schofield, D., Thomas, R.J., Crowley, Q.C., Lilly, R.M., McKervey, J., Stephenson, D., Carney, J.N., 2010. Architecture of the Oman-UAE ophiolite: evidence for multi-phase magmatic history. Arabian Journal of Geosciences 3, 439–458.
Gonzáles-Menéndez, L., Gallastegui, G., Cuesta, A., Heredia, N., Rubio-Ordóñez, A., 2013. Petrogenesis of Early Paleozoic basalts and gabbro in the western Cuyania terrane: constraints on the tectonic setting of the southwestern Gondwana margin (Sierra del Tigre, Andean Argentine Precordillera). Gondwana Research 24, 359–376.
Goscombe, B.D., Everard, J.L., 1999. Macquarie Island mapping reveals three tectonic phases. Eos, Transactions American Geophysical Union 80 (5), 50–55.
Grenne, T., 1989. Magmatic evolution of the Løkken SSZ Ophiolite, Norwegian Caledonides: relationships between anomalous lavas and high-level intrusions. Geological Journal 24, 251–274.
Grove, T.L., Parman, S.W., 2004. Thermal evolution of the Earth as recorded by komatiites. Earth and Planetary Science Letters 219, 173–187.
Guilmette, C., Hébert, R., Wang, S.C., Villeneuve, M., 2009. Geochemistry and geochronology of the metamorphic sole underlying the Xigaze ophiolite, Yarlung Zangbo Suture Zone, Tibet. Lithos 112, 149–162.
Guivel, C., Lagabrielle, Y., Bourgois, J., Maury, R.C., Fourcade, S., Martin, H., Arnaud, N., 1999. New geochemical constraints for the origin of ridge-subducted-related plutonic and volcanic suites from the Chile Triple Junction (Taitao Peninsula and Site 862, LEG ODP141 on the Taitao Ridge). Tectonophysics 311, 83–111.
Hall, R., 2012. Late Jurassic-Cenozoic reconstruction of the Indonesian region and the Indian Ocean. Tectonophysics 570–571, 1–41.
Hamilton, W.B., 1998. Archean magmatism and deformation were not the products of plate tectonics. Precambrian Research 91, 109–142.
Hamilton, W.B., 2007. Earth's First Two Billion Years – the Era of Internally Mobile Crust. In: Geological Society of America, Memoir 200, pp. 233–296.
Hamilton, W.B., 2011. Plate tectonics began in Neoprotrozoic time, and plumes from deep mantle have never operated. Lithos 123, 1–20.
Harper, G.D., 2003. Fe-Ti basalts and propagating-rift tectonics in the Josephine Ophiolite. Geological Society of America Bulletin 115 (7), 771–787.
Harper, G.D., Wright, J.E., 1984. Middle to Late Jurassic tectonic evolution of the Klamath Mountains, California-Oregon. Tectonics 3, 759–772.
Harris, R.A., 1995. Geochemistry and tectonomagmatic affinity of the Misheguk massif, Brooks Range ophiolite, Alaska. Lithos 35, 1–25.
Harrison, T.M., Schmitt, A.K., McCulloch, M.T., Lovera, O.M., 2008. Early (≥4.5 Ga) formation of terrestrial crust: Lu-Hf, $\delta^{18}O$, and Ti thermometry results for Hadean zircons. Earth and Planetary Science Letters 268, 476–486.
Hassanipak, A.A., Ghazi, A.M., 2000. Petrology, geochemistry and tectonic setting of the Khoy ophiolite, northwest Iran: implications for the Tethyan tectonics. Journal of Asian Earth Sciences 18, 109–121.
Hastie, A.R., Kerr, A.C., Mitchell, S.F., Millar, I.L., 2008. Geochemistry and petrogenesis of Cretaceous oceanic plateau lavas in eastern Jamaica. Lithos 101, 323–343.
Hauff, F., Hoernle, K., van den Bogaard, P., Alvarado, G., Garbe-Schönberg, D., 2000. Age and geochemistry of basaltic complexes in western Costa Rica: contributions to the geotectonic evolution of Central America. Geochemistry, Geophysics, Geosystems 1. http://dx.doi.org/10.1029/1999GCC000020.
Hébert, R., Bezard, R., Guilmette, C., Dostal, J., Wang, C.S., Liu, Z.F., 2012. The Indus-Yarlung Zangbo ophiolites from Nanga Parbat to Namche Barwa syntaxes, southern Tibet: First synthesis of petrology, geochemistry, and geochronology

with incidences on geodynamic reconstructions of the Neo-Tethys. Gondwana Research 22, 377–397.
Heim, M., Grenne, T., Prestvik, T., 1987. The Resfjell ophiolite fragment, southwest Trondheim region, central Norwegian Caledonides. Norges Geologiske Undersøkelse Bulletin 409, 49–71.
Hemond, C., Arndt, N.T., Lichtenstein, U., Hofmann, A.W., 1993. The heterogeneous Iceland plume: Nd-Sr-O isotopes and trace element constraints. Journal of Geophysical Research 98 (B9), 15833–15850.
Herzberg, C., Condie, K., Korenaga, J., 2010. Thermal history of the Earth and its petrological expression. Earth and Planetary Science Letters 292, 79–88.
Heskestad, B., Hofshagen, H.H., Furnes, H., Pedersen, R.B., 1994. The geochemical evolution of the Gulfjellet Ophiolite Complex, west Norwegian Caledonides. Norsk Geologisk Tidsskrift 74, 77–88.
Hildebrand, R.S., 2009. Did Westward Subduction Cause Cretaceous-Tertiary Orogeny in the North American Cordillera? In: Geological Society of America Special Paper 457, pp. 1–71.
Hildebrand, R.S., 2013. Westward subduction of North America during the Sevier event. In: Geological Society of America Annual Meeting and Exploration, Denver 27–30 October. Abstracts with Programs, p. 441.
Hirano, N., Ogawa, Y., Saito, K., Yoshida, T., Sato, H., Taniguchi, H., 2003. Multi-stage evolution of the Tertiary Mineoka ophiolite, Japan: new geochemical and age constraints. In: Dilek, Y., Robinson, P.T. (Eds.), Ophiolites in Earth History, The Geological Society, London, Special Publications 218, pp. 79–298.
Hoffmann, J.E., Münker, C., Polat, A., König, S., Mezger, K., Rosing, M.T., 2010. Highly depleted Hadean mantle reservoirs in the sources of early Archean arc-like rocks, Isua supracrustal belt, southern West Greenland. Geochimica et Cosmochimica Acta 74, 7236–7260.
Hofmann, A., Kusky, T., 2004. The Belingwe greenstone belt: ensialic or oceanic? In: Kusky, T.M. (Ed.), Precambrian Ophiolites and Related Rocks, Developments in Precambrian Geology 13. Elsevier, Amsterdam, pp. 486–536.
Hofmann, A., Wilson, A.H., 2007. Silicified basalts, bedded cherts and other sea floor alteration phenomena of the 3.4 Ga Nondweni greenstone belt, South Africa. In: Van Kranendonk, M.J., Smithies, R.H., Bennett, V.C. (Eds.), Earth's Oldest Rocks, Developments in Precambrian Geology 15. Elsevier, Amsterdam, pp. 571–605.
Hollis, S.P., Roberts, S., Cooper, M.R., Earls, G., Herrington, R., Condon, D.J., Cooper, M.J., Archibald, S.M., Piercey, S.J., 2012. Episodic arc-ophiolite emplacement and the growth of continental margins: late accretion in the Northern Irish sector of the Grampian-Taconic orogeny. Geological Society of America Bulletin 124, 1702–1723.
Hollis, S.P., Cooper, M.R., Roberts, S., Earls, G., Herrington, R., Condon, D.J., Daly, J.S., 2013. Evolution of the Tyrone ophiolite, Northern Ireland, during the Grampian-Taconic orogeny: a correlative of the Annieopsquotch Ophiolite Belt of central Newfoundland? Journal of the Geological Society, London 170, 861–876.
Hollocher, K., Robinson, P., Walsh, E., Roberts, D., 2012. Geochemistry of amphibolefacies volcanics and gabbros of the Støren Nappe in extensions west and southwest of Trondheim, Western Gneiss Region, Norway: a key to correlations and paleotectonic settings. American Journal of Science 312, 357–416.
Hou, Q., Zhao, Z., Zhang, H., Zhang, B., Chen, Y., 2006. Indian Ocean-MORB-type isotopic signature of Yushigou ophiolite in North Qilian Mountains and its implications. Science in China: Series D Earth Science 49 (6), 561–572.
Ishikawa, A., Kaneko, Y., Kadarusman, A., Ota, T., 2007. Multiple generations of forearc mafic-ultramafic rocks in the Timor – Tanimbar ophiolite, eastern Indonesia. Gondwana Research 11, 200–217.
Ichiyama, Y., Ishiwatari, A., 2004. Petrochemical evidence for off-ridge magmatism in a back-arc setting from the Yakuno ophiolite, Japan. Island Arc 13, 157–177.
Ichiyama, Y., Ishiwatari, A., Koizumi, K., 2008. Petrogenesis of greenstones from the Mino-Tamba belt, SW Japan: evidence for an accreated Permian oceanic plateau. Lithos 100, 127–146.
Ingersoll, R.V., 2000. Models for Origin and Emplacement of Jurassic Ophiolites of Northern California. In: Geological Society of America Special Paper 349, pp. 395–402.
Ishizuka, O., Tani, K., Reagan, M.K., 2014. Izu-Bonin-Mariana forearc crust as a modern ophiolite analogue. Elements 10 (in press).
Isozaki, Y., 1997. Contrasting two types of orogen in Permo-Triassic Japan: accretionary versus collisional. Island Arc 6, 2–24.
Isozaki, Y., Aoki, K., Nakama, T., Yanai, S., 2010. New insight into a subduction-related orogen: A reappraisal of the geotectonic framework and evolution of the Japanese Islands. Gondwana Research 18, 82–105.
Jian, P., Liu, D., Kröner, A., Zhang, Q., Wang, Y., Sun, X., Zhang, W., 2009. Devonian to Permian plate tectonic cycle of the Paleo-Tethys Orogen in southwest China (I): geochemistry of ophiolites, arc/back-arc assemblages and within-plate igneous rocks. Lithos 113, 748–766.
Jian, P., Kröner, A., Windley, B.F., Shi, Y., Zhang, F., Miao, L., Tomurhuu, D., Zhang, W., Liu, D., 2010. Zircon ages of the Bayankhongor ophiolitr mélange and associated rocks: time constraints on Neoproterozoic to Cambrian accretionary and collisional orogenesis in Central Mongolia. Precambrian Research 177, 162–180.
Jian, P., Kröner, A., Windley, B.F., Shi, Y., Zhang, W., Zhang, L., Yang, W., 2012. Carboniferous and Cretaceous mafic-ultramafic massifs in Inner Mongolia (China): a SHRIMP zircon and geochemical study of the previous presumed integral "Hegenshan ophiolite". Lithos 142–143, 48–66.
John, T., Scherer, E.E., Schenk, V., Herms, P., Halama, R., Garbe-Schönberg, D., 2010. Subducted seamounts in an eclogite-facies ophiolite sequence: the Andean Raspas Complex, SW Ecuador. Contributions to Mineralogy and Petrology 159, 265–284.
Kadarusman, A., Miyashita, S., Maruyama, S., Parkinson, C.D., Ishikawa, A., 2004. Petrology, geochemistry and paleogeographic reconstruction of the East Sulawesi Ophiolite, Indonesia. Tectonophysics 392, 55–83.
Kamenetsky, V.S., Everard, J.L., Crawford, A.J., Varne, R., Eggins, S.M., Lanyon, R., 2000. Enriched end-member of primitive MORB melts: petrology and geochemistry of glasses from Macquarie Island (SW Pacific). Journal of Petrology 41, 411–430.
Kerr, A.C., Tarney, J., Marriner, G.F., Klaver, G.Th, Saunders, A.D., Thirlwall, M.F., 1996a. The geochemistry and petrogenesis of the late-Cretaceous picrites and basalts of Curaçao, Netherlands Antilles: a remnant of an oceanic plateau. Contributions to Mineralogy and Petrology 124, 29–43.
Kerr, A.C., Marriner, G.F., Arndt, N.T., Tarney, J., Nivia, A., Saunders, A.D., Duncan, R.A., 1996b. The petrogenesis of Gorgona komatiites, picrites and basalts: new field, petrographical and geochemical constraints. Lithos 37, 245–260.
Kerr, A.C., Marriner, G.F., Tarney, J., Nivia, A., Saunders, A.D., Thirlwall, M.F., Sinton, C.W., 1997. Cretaceous basaltic terranes in Western Colombia: elemental, chronological and Sr-Nd isotopic constraints on petrogenesis. Journal of Petrology 38, 677–702.
Kerr, A.C., Pearson, D.G., Nowell, G.M., 2009. Magma source evolution beneath the Caribbean oceanic plateau: new insights from elemental and Sr-Nd-Pb-Hf isotopic studies of ODP Leg 165 Site 1001 basalts. In: James, K.H., Lorente, M.A., Pindell, J.L. (Eds.), The Origin and Evolution of the Caribbean Plate, The Geological Society, London, Special Publications 328, pp. 809–827.
Khalatbari-Jafari, M., Juteau, T., Cotten, J., 2006. Petrology and geochemical study of the Late Cretaceous ophiolite of Khoy (NW Iran), and related geological formations. Journal of Asian Earth Sciences 27, 465–502.
Khan, M., Kerr, A.C., Mahmood, K., 2007a. Formation and tectonic evolution of the Cretaceous-Jurassic Muslim Bagh ophiolitic complex, Pakistan: Implications for the composite tectonic setting of ophiolites. Journal of Asian Earth Sciences 31, 112–127.
Khan, S.R., Jan, M.Q., Khan, T., Khan, M.A., 2007b. Petrology of the dykes from the Waziristan Ophiolite, NW Pakistan. Journal of Asian Earth Sciences 29, 369–377.
Kirby, G.A., 1979. The Lizard complex as an ophiolite. Nature 282, 58–61.
Klaver, G.Th, 1987. The Curaçao Lava Formation: an Ophiolitic Analogue of an Anomalous Thick Layer 2B of the Mid-Cretaceous Oceanic Plateau in the Western Pacific and Central Caribbean. PhD thesis. University of Amsterdam, 168 pp.
Klootwijk, C.T., Gee, J.S., Peirce, J.W., Smith, G.M., MacFadden, P.L., 1992. An early India-Asia contact: paleomagnetic constraints from the Ninetyeast Ridge, ODP Leg 121. Geology 20, 395–398.
Komiya, T., 2004. Material circulation model including chemical differentiation within the mantle and secular variation of temperature and composition of the mantle. Physics of the Earth and Planetary Interiors 146, 333–367.
Komiya, T., Maruyama, S., Masuda, T., Nohda, S., Hayashi, M., Okamoto, K., 1999. Plate tectonics at 3.8–3.7 Ga: field evidence from the Isua accretionary complex, Southern West Greenland. The Journal of Geology 107, 515–554.
Komiya, T., Maruyama, S., Hirata, T., Yurimoto, H., Nohda, S., 2004. Geochemistry of the oldest MORB and OIB in the Isua Supracrustal Belt, southern West Greenland: implications for the composition and temperature of early Archean upper mantle. Island Arc 13 (1), 47–72.
Korenaga, J., 2006. Archean geodynamics and the thermal evolution of Earth. In: Benn, K., Mareschal, J.-C., Condie, K. (Eds.), Archean Geodynamics and Environments, AGU Geophysical Monograph Series, 164. AGU, Washington DC, pp. 7–32.
Kramer, J., Abart, R., Müntener, O., Schmid, S.M., Stern, W.-B., 2003. Geochemistry of metabasalts from ophiolitic and adjacent distal continental margin units: evidence from the Monte Rosa region (Swiss and Italian Alps). Swiss Bulletin of Mineralogy and Petrology 83, 217–240.
Kroner, U., Romer, R.L., 2013. Two plates – many subduction zones: the Variscan orogeny reconsidered. Gondwana Research 24, 298–329.
Kröner, A., Hegner, E., Lehmann, B., Heinhorst, J., Wingate, M.T.D., Liu, D.Y., Ermelow, P., 2008. Paleozoic arc magmatism in the Central Asian Orogenic Belt of Kazakhstan: SHRIMP zircon ages and whole-rock Nd isotopic systematics. Journal of Asian Earth Sciences 32, 118–130.
Kvassnes, A.J.S., Hetland Strand, A., Moen-Eikeland, H., Pedersen, R.B., 2004. The Lyngen Gabbro: the lower crust of an Ordovician incipient arc. Contributions to Mineralogy and Petrology 148, 358–379.
Kump, L.R., Kasting, J.F., Barley, M.E., 2001. Rise of atmospheric oxygen and the "upside-down" Archean mantle. Geochemistry, Geophysics, Geosystems 2, 2000GC000114.
Kurth-Velz, M., Sassen, A., Galer, S.J.G., 2004. Geochemical and isotopic heterogeneities along an island arc-speading ridge intersection: evidence from the Lewis Hills, Bay of Islands ophiolite, Newfoundland. Journal of Petrology 45 (3), 635–668.
Kusky, T.M., 1990. Evidence of Archean ocean opening and closing in the southern Slava Province. Tectonics 9, 1533–1563.
Kusky, T.M., Young, C.P., 1999. Emplacement of the Resurrection Peninsula ophiolite in the southern Alaska forearc during a ridge-trench encounter. Journal of Geophysical Research 104 (B12), 29025–29054.
Kusky, T.M., Windley, B.F., Safonova, I., Wakita, K., Wakabayashi, J., Polat, A., Santosh, M., 2013. Recognition of ocean plate stratigraphy in accretionary orogens through Earth history: a record of 3.8 billion years of sea floor spreading, subduction, and accretion. Gondwana Research 24, 501–547.

Please cite this article in press as: Furnes, H., et al., Four billion years of ophiolites reveal secular trends in oceanic crust formation, Geoscience Frontiers (2014), http://dx.doi.org/10.1016/j.gsf.2014.02.002

Lagabrielle, Y., Lemoine, M., 1997. Alpine, Corsican and Apennine ophiolites: the slow-spreading ridge model. Comptes Rendus de l'Acadciencedirect.com/science/journ 325, 909–920.

Le Moigne, J., Lagabrielle, Y., Whitechurch, H., Girardeau, J., Bourgois, J., Maury, R.C., 1996. Petrology and geochemistry of the Ophiolitic and Volcanic Suites of the Taitao Peninsula – Chile Triple Juction Area. Journal of South American Earth Sciences 9 (1/2), 43–58.

Leslie, A.G., Smith, M., Soper, N.J., 2008. Laurentian margin evolution and the Caledonian orogeny - a template for Scotland and East Greenland. In: Higgins, A.K., Gilotti, A.J., Smith, M.P. (Eds.), The Greenland Caledonides: Evolution of the Northeast Margin of Laurentia, Geological Society of America Memoir 202, pp. 307–343.

Liberi, F., Morten, L., Piluso, E., 2006. Geodynamic significance of ophiolites within the Calabrian Arc. Island Arc 15, 26–43.

Lissenberg, C.J., van Staal, C.R., Bédard, J.H., Zagorevski, A., 2005. Geochemical constraints on the origin of the Annieopsquotch ophiolite belt, Newfoundland Appalachians. Geological Society of America Bulletin 117 (11/12), 1413–1426.

Lucas, S.B., Stern, R.A., Syme, E.C., Reilly, B.A., Thomas, D.J., 1996. Intraoceanic tectonics and the development of continental crust: 1.92–1.84 Ga evolution of the Flin Flon Belt, Canada. Geological Society of America Bulletin 108 (5), 602–629.

Lytwyn, J., Casey, J., Gilbert, S., Kusky, T., 1997. Arc-like mid-ocean ridge formed seaward of a trench-forearc system just prior to ridge subduction: an example from subaccreted ophiolites in southern Alaska. Journal of Geophysical Research 102 (B5), 10225–10243.

MacDonald Jr., J.H., Harper, G.D., Miller, R.B., Miller, J.S., Mlinarevic, A.N., Schultz, C.E., 2008. The Ingalls ophiolite complex, central Cascades, Washington: geochemistry, tectonic setting, and regional correlations. In: Wright, J.E., Shervais, J.W. (Eds.), Ophiolites, Arcs, and Batholiths: A Tribute to Cliff Hopson, Geological Society of America Special Paper 438, pp. 133–159.

Mahéo, G., Bertrand, H., Guillot, S., Villa, I.M., Keller, F., Capiez, P., 2004. The South Ladakh ophiolites (NW Himalaya, India): an intra-oceanic tholeiitic arc origin with implication for the closure of the Neo-Tethys. Chemical Geology 203, 273–303.

Mahoney, J.J., Frei, R., Tejada, M.L.G., Mo, X.X., Leat, P.T., Nägler, T.F., 1998. Tracing the Indian Ocean mantle domain through time: isotopic results from old West Indian, East Tethyan, and South Pacific seafloor. Journal of Petrology 39, 1285–1306.

Maier, W.D., Roelofse, F., Barnes, S.-J., 2003. The concentration of the platinum-group elements in South Africa komatiites: Implications for mantle sources, melting regime and PGE fractionation during crystallization. Journal of Petrology 44 (10), 1787–1804.

Malpas, J., Zhou, M.-F., Robinson, P.T., Reynolds, P.H., 2003. Geochemical and geochronological constraints on the origin and emplacement of the Yarlung Zangbo ophiolites, Southern Tibet. In: Dilek, Y., Robinson, P.T. (Eds.), Ophiolites in the Earth History, The Geological Society, London, Special Publications 218, pp. 191–206.

Manatschal, G., Müntener, O., 2009. A type sequence across an ancient magma-poor ocean-continent transition: the example of the western Alpine Tethys ophiolites. Tectonophysics 473, 4–19.

Manatschal, G., Sauter, D., Karpoff, A.M., Masini, E., Mohn, G., Lagabrielle, Y., 2011. The Chenaillet Ophiolite in the French/Italian Alps: an ancient analogue for an Oceanic Core Complex? Lithos 124, 169–184.

Maruyama, S., Komiya, T., 2011. The oldest pillow lavas, 3.8–3.7 Ga from Isua supracrustal belt, SW Greenland: plate tectonics had already begun at 3.8 Ga. Journal of Geography 120 (5), 869–876.

Maruyama, S., Ikoma, M., Genda, H., Hirose, K., Yokoyama, T., Santosh, M., 2013. The naked planet Earth: most essential pre-requisite for the origin and evolution of life. Geoscience Frontiers 4, 141–165.

Matte, P., 1991. Accretionary history and crustal evolution of the Variscan belt in Western Europe. Tectonophyscis 196, 309–337.

Matte, Ph, Mattauer, M., Olivet, J.M., Griot, D.A., 1997. Continental subductions beneath Tibet and the Himalayan orogeny: a review. Terra Nova 9, 264–270.

Maurice, C., David, J., Bédard, J.H., Francis, D., 2009. Evidence for a mafic cover sequence and its implications for continental growth in the northeastern Superior Province. Precambrian Research 168, 45–65.

McDonough, W.F., McCulloch, M.T., Sun, S.S., 1985. Isotopic and geochemical systematics in Tertiary-Recent basalts from southeastern Australia and implications for the evolution of the sub-continental lithosphere. Geochimica et Cosmochimica Acta 49, 2051–2067.

Meffre, S., Aitchison, J.C., Crawford, A.J., 1996. Geochemical evolution and tectonic significance of boninites and tholeiites from the Koh ophiolite, New Caledonia. Tectonics 15 (1), 67–83.

Monnier, C., Girardeau, J., Pubellier, M., Polve, M., Permana, H., Bellon, H., 1999a. Petrology and geochemistry of the Cyclops ophiolites (Irian Jaya, East Indonesia): consequences for the Cenozoic evolution of the north Australian margin. Mineralogy and Petrology 65, 1–28.

Monnier, C., Polve, M., Girardeau, J., Pubellier, M., Maury, R.C., Bellon, H., Permana, H., 1999b. Extensional to compressive Mesozoic magmatism at the SE Eurasia margin as recorded from the Meratus ophiolite (SE Borneo, Indonesia). Geodinamica Acta 12 (1), 43–55.

Monnier, C., Girardeau, J., Permana, H., Rehault, J.-P., Bellon, H., Cotten, J., 2003. Dynamics and age of formation of the Seram-Ambol ophiolites (Central Indonesia). Bulletin de la Société Géologique de France 174 (6), 529–543.

Montanini, A., Tribuzio, R., Vernia, L., 2008. Petrogenesis of basalts and gabbros from an ancient continent-ocean transition (External Liguride ophiolites, Northern Italy). Lithos 101, 453–479.

Moores, E.M., Day, H.W., 1984. Overthrust model for the Sierra Nevada. Geology 12, 416–419.

Mukhopadhyay, J., Ghosh, G., Zimmermann, U., Guha, S., Mukherjee, T., 2012. A 3.51 Ga bimodal volcanics-BIF-ultramafic succession from Singhbhum Craton: implications for Palaeoarchaean geodynamic processes from the oldest greenstone succession of the Indian subcontinent. Geological Journal 47, 284–311.

Nicholson, K.N., Black, P.M., Picard, C., 2000. Geochemistry and tectonic significance of the Tangihua Ophiolite Complex, New Zealand. Tectonophysics 321, 1–15.

Nutman, A.P., Green, D.H., Cook, C.A., Styles, M.T., Holdsworth, R.E., 2001. SHRIMP U-Pb zircon dating of the exhumation of the Lizard Peridotite and its emplacement over crustal rocks: constraints for tectonic models. Journal of the Geological Society, London 158, 809–820.

Nutman, A.P., Friend, C.R.L., Horie, K., Hidaka, H., 2007. The Itsaq Gneiss complex of southern west Greenland and the construction of Eoarchean crust at convergent plate boundaries. In: Van Kranendonk, M.J., Smithies, R.H., Bennet, V.C. (Eds.), Earth's Oldest Rocks, Development in Precambrian Geology 15. Elsevier B.V, pp. 187–218.

Olive, V., Hébert, R., Loubet, M., 1997. Isotopic and trace element constraints on the genesis of a boninitic sequence in he Thetford Mines ophiolitic complex, Quebec, Canada. Canadian Journal of Earth Sciences 34, 1258–1271.

Oliver, G.J.H., McAlpine, R.R., 1998. Occurrence of a sheeted dyke complex in the Ballantrae ophiolite, Scotland Geological Magazine 135, 509–517.

Oncken, O., Cheng, G., Franz, G., Giese, P., Götze, H.-J., Ramos, V.A., Strecker, M.R., Wigger, P. (Eds.), 2006. The Andes – Active Subduction Orogeny. Frontiers in Earth Sciences. Springer, Berlin, Heidelberg, p. 569.

O'Neil, J., Carlson, R.W., Francis, D., Stevenson, R.K., 2008. Neodymium-142 evidence for Hadean mafic crust. Science 321, 1828–1831.

O'Neil, J., Francis, D., Carlson, R.W., 2011. Implications of the Nuvvuagittuq greenstone belt for the formation of Earth's early crust. Journal of Petrology 52 (5), 985–1009.

Ottonello, G., Joron, J.L., Piccardo, G.B., 1984. Rare earth and 3d transition element geochemistry of peridotitic rocks: II. Ligurian peridotites and associated basalts. Journal of Petrology 25, 373–393.

Page, P., Bédard, J.H., Tremblay, A., 2009. Geochemical variations in a depleted fore-arc mantle: the Ordovician Thetford Mines Ophiolite. Lithos 113, 21–47.

Pallister, J.S., Budahn, J.R., Murchey, B.L., 1989. Pillow basalts of the Angayucham Terrane: oceanic plateau and island crust accreted to the Brooks Range. Journal of Geophysical Research 94 (B11), 15901–15923.

Parman, S.W., Grove, T.L., 2004. Petrology and geochemistry of Barberton komatiites and basaltic komatiites: evidence of Archean fore-arc magmatism. In: Kusky, T.M. (Ed.), Precambrian Ophiolites and Related Rocks, Developments in Precambrian Geology 13. Elsevier, Amsterdam, pp. 539–565.

Pearce, J.A., 2008. Geochemical fingerprinting of oceanic basalts with implications for the classification of ophiolites and search for Archean oceanic crust. Lithos 100, 14–48.

Pearce, J.A., 2014. Immobile elements fingerprinting of ophiolites. Elements 10 (in press).

Pearce, J.A., Parkinson, I.J., 1993. Trace element models for mantle melting: application to volcanic arc petrogenesis. In: Prichard, H.M., Alabaster, T., Harris, N.B.W., Neary, C.R. (Eds.), Magmatic Processes and Plate Tectonics, Geological Society of London, Special Publication 76, pp. 373–403.

Pearce, J.A., Robinson, P.T., 2010. The Troodos ophiolitic complex probably formed in a subduction initiation, slab edge setting. Gondwana Research 18, 60–81.

Pedersen, R.B., Hertogen, J., 1990. Magmatic evolution of the Karmøy Ophiolite Complex, SW Norway: relationships between MORB-IAT-boninitic-calc-alkaline and alkaline magmatism. Contributions to Mineralogy and Petrology 104, 277–293.

Pedersen, R.B., Furnes, H., Dunning, G., 1991. A U/Pb age for the Sulitjelma Gabbro, North Norway: further evidence for the development of a Caledonian marginal basin in Ashgill-Llandovery time. Geological Magazine 128, 141–143.

Pedersen, R.B., Searle, M.P., Carter, A., Bandopadhyay, P.C., 2010. U-Pb zircon age of the Andaman ophiolite: implications for the beginning of subduction beneath the Andaman-Sumatra arc. Journal of the Geological Society, London 167, 1105–1112.

Pedro, J., Araújo, A., Fonseca, P., Tassinari, C., Ribeiro, A., 2010. Geochemistry and U-Pb zircon age of the internal Ossa-Morena zone ophiolite sequences: a remnant of Rheic ocean in SW Iberia. Ofioliti 35, 117–130.

Peltonen, P., Kontinen, A., Huhma, H., 1996. Petrology and geochemistry of metabasalts from the 1.95 Ga Jormua ophiolite, Northeastern Finland. Journal of Petrology 37 (6), 1359–1383.

Pe-Piper, G., Tsikouras, B., Hatzipanagiotou, K., 2004. Evolution of boninites and island-arc tholeiites in the Pindos Ophiolite, Greece. Geological Magazine 141, 455–469.

Peters, T., Mercolli, I., 1998. Extremely thin oceanic crust in the Proto-Indian Ocean: evidence from the Masirah Ophiolite, Sultanate of Oman. Journal of Geophysical Research 103, 677–689.

Polat, A., Kerrich, R., Wyman, D.A., 1998. The late Archean Schreiber – Hemlo and White River – Dayohessarah greenstone belts, Superior Province: collages of oceanic plateaus, oceanic arcs, and subduction-accretion complexes. Tectonophysics 289, 295–326.

Polat, A., Hofmann, A.W., Rosing, M.T., 2002. Boninite-like volcanic rocks in the 3.7–3.8 Ga Isua Greenstone Belt, West Greenland: geochemical evidence for

Please cite this article in press as: Furnes, H., et al., Four billion years of ophiolites reveal secular trends in oceanic crust formation, Geoscience Frontiers (2014), http://dx.doi.org/10.1016/j.gsf.2014.02.002

intra-oceanic subduction zone processes in the early Earth. Chemical Geology 184, 231–254.
Polat, A., Li, J., Fryer, B., Kusky, T., Gagnon, J., Zhang, S., 2006. Geochemical characteristics of the Neoarchean (2800–2700 Ma) Taishan greenstone belt, North China Craton: evidence for plume-craton interaction. Chemical Geology 230, 60–87.
Pollack, N.H., 1997. Thermal characteristics of the Archean. In: de Wit, M.J., Ashwal, L.D. (Eds.), Greenstone Belts. Oxford University Press, Oxford, pp. 223–232.
Prichard, H.M., 1985. The Shetland ophiolites. In: Gee, D.G., Sturt, B.A. (Eds.), The Caledonide Orogen: Scandinavia and Related Areas. John Wiley & Sons, London, pp. 1173–1184.
Pushkov, V.N., 2009. The evolution of the Uralian orogen. In: Murphy, J.B., Keppie, J.D., Hynes, A.J. (Eds.), Ancient Orogens and Modern Analogues, The Geological Society, London, Special Publications 327, pp. 161–195.
Puchtel, I.S., Haase, K.M., Hofmann, A.W., Chauvel, C., Kulikov, V.S., Garbe-Schönberg, C.-D., Nemchin, A.A., 1997. Petrology and geochemistry of crustally contaminated komatiitic basalts from the Vetreny Belt, southeastern Baltic Shield: evidence for an early Proterozoic mantle plume beneath rifted Archean continental lithosphere. Geochimica et Cosmochimica Acta 61, 1205–1222.
Puchtel, I.S., Hofmann, A.W., Mezger, K., Jochum, K.P., Shchipansky, A.A., Samsonov, A.V., 1998. Oceanic plateau model for continental crustal growth in the Archaean: a case study from the Kostomuksha greenstone belt, NW Baltic Shield. Earth and Planetary Science Letters 155, 57–74.
Puga, E., Fanning, M., de Federico, Diaz, Nieto, J.M., Beccaluva, L., Bianchini, G., Diaz Puga, M.A.D., 2011. Petrology, geochemistry and U-Pb geochronology of the Betic Ophiolites: inferences for Pangaea break-up and birth of the westernmost Tethys Ocean. Lithos 124, 255–272.
Rampone, E., Hofmann, A.W., Raczek, I., 1998. Isotopic contrasts within the Internal Liguride ophiolite (N. Italy): the lack of a genetic mantle-crust link. Earth and Planetary Science Letters 163, 175–189.
Ramos, V.A., 2009. Anatomy and global context of the Andes: main geologic features and the Andean orogenic cycle. In: Kay, S.M., Ramos, V.A., Dickinson, W.R. (Eds.), Backbone of the Americas: Shallow Subduction, Plateau Uplift, and Ridge and Terrane Collision, Geological Society of America Memoir 204, pp. 31–65.
Ramos, V.A., Escayola, M., Mutti, D.I., Vujovich, G.I., 2000. Proterozoic-early Paleozoic ophiolites of the Andean basement of southern South America. In: Dilek, Y., Moores, E.M., Elthon, D., Nicolas, A. (Eds.), Ophiolites and Oceanic Crust: New Insights from Field Studies and the Ocean Drilling Program. Boulder, Colorado, Geological Society of America, Special Paper 349, pp. 331–349.
Rautenschlein, M., Jenner, G.A., Hertogen, J., Hofmann, A.W., Kerrich, R., Schmincke, H.-U., White, W.M., 1985. Isotopic and trace element composition of volcanic glasses from the Akaki Canyon, Cyprus: implications for the origin of the Troodos ophiolite. Earth and Planetary Science Letters 75, 369–383.
Redman, B.A., Keays, R.R., 1985. Archean volcanism in the eastern Goldfields Province, Western Australia. Precambrian Research 30, 113–152.
Revillion, S., Arndt, N.T., Chauvel, C., Hallot, E., 2000. Geochemical study of ultramafic volcanic and plutonic rocks from Gorgona Island, Colombia: the plumbing system of an oceanic plateau. Journal of Petrology 41 (7), 1127–1153.
Roberts, D., 2003. The Scandinavian Caledonides: event chronology, palaeogeographic settings and likely modern analogues. Tectonophysics 365, 283–299.
Roberts, D., Sturt, B.A., Furnes, H., 1985. Volcanite assemblages and environments in the Scandinavian Caledonides and the sequential development history of the mountain belt. In: Gee, D.G., Sturt, B.A. (Eds.), The Caledonide Orogen – Scandinavia and Related Areas. John Wiley & Sons, London, pp. 919–930.
Roberts, D., Nordgulen, Ø., Melezhik, V., 2007. The Uppermost Allochthon in the Scandinavian Caledonides: from a Laurentian ancestry through Taconian orogeny to Scandian crustal growth on Baltica. In: Hatcher Jr., R.D., Carlson, M.P., McBride, J.H., Martínez Catalán, J.R. (Eds.), 4-D Framework of Continental Crust, Geological Society of America Memoir 200, pp. 357–377.
Robertson, A.H.F., 2000. Mesozoic–Tertiary tectonic–sedimentary evolution of a south Tethyan oceanic basin and its margins in southern Turkey. In: Winchester, J.A., Piper, J.D.A. (Eds.), Tectonics and Magmatism in Turkey and the Surrounding Area, Geological Society, London, Special Publications 173, pp. 97–138.
Robinson, P.T., Zhou, M.-F., Hu, X.-F., Reynolds, P., Wenji, B., Yang, J., 1999. Geochemical constraints on the origin of the Hegenshan Ophiolite, Inner Mongolia, China. Journal of Asian Earth Sciences 17, 423–442.
Robinson, P.T., Malpas, J., Dilek, Y., Zhou, M.-F., 2008. The significance of sheeted dike complexes in ophiolites. GSA Today 18, 4–10.
Ryazantsev, A.V., Dubinina, S.V., Kuznetsov, N.B., Belova, A.A., 2008. Ordovician lithoteconic complexes in allochthons of the Southern Urals. Geotectonics 42 (5), 368–395.
Saccani, E., Pricipi, G., Garfagnoli, F., Menna, F., 2008. Corsica ophiolites: geochemistry and petrogenesis of basaltic and metabasaltic rocks. Ofioliti 33, 187–207.
Saccani, E., Delavari, M., Beccaluva, L., Amini, S., 2010. Petrological and geochemical constraints on the origin of the Nehbandan ophiolitic complex (eastern Iran): implications for the evolution of the Sistan Ocean. Lithos 117, 209–228.
Saleeby, J.B., 1983. Accretionary tectonics of the North American Cordillera. Annual Review of Earth and Planetary Sciences 15, 45–73.
Sager, W.W., Zhang, J., Korenaga, J., Sano, T., Koppers, A.A., Widdowson, M., Mahoney, J.J., 2013. An immense shield volcano in the Shatsky Ridge oceanic plateau, northwest Pacific Ocean. Nature Geoscience 6 (11), 976–981.
Sandstå, N.R., Robins, B., Furnes, H., de Wit, M., 2011. The origin of large varioles in flow-banded pillow lava from the Hooggenoeg Complex, Barberton Greenstone Belt, South Africa. Contributions to Mineralogy and Petrology 162, 365–377.
Santosh, M., 2010. A synopsis of recent conceptual models on supercontinent tectonics in relation to mantle dynamics, life evolution and surface environment. Journal of Geodynamics 50, 116–133.
Sarifakioglu, E., Dilek, Y., Sevin, M., 2013. Jurassic–Paleogene intra-oceanic magmatic evolution of the Ankara Mélange, North-Central Anatolia, Turkey. Solid Earth 5, 1941–2004. http://dx.doi.org/10.5194/sed-5-1941-2013.
Saunders, A.D., Tarney, J., Stern, C.R., Dalziel, I.W.D., 1979. Geochemistry of Mesozoic basin floor igneous rocks from southern Chile. Geological Society of America Bulletin 90, 237–258.
Savelieva, G.N., 2011. Ophiolites in European Variscides and Uralides: geodynamic settings and metamorphism. Geotectonics 45, 439–452.
Savelieva, G.N., Sharaskin, A.Ya, Saveliev, A.A., Spadea, P., Gaggero, L., 1997. Ophiolites of the southern Uralides adjacent to the East European continental margin. Tectonophysics 276, 117–137.
Sawaki, Y., Shibuya, T., Kawai, T., Komiya, T., Omori, S., Iizuka, T., Hirata, T., Windley, B.F., Maruyama, S., 2010. Imbricated ocean-plate stratigraphy and U-Pb zircon ages from tuff beds in cherts in the Ballantrae complex, SW Scotland. Geological Society of America Bulletin 122 (3/4), 454–464.
Searle, M.P., Law, R.D., Jessup, M.J., 2006. Crustal structure, restoration and evolution of the Greater Himalaya in Nepal, South Tibet: implications for channel flow and ductile extrusion of the middle crust. In: Law, R.D., Searle, M.P., Godin, L. (Eds.), Ductile Extrusion and Exhumation in Continental Collision Zones, Geological Society, London, Special Publications 268, pp. 355–378.
Selbekk, R.S., Furnes, H., Pedersen, R.B., Skjerlie, K.P., 1998. Contrasting tonalite genesis in the Lyngen magmatic complex, north Norwegian Caledonides. Lithos 42, 243–268.
Scott, R.B., Hajash Jr., A., 1976. Initial submarine alteration of basaltic pillow lavas: a microprobe study. American Journal of Science 276, 480–501.
Scott, D.J., Helmstaedt, H., Bickle, M.J., 1992. Purtuniq ophiolite, Cape Smith belt, northern Quebec, Canada: a reconstructed section of Early Proterozoic oceanic crust. Geology 20, 173–176.
Seyfried, W.E., Berndt, M.E., Seewald, J.S., 1988. Hydrothermal alteration processes at mid-ocean ridges: constraints from diabase alteration experiments, hot-spring fluids and composition of the oceanic crust. The Canadian Mineralogist 26, 787–804.
Shafaii Moghadam, H., Rahgoshay, M., Whitechurch, H., 2008. Mesozoic back-arc extension in the active margin of the Iranian continental block: constraints from age and geochemistry of the mafic lavas. Ofioliti 33, 95–103.
Shafaii Moghadam, H., Stern, R.J., Rahgoshay, M., 2010. The Dehshir ophiolite (central Iran): geochemical constraints on the origin and evolution of the Inner Zagros ophiolite belt. Geological Society of America Bulletin 122 (9/10), 1516–1547.
Shariff, A., Omang, K., Barber, A.J., 1996. Origin and tectonic significance of the metamorphic rocks associated with the Darvel Bay Ophiolite, Sabah, Malaysia. In: Hall, R., Blundell, D. (Eds.), Tectonic Evolution of Southeast Asia, The Geological Society, London, Special Publications 106, pp. 263–279.
Shervais, J.W., 1982. Ti-V plots and the petrogenesis of modern and ophiolitic lavas. Earth and Planetary Science Letters 32, 114–120.
Shervais, J.W., 2008. Tonalites, trondhjemites, and diorites of the Elder Creek ophiolite, California: low-pressure slab melting and reaction with the mantle wedge. In: Wright, J.E., Shervais, J.W. (Eds.), Ophiolites, Arcs, and Batholiths: A Tribute to Cliff Hopson, Geological Society of America Special Paper 438, pp. 113–132.
Shirey, S.B., Richardson, S.H., 2011. Start of the Wilson Cycle at 3 Ga shown by diamonds from subcontinental mantle. Science 333, 434–436.
Shojaat, B., Hassanipak, A.A., Mobasher, K., Ghazi, A.M., 2003. Petrology, geochemistry and tectonics of the Sabzevar ophiolite, North Central Iran. Journal of Asian Earth Sciences 21, 1053–1067.
Singh, A.K., Singh, N.I., Devi, L.D., Singh, R.K.B., 2012. Geochemistry of Mid-Ocean Ridge Mafic intrusives from the Manipur Ophiolite Complex, Indo-Myanmar Orogenic Belt, NE India. Journal of the Geological Society of India 80, 231–240.
Slagstad, T., 2003. Geochemistry of trondhjemites and mafic rocks in the Bymarka ophiolite fragment, Trondheim, Norway: petrogenesis and tectonic implications. Norwegian Journal of Geology 83, 167–185.
Smellie, J.L., Stone, P., Evans, J., 1995. Petrogenesis of boninites in the Ordovician Ballantrae ophiolite, southwestern Scotland. Journal of Volcanology and Geothermal Research 69, 323–342.
Smith, I.E.A., 2013. The chemical characterization and tectonic significance of ophiolite terrains in southeastern Papua New Guinea. Tectonics 32 (2), 159–170.
Smithies, R.H., Champion, D.C., Van Kranendonk, M.J., Howard, H.M., Hickman, A.H., 2005. Modern-style subduction processes in the Mesoarchaean: geochemical evidence from the 3.12 Ga Whundo intra-oceanic arc. Earth and Planetary Science Letters 231, 221–237.
Song, S., Niu, Y., Su, L., Zia, X., 2013. Tectonics of the North Qilian orogen, NW China. Gondwana Research 23, 1378–1401.
Spadea, P., Delaloye, M., Espinosa, A., Orrego, A., Wagner, J.J., 1987. Ophiolite complex from La Tetilla, Southwestern Colombia, South America. The Journal of Geology 95, 377–395.
Spadea, P., Kabanova, L.Y., Scarrow, J.H., 1998. Petrology, geochemistry, and geodynamic significance of Mid-Devonian boninitic rocks from the Baimak-Buribai area (Magnitogorsk Zone, Southern Urals). Ofioliti 23, 17–36.
Spadea, P., D'Antonio, M., Kosarev, A., Gorozhanina, Y., Brown, D., 2002. Arc-continent collision in the Southern Urals: Petrogenetic aspects of the forearc-arc

Please cite this article in press as: Furnes, H., et al., Four billion years of ophiolites reveal secular trends in oceanic crust formation, Geoscience Frontiers (2014), http://dx.doi.org/10.1016/j.gsf.2014.02.002

complex. In: Brown, D., Juhlin, C., Puchkov, V. (Eds.), Mountain Building in the Uralides: Pangea to Present, Geophysical Monograph 132. American Geophysical Union, pp. 101–134.
Spadea, P., Scarrow, J.H., 2000. Early Devonian boninites fron the Magnitogorsk arc, southern Urals (Russia): Implications for early development of a collisional orogeny. In: Dilek, Y., Moores, E.M., Elthon, D., Nicolas, A. (Eds.), Ophiolites and Oceanic Crust: New Insights from Field Studies and the Ocean Drilling Program. Boulder, Colorado, Geological Society of America, Special Paper 349, pp. 461–472.
Spadea, P., D'Antonio, M., 2006. Initiation and evolution of intra-oceanic subduction in the Uralides: geochemical and isotopic constraints from Devonian oceanic rocks of the Southern Urals, Russia. Island Arc 15, 7–25.
Stampfli, G.M., Borel, G.D., 2002. A plate tectonic model for the Paleozoic and Mesozoic constrained by dynamic plate boundaries and restored synthetic oceanic isochrons. Earth and Planetary Science Letters 196 (1–2), 17–33.
Stampfli, G.M., Hochard, C., 2009. Plate tectonics of the Alpine realm. In: Murphy, J.B., Keppie, J.D., Hynes, A.J. (Eds.), Ancient Orogens and Modern Analogues, The Geological Society, London, Special Publications 327, pp. 89–111.
Staudigel, H., Hart, R., 1983. Alteration of basaltic glass: mechanism and significance for the oceanic crust-seawater budget. Geochimica et Cosmochimica Acta 47, 37–50.
Stephens, M.B., Furnes, H., Robins, B., Sturt, B.A., 1985. Igneous activity within the Scandinavian Caledonides. In: Gee, D.G., Sturt, B.A. (Eds.), The Caledonide Orogen – Scandinavia and Related Areas. John Wiley & Sons, London, pp. 623–656.
Stern, C., 1979. Open and closed system igneous fractionation within two Chilean ophiolites and tectonic implication. Contributions to Mineralogy and Petrology 68, 243–258.
Stern, C., 1980. Geochemistry of Chilean ophiolites: evidence for the compositional evolution of the mantle source of back-arc basin basalts. Journal of Geophysical Research 85 (B2), 955–966.
Stern, C., Elthon, D., 1979. Vertical variations in the effects of hydrothermal metamorphism in Chilean ophiolites: their implications for ocean floor metamorphism. Tectonophysics 55, 179–213.
Stern, R.J., 2005. Evidence from ophiolites, blueschists, and ultra-high pressure metamorphic terranes that the modern episode of subduction tectonics began in Neoproterozoic time. Geology 33, 557–560.
Stern, R.J., 2008. Modern-style plate tectonics began in Neopreoterozoic time: an alternative interpretation of Earth's tectonic history. In: Condie, K.C., Pease, V. (Eds.), When Did Plate Tectonics Begin on Planet Earth?, Geological Society of America, Special Paper 440, pp. 265–280.
Sylvester, P.J., Attoh, K., 1992. Lithostratigraphy and composition of 2.1 Ga greenstone belts of West African craton and their bearing on crustal evolution of the Archean-Proterozoic boundary. The Journal of Geology 100, 377–393.
Tadesse, G., Allen, A., 2005. Geology and geochemistry of the Neoproterozoic Tuludimtu Ophiolite suite, western Ethiopia. Journal of African Earth Sciences 41, 192–211.
Tortorici, L., Catalano, S., Monaco, C., 2009. Ophiolite-bearing mélanges in southern Italy. Geological Journal 44, 153–166.
Tseng, C.-Y., Yang, H.-J., Yang, H.-Y., DunYi, L., Tsai, C.-L., HanQuan, W., GuoChao, Z., 2007. The Dongcaoche ophiolite from the North Qilian Mountains: a fossil oceanic crust of the Paleo-Qilian ocean. Chinese Science Bulletin 52 (17), 2390–2401.
Tsukanov, N.V., Kramer, W., Skolotnev, S.G., Luchitskaya, M.V., Seifert, W., 2007. Ophiolites of the Eastern Peninsulas zone (Eastern Kamchatka): age, composition, and geodynamic diversity. Island Arc 16, 431–456.
Upadhyay, H.D., 1982. Ordovician komatiites and associated boninite-type magnesian lavas from Betts Cove, Newfoundland. In: Arndt, N.T., Nisbet, E.G. (Eds.), Komatiites. George Allen & Unwin, London, pp. 187–198.
Uysal, I., Ersoy, Y., Dilek, Y., Escayola, M., Sarifakioglu, E., Saka, S., Hirata, T., 2013. Depletion and refertilization of the Tethyan oceanic upper mantle as revealed by the early Jurassic Refahiye ophiolite, NE Anatolian Kamch. Gondwana Research. http://dx.doi.org/10.1016/j.gr.2013.09.008.
van Hunen, J., Moyan, J.-F., 2012. Archean subduction: fact or fiction? Annual Review of Earth and Planetary Sciences 40, 195–219.
Van Kranendonk, M.J., 2007. Tectonics of early Earth. In: Van Kranendonk, M.J., Smithies, R.,H., Bennet, V.C. (Eds.), Earth's Oldest Rocks, Development in Precambrian Geology 15. Elsevier, Amsterdam, pp. 1105–1116.
Van Kranendonk, M.J., 2011. Onset of plate tectonics. Science 333, 413–414.
van Staal, C.R., Whalen, J.B., Valverde-Vaquero, P., Zagorevski, A., Rogers, N., 2009. Pre-Carboniferous, episodic accretion-related, orogenesis along the Laurentian margin of the northern Appalachians. In: Murphy, J.B., Keppie, J.D., Hynes, A.J. (Eds.), Ancient Orogens and Modern Analogues, Geological Society, London, Special Publications 327, pp. 271–316.
van Staal, C.R., Chew, D.M., Zagorevski, A., McNicoll, V., Hibbard, J., Skulski, T., Castonguay, S., Escayola, M., Sylvester, P.J., 2013. Evidence of Late Ediacaran Hyperextension of the Lauretian Iapetan Margin in the Birchy Complex, Baie Verte Peninsula, Northwest Newfoundland: Implications for the Opening of Iapetus, Formation of Peri-Laurentian Microcontinents and Taconic – Grampian Orogenesis. Geoscience Canada 40, 1–25.
Varne, R., Brown, A.V., Jenner, G.A., Falloon, T., 2000. Macquarie Island: its geology and structural history, and the timing and tectonic setting of its N-MORB to E-MORB magmatism. In: Dilek, Y., Moores, E.M., Elthon, D., Nicolas, A. (Eds.), Ophiolites and Oceanic Crust: New Insights from Field Studies and Ocan Drilling Program, Geological Society of America, Special Publication 349, pp. 301–320.
Velozo, E.A.E., Anma, R., Yamazaki, T., 2005. Tectonic rotations during the Chile Ridge collision and obduction of the Taitao ophiolite (southern Chile). Island Arc 14, 599–615.
Wakita, K., Bubellier, M., Windley, B.F., 2013. Tectonic processes, from rifting to collision via subduction, in SE Asia and the western Pacific: a key to understanding the architecture of the Central Asian Orogenic Belt. Lithosphere 5 (3), 265–276.
Wang, Z., Sun, S., Li, J., Hou, Q., 2002. Petrogenesis of tholeiite associations in Kudi ophiolite (western Kunlun Mountains, northwestern China): implications for the evolution of back-arc basins. Contributions to Mineralogy and Petrology 143, 471–483.
Whattam, S.A., Malpas, J., Smith, I.E.M., Ali, J.R., 2006. Link between SSZ ophiolite formation, emplacement and arc inception, Northland, New Zealand: U-Pb SHRIMP constraints; Cenozoic SW Pacific tectonic implications. Earth and Planetary Science Letters 250, 606–632.
Whitechurch, H., Juteau, T., Montigny, R., 1984. Role of the Eastern Mediterranean Ophiolites (Turkey, Syria, Cyprus) in the History of the Neo-Tethys. In: Geological Society, London, Special Publications 17, pp. 301–317.
Wilhem, C., Windley, B.F., Stampfli, G.M., 2011. The Altaids of Central Asia: a tectonic and evolutionary innovative review. Earth-Science Reviews 113, 303–341.
Windley, B.F., 1988. Tectonic framework of the Himalaya, Karakoram and Tibet, and problems of their evolution. Philosophical Transactions of the Royal Society A 326, 3–16.
Windley, B.F., Alexeiev, D., Xiao, W., Kröner, A., Badarch, G., 2007. Tectonic models for accretion of the Central Asian Orogenic Belt. Journal of the Geological Society, London 164, 31–47.
Wyman, D.A., O'Neill, C., Ayer, J.A., 2008. Evidence for moderen-style subduction to 3.1 Ga: a plateau-adakite-gold (diamond) association. In: Condie, K.C., Pease, V. (Eds.), When Did Plate Tectonics Begin on Planet Earth?, Geological Society of America, Special Paper 440, pp. 129–148.
Xia, B., Yu, H.-X., Chen, G.-W., Qi, L., Zhao, T.-P., Zhou, M.-F., 2003. Geochemistry and tectonic environment of the Dagzhuka ophiolite in the Yarlung-Zangbo suture zone, Tibet. Geochemical Journal 37, 311–324.
Xia, X., Song, S., 2010. Forming age and tectono-petrogenises of the Jiugequan ophiolite in the North Qilian Mountain, NW China. Chinese Science Bulletin 55 (18), 1899–1907.
Xiao, W., Windley, B.F., Hao, J., Li, J., 2002. Arc-ophiolite obduction in the Western Kunlun Range (China): implications for the Palaeozoic evolution of central Asia. Journal of the Geological Society, London 159, 517–528.
Yang, J.-S., Dobrzhinetskaya, L., Bai, W.-J., Fang, Q.-S., Robinson, P.T., Zhang, J., Green II, H.W., 2007. Diamond- and coesite-bearing chromitites from the Loubusa ophiolite, Tibet. Geology 35 (10), 875–878.
Yin, A., Harrison, T.M., 2000. Geologic evolution of the Himalayan-Tibetan orogeny. Annual Review of Earth and Planetary Sciences 28, 211–280.
Yumul Jr., G.P., Dimalanta, C.B., Jumawan, F.T., 2000. Geology of the southern Zambales Ophiolite Complex, Luzon, Philippines. Island Arc 9, 542–555.
Zagorevski, A., van Staal, C.R., 2011. The record of Ordovician arc-arc and arc-continent collisions in the Canadian Appalachians during the closure of Iapetus. In: Brown, D., Ryan, P.D. (Eds.), Arc-Continent Collisions, Frontiers in Earth Sciences. Springer-Verlag, Berlin Heidelberg, pp. 341–371.
Zhai, Q-g., Jahn, B-m., Wang, J., Su, L., Mo, X.-X., Wang, K-l., Tang, S-h., Lee, H-y., 2013. The Carboniferous ophiolite in the middle of the Qiangtang terrane, Northern Tibet: SHRIMP U-Pb dating, geochemical and Sr-Nd-Hf isotopic characteristics. Lithos 168–169, 186–199.
Zheng, R., Wu, T., Zhang, W., Xu, C., Meng, Q., 2013. Late Paleozoic subduction system in the southern Central Asian Orogenic Belt: evidences from geochronology and geochemistry of the Xiaohuangshan ophiolite in the Beishan orogenic belt. Journal of Asian Earth Sciences 62, 463–475.
Zonenshain, L.P., Korinevski, V.G., Kazmin, V.G., Pechersky, D.M., Khain, V.V., Matveenkov, V.V., 1985. Plate tectonic model of the South Urals development. Tectonophysics 109, 95–135.
Zwart, H.J., 1967. The duality of orogenic belts. Geol. Mijnb. 46, 283–309.

Harald Furnes is professor at the Department of Earth Science, University of Bergen, Norway, since 1985. He received his D.Phil. at Oxford University, UK, in 1978. His main research interests have been connected to volcanic rocks. This involves physical volcanology, geochemistry and petrology, mainly related to ophiolites and island arc development of various ages. During the last 10 years the main research has been focussed on Precambrian greenstones, in particular the Paleoarchean Barberton Greenstone Belt. Another research focus has been related to the alteration of volcanic glass, which again led to a long-term study on the interaction between submarine basaltic volcanic rocks and micro-organisms, and the search for traces of early life.

Please cite this article in press as: Furnes, H., et al., Four billion years of ophiolites reveal secular trends in oceanic crust formation, Geoscience Frontiers (2014), http://dx.doi.org/10.1016/j.gsf.2014.02.002

Maarten Johan de Wit was born in Holland, went to school in Holland and Ireland, and completed his BSc/MA in Ireland (Trinity College, Dublin), and his PhD in England (Cambridge University), and was a postdoc at the Lamont Doherty Earth Observatory, Columbia University, USA, and at the BPI Geophysics University of the Witwatersrand, Johannesburg, South Africa. Presently he holds the chair of Earth Stewardship Science at the Nelson Mandela Metropolitan University in Port Elizabeth, South Africa. He was the Founding Director of AEON (Africa Earth Observatory Network), a trans-disciplinary research institute (www.aeon.org.za). His scientific interests lie in how the Earth works (particular in its youthful stage); in global tectonics; the evolution of Africa and Gondwana; the origin of continents, life and mineral resources; and in the economics of natural-resources and sharing of the 'commons'. He has mapped in the Barberton Greenstone Belt since 1979.

Yildirim Dilek is a Distinguished Professor of Geology at Miami University (USA), and the Vice President of the International Union of Geosciences (IUGS). He received his PhD from the University of California. He has been a Visiting Professor at Ecole Normal Superieur in Paris-France, University of Bergen-Norway, University of Tsukuba-Japan, University of Kanazawa-Japan, and China University of Geosciences in Beijing. He has worked extensively on the Phanerozoic ophiolites in the Alpine-Himalayan, North American Cordilleran and Caledonian orogenic belts. His other research interests include Precambrian tectonics, mantle dynamics and magmatism in collisional orogenic belts, extensional tectonics and metamorphic core complex development, and accretionary convergent margin tectonics. Recently, he has been studying the structural architecture and geochemical make up of the Mesozoic ophiolites and suture zones in Iran, Tibet and the Qinling-Qilian orogenic belt in China.

Please cite this article in press as: Furnes, H., et al., Four billion years of ophiolites reveal secular trends in oceanic crust formation, Geoscience Frontiers (2014), http://dx.doi.org/10.1016/j.gsf.2014.02.002